

AD-A273 095



NPS-69SL77071

2

NAVAL POSTGRADUATE SCHOOL

Monterey, California



DTIC
ELECTE
NOV 29 1993
S B D

TRANSVERSE OSCILLATIONS OF A CIRCULAR CYLINDER

IN UNIFORM FLOW

PART-I

By

TURGUT SARPKAYA

20 JULY 1977

Approved for public release; distribution unlimited.

93-27195



NPS-69SL77071

93

11

5

073



DEPARTMENT OF THE NAVY

NAVAL POSTGRADUATE SCHOOL
MONTEREY CA 93943-5100

IN REPLY REFER TO:

Defense Technical Information Center
ATTN: DTIC-OCC (Selection Group), **MR. Chester Becks**
Building 5
Cameron Station
Alexandria, VIRGINIA 22304-6145

26 October 1993

Dear Mr. Becks:

This is a follow-up to your conversation with Ms. Margery Cline of the Research Reports Division of the Library of the Naval Postgraduate School regarding two reports of identical title, with different dates of issue.

Briefly, you have been provided in July 1977 with two copies of a technical report (enclosed herewith are **two additional copies of these originals**). Subsequently, a small change has been made in the original report, its number has been modified with a letter -R, and the report date has been changed to 25 December 1977. Apparently, upon the receipt of the revised version, DTIC has taken off the original report from its documentation list, since the original does not appear in your data base.

The changes I have made caused a great deal of confusion through the years. More importantly, time has shown that the changes *did not improve either the originality or the quality of the first report*. With hindsight, I have realized that it would have been better had I kept the original remain ~~as~~ is (i.e., no revisions).

It is because of the foregoing reasons, I respectfully request that:

1. Report NPS-69SL77071-R (AD-A049 825), dated 25 Dec 1977 be taken off your records and destroyed once and for all; and
2. The original report (two copies of which are attached herewith) be entered into your documentation system as:
Report NPS-69SL77071 (AD-A049 825), dated 20 July 1977.

If my request is too difficult to implement, then please feel free to list both of the reports. In any case, it is important that the original report appear in your documentation ~~either alone or~~ together with the revised version.

With many thanks for your help and best wishes, I remain

Sincerely yours,

Prof. T. Sarpkaya, Code: ME-SL
Mechanical Engineering
Naval Postgraduate School
Monterey, CA 93943-5100

PH: (408) 656-3425
FAX: (408) 656-2238

Encls: as noted

NAVAL POSTGRADUATE SCHOOL
Monterey, California

Rear Admiral Isham Linder
Superintendent

J. R. Borsting
Provost

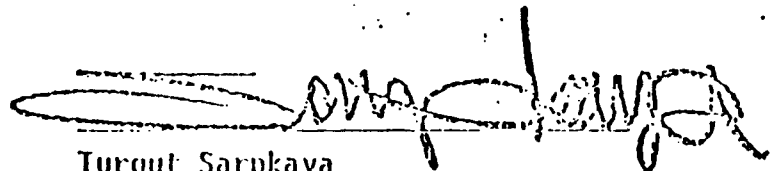
TRANSVERSE OSCILLATIONS OF A CIRCULAR CYLINDER
IN UNIFORM FLOW
PART-I

This report presents the results of an experimental and analytical investigation of the forced oscillations of a circular cylinder in uniform flow. The transverse force has been decomposed into two components and the appropriate force coefficients have been determined experimentally through the use of a Fourier-averaging technique. The results were then incorporated into the equation of motion to predict the dynamic response of elastically-mounted cylinders. The numerical predictions were found to be in good agreement with those obtained experimentally.

The results obtained with the discrete-vortex representation of the separated flow field about an oscillating cylinder will be described in a separate report.

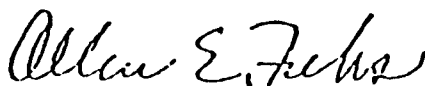
The work reported herein has been supported by the Civil Engineering Laboratory of the Naval Construction Battalion Center, Port Hueneme, CA.

This report was prepared by:



Turgut Sarpkaya
Professor of Mechanical Engineering

Approved by:



Allen E. Fuhs, Chairman
Department of Mechanical
Engineering



Robert R. Fossum
Dean of Research

REPORT DOCUMENTATION PAGE		READ INSTRUCTIONS BEFORE COMPLETING FORM
1. REPORT NUMBER NPS-69SL77071	2. GOVT ACCESSION NO.	3. RECIPIENT'S CATALOG NUMBER
4. TITLE (and Subtitle) TRANSVERSE OSCILLATIONS OF A CIRCULAR CYLINDER IN UNIFORM FLOW - Part I.		5. TYPE OF REPORT & PERIOD COVERED Interim Report 1 Sept. 76 -- 30 Aug. 1977.
7. AUTHOR(s) Prof. TURGUT SARPKAYA Mechanical Engineering, NPS.		6. PERFORMING ORG. REPORT NUMBER
9. PERFORMING ORGANIZATION NAME AND ADDRESS Naval Postgraduate School Monterey, Calif. 93940		8. CONTRACT OR GRANT NUMBER(s)
11. CONTROLLING OFFICE NAME AND ADDRESS Naval Construction Battalion Center Civil Engineering Laboratory Port Hueneme, California		10. PROGRAM ELEMENT, PROJECT, TASK AREA & WORK UNIT NUMBERS
14. MONITORING AGENCY NAME & ADDRESS (if different from Controlling Office) Mr. Dallas J. Meggitt Civil Engineering Laboratory Naval Construction Battalion Center Port Hueneme, Calif.		12. REPORT DATE 20 July 1977
16. DISTRIBUTION STATEMENT (of this Report) Approved for public release; distribution unlimited.		13. NUMBER OF PAGES 95
17. DISTRIBUTION STATEMENT (of the abstract entered in Block 20, if different from Report) The source must be acknowledged in using or referring to the data presented in this report.		15. SECURITY CLASS. (of this report) Unclassified
18. SUPPLEMENTARY NOTE FOR ADDITIONAL INFORMATION SEE NPS-69SL77071R, (ADAO49 825)		
19. KEY WORDS (Continue on reverse side if necessary and identify by block number) Flow-induced vibrations, transverse oscillations, cable strumming, resonant vibrations.		
20. ABSTRACT (Continue on reverse side if necessary and identify by block number) This report presents the results of an experimental and analytical investigation of the forced oscillations of a circular cylinder in uniform flow. The transverse force has been decomposed into two components and the appropriate force coefficients have been determined experimentally through the use of a Fourier-averaging technique. The results were then incor- porated into the equation of motion to predict the dynamic response of elastically-mounted cylinders. The numerical predictions were found to be		

in good agreement with those obtained experimentally.

The results of the discrete-vortex model of the separated flow field about an oscillating cylinder will be described in a separate report entitled: "Transverse Oscillations of a Circular Cylinder in Uniform Flow-Part-II."

Accession For	
NTIS GRA&I	<input checked="checked" type="checkbox"/>
DTIC TAB	<input type="checkbox"/>
Unannounced	<input type="checkbox"/>
Justification	
By	
Distribution/	
Availability Codes	
Dist	Avail and/or Special
A-1	

TABLE OF CONTENTS

INTRODUCTION	9
A. General Remarks	9
B. Self-Excited Oscillations	12
C. Discussion of Relevant Physical Parameters	15
a. Strouhal Number	15
b. Damping Coefficient	18
c. Natural Frequency and Added Mass	20
EXPERIMENTAL EQUIPMENT AND PROCEDURES	24
DATA ANALYSIS	29
DRAG AND INERTIA COEFFICIENTS	34
ANALYSIS	40
CONCLUSIONS	49
REFERENCES	50
FIGURES	51-92
APPENDIX-A	93
INITIAL DISTRIBUTION LIST	95

LIST OF FIGURES

1.	NPS Water Tunnel	51
2.	Motor, Flywheel and Pivot Assembly	52
3.	Aluminum Yoke-Force Transducer	53
4.	Force and Acceleration Traces	54
5.	Comparison of Calculated and Measured Lift Forces, $\Lambda/D = 0.84$, $\bar{V}T/D = 4.98$	55
6.	Comparison of Calculated and Measured Lift Forces, $\Lambda/D = 0.84$, $\bar{V}T/D = 5.15$	56
7.	Comparison of Calculated and Measured Lift Forces, $\Lambda/D = 0.84$, $\bar{V}T/D = 5.49$	57
8.	Comparison of Calculated and Measured Lift Forces, $\Lambda/D = 0.84$, $\bar{V}T/D = 5.81$	58
9.	Comparison of Calculated and Measured Lift Forces, $\Lambda/D = 0.84$, $\bar{V}T/D = 6.50$	59
10.	Mean In-Line Drag Coefficient versus $D/\bar{V}T$ for $\Lambda/D = 0.25$.	60
11.	Mean In-Line Drag Coefficient versus $D/\bar{V}T$ for $\Lambda/D = 0.50$.	61
12.	Mean In-Line Drag Coefficient versus $D/\bar{V}T$ for $\Lambda/D = 0.75$.	62
13.	Comparison Curves: Mean In-Line Drag Coefficient versus $D/\bar{V}T$ for $\Lambda/D = 0.25, 0.50, 0.75$, and 0.84	63
14.	Phenomenological Demonstration: In-Line Force versus Time while Increasing Oscillation Frequency	64
15.	C_{dl} versus V_r for $\Lambda/D = 0.13$	65
16.	C_{dl} versus V_r for $\Lambda/D = 0.25$	66
17.	C_{dl} versus V_r for $\Lambda/D = 0.50$	67
18.	C_{dl} versus V_r for $\Lambda/D = 0.75$	68
19.	C_{dl} versus V_r for $\Lambda/D = 1.03$	69
20.	C_{ml} versus V_r for $\Lambda/D = 0.13$	70

21.	C_{mh} versus V_r for $\Lambda/D = 0.25$	71
22.	C_{mh} versus V_r for $\Lambda/D = 0.50$	72
23.	C_{mh} versus V_r for $\Lambda/D = 0.75$	73
24.	C_{mh} versus V_r for $\Lambda/D = 1.03$	74
25.	C_{dh} versus V_r for $\Lambda/D = 0.13$	75
26.	C_{dh} versus V_r for $\Lambda/D = 0.25$	76
27.	C_{dh} versus V_r for $\Lambda/D = 0.50$	77
28.	C_{dh} versus V_r for $\Lambda/D = 0.75$	78
29.	C_{dh} versus V_r for $\Lambda/D = 1.03$	79
30.	C_{mh} versus V_r for $\Lambda/D = 0.13$	80
31.	C_{mh} versus V_r for $\Lambda/D = 0.25$	81
32.	C_{mh} versus V_r for $\Lambda/D = 0.50$	82
33.	C_{mh} versus V_r for $\Lambda/D = 0.75$	83
34.	C_{mh} versus V_r for $\Lambda/D = 1.03$	84
35.	Elastically-Mounted, Linearly-Damped Cylinder	40
36.	Sample Transient and Steady-State Oscillation Simulation . .	85
37.	Sample Transient and Steady-State Oscillation Simulation . .	86
38.	Sample Transient and Steady-State Oscillation Simulation . .	87
39.	Predicted Response of an Elastically-Mounted Cylinder with $\zeta = 0.000678$, 'a' = 0.00862, and $S_G = 0.079$	88
40.	Predicted Response of an Elastically-Mounted Cylinder with $\zeta = 0.000331$, 'a' = 0.00243, and $S_G = 0.14$	89
41.	Predicted Response of an Elastically-Mounted Cylinder with $\zeta = 0.000162$, 'a' = 0.000517, and $S_G = 0.31$	90
42.	$2\Lambda/D$ versus Response Parameter S_G	91
43.	Unstable Dynamic Response of an Elastically-Mounted Cylinder with $\zeta = 0.017$, 'a' = 0.0086, and $S_G = 2$	92

NOMENCLATURE

A	Amplitude of transverse oscillations
a	Mass ratio, (see Eq. 11-a))
C_d	Drag coefficient, see Eq. (1)
C_{dl}	Another drag coefficient, see Eqs. (2) and (4)
C_{dlh}	Another drag coefficient, see Eqs. (6) and (7)
C_{ds}	Steady-Flow drag coefficient
\bar{C}_{di}	Mean in-line drag coefficient
C_L	Lift coefficient
C_m	An inertia coefficient, see Eq. (1)
C_{ml}	An inertia coefficient, See Eqs. (2) and (5)
C_{mlh}	An inertia coefficient, see Eqs. (6) and (8)
D	Cylinder diameter
f	A frequency
f_c	Cylinder oscillation frequency
f_n	Natural frequency of an elastically-mounted cylinder
f_v^o	Vortex shedding frequency for a cylinder at rest
L	Length of the test cylinder
m	Mass of the oscillating cylinder
Re	Reynolds number
S	Strouhal number
S_G	Response parameter, material damping ratio/mass ratio
t	Time
T	Period of transverse oscillations
u	Velocity
U	Velocity

U_m	Maximum velocity in a cycle
\bar{V}	Velocity of the ambient flow
V_r	Reduced velocity, $\bar{V}T/D$
x	Displacement
x_r	$= x/D$
y_r	$= x/\Lambda$
ζ	Material damping ratio unless otherwise stated
ν	Kinematic viscosity of fluid
ρ_f	Density of fluid
ρ_s	Density of the cylinder, (apparent density)
ρ_r	Fluid density/apparent structural density
ω	Circular frequency
ω_0	f_s/f_n , Strouhal frequency/natural frequency
Ω	f_c/f_n , Cylinder oscillation frequency/natural frequency

ACKNOWLEDGMENTS

The work described in this report represents part of a research program supported by the Civil Engineering Laboratory of the Naval Construction Battalion Center, Port Hueneme, California. This support is gratefully acknowledged.

The writer is indebted to the many people whose help and co-operation made this investigation possible. Mr. Dallas J. Meggitt provided much valuable insight and encouragement. Messrs. D. W. Meyers, D. Fortik, P. Raposo, Z. Demirbilek, and R. L. Shoaff, all graduate students at the Naval Postgraduate School, assisted with the experiments and data evaluation. Mr. Jack McKay, an artist and ingenious model maker, built all the critical parts of the instrumentation. The computer time was donated by the Naval Postgraduate School and the Fleet Numerical Weather Central.

The writer wishes to express his sincere thanks to Drs. O. M. Griffin and G. H. Koopmann for an advance copy of their paper on "the vortex-excited lift and resistance forces on resonantly vibrating cylinders."

1. INTRODUCTION

A. GENERAL REMARKS

The linear or nonlinear transient or steady-state response of a body to forces acting on it has long been a source of interesting and practically applicable research. In fluid flow, the problem arises from the fundamentally unstable nature of the shear layers and the feed-back from the wake to the shear layers. The resulting vortex motion gives rise, in addition to a mean drag force, to a significant fluctuating transverse force provided that part of the body contour lies in the region of the transverse pressure gradient, i.e., downstream of the separation points. Evidently, the shape of the afterbody and the pressure gradient are related and an afterbody which prevents the nonlinear interaction between the two shear layers may eliminate the transverse pressure gradient without preventing the symmetric vortex formation.

Experiments have shown that elastic bodies or elastically-mounted rigid bodies with a suitable afterbody subjected to steady or time-dependent flow can develop self-excited oscillations with limit-cycle behavior and that energy may be transferred from the fluid to the body when the vortex-shedding frequency brackets the natural frequency of oscillation of the body. Thus, not only the shape of the body but also its material characteristics (e.g., density, elasticity, internal friction, tension, type of mounting, surface condition, yaw angle, proximity of other bodies or free surface, etc.) play significant roles in the overall mechanism. Some of these variables controls the spanwise coherence of the vortices and hence the integrated transverse force along the body; some controls the natural frequency of the body and the mode

of its vibration; and some changes the internal damping of the body and the work done by its surroundings. Evidently, means may be discovered through painstakingly-difficult experiments to reduce or destroy the spanwise coherence so as to minimize the exciting force, to increase the internal damping so as to minimize the net energy transfer, or to increase the natural frequency (stiffening of the body or of its supports) so that the vortex-shedding frequencies are well below or above the natural frequency of the body. In doing so, however, the objective is not only the reduction or elimination of the hydroelastic oscillations but also the minimization of an in-line drag-force parameter such as $(1+A/D)C_d$. In other words, the penalty for the reduced transverse oscillations should not be a large in-line drag force.

The phenomenon is relatively more complex since one is concerned not only with the oscillations of the body and the in-line and transverse forces acting on it but also with fatigue and the sound generated by the oscillations and vortices. Furthermore, in affecting the natural frequency of the body by additional tension or mass, the question is not merely the determination of the separation needed between the vortex-shedding and natural frequencies but also of the range over which the exciting mechanism can lock onto the frequency of the body.

The material damping which is often combined or confused with fluid damping, cannot be increased to desired levels without severe penalties. As to the efforts to change the body shape, it is obvious that a circular cross-section is most desirable partly because of ease of its construction and partly because of the fact that often the flow is omnidirectional as well as time-dependent. It is for the reasons cited above that the reduction of the integrated transverse force by a reduction

of the spanwise coherence (increasing the force-cancelling effects of phase shifts which may be brought about by three-dimensional effects) by means of helical strakes, eccentric rings, uneven roughness, and various types of fairings has been the primary method of vibration suppression. It should be noted that such devices are often referred to as the "vortex suppression" devices even though they do not actually suppress the vortex shedding. They merely reduce the integrated lift force through phase shifts.

It is evident from the foregoing remarks that there are substantial gaps in the understanding of the fundamental mechanisms at work in the forcing of a body by the forces acting on its afterbody and in the prediction of the lock-in range in which resonant and pseudo-resonant oscillations occur. It is also evident that the control or prevention of the oscillations requires first of all the prediction of whether such oscillations will at all occur and if so for what range of the controlling parameters.

In view of the foregoing considerations, the present research program was undertaken with two main objectives: (a) to determine the in-phase and out-of-phase components of the time-dependent force acting on a rigid circular cylinder undergoing forced transverse oscillations in a uniform stream and to predict through the use of these force components the dynamic response of an elastically mounted cylinder for which the material damping coefficient and the 'mass parameter' are known; and (b) to predict through the use of the discrete vortex model the kinematic and dynamic characteristics of the fluid motion about a circular cylinder undergoing harmonic oscillations. The second objective will, hopefully, help to synthesize the information gathered during the past decade from specific

practical vibration problems and from highly idealized experimental and theoretical investigations.

This report does not deal with vibration suppression methods, the effect of time-dependence and shear of the ambient flow, galloping motion, the effect of yaw, coupled in-line and transverse oscillations of flexible cylinders or cables, the proximity effect of other tubes or bodies, etc. Furthermore, no attempt has been made to offer a chronological survey or a state-of-the art appraisal of the flow induced oscillations. Only those works which have a direct bearing on the evaluation and/or discussion of the present results are reviewed in some detail wherever appropriate.

B. SELF-EXCITED OSCILLATIONS

The net result of alternate vortex shedding is an oscillating side thrust, upon a cylinder of suitable form, in a direction away from the last vortex. This side thrust or lift force exists practically at all Reynolds numbers regardless of whether the body is allowed to respond dynamically or not. For a body held at rest, there is a finely-tuned, relatively delicate, interaction and balance between various features of the flow. Upstream boundary layers generate the vorticity which feeds the vortices. Downstream boundary layers, interaction between the oppositely-signed shed vortices, and turbulence control the dissipation mechanism, the amount of vorticity each vortex receives or retains, the mobility of the separation points, the average vortex shedding frequency, etc. The fact that the various components of such a flow is delicately interrelated and susceptible to interference has been amply demonstrated. The appreciation of the fact that the alternate vortex shedding is a consequence of flow instability, or of the breakdown of the cause and

effect symmetry, is particularly important in understanding as to why the vortex-induced oscillation is not a simple cause-and-effect phenomenon. From a fundamental point of view the question is the understanding of both the modification of the steady flow mechanisms and the interdependence between the resulting time-dependent force that causes the body to oscillate and the oscillation. From a practical point of view the question is how to prevent the body from taking control of vortex shedding.

Numerous experiments have shown that (e.g., Blevins 1977) when the vortex shedding frequency brackets the natural frequency of a body with a suitable afterbody, the body takes control of the shedding in apparent violation of the Strouhal relationship. Furthermore, the spanwise correlation of the wake, the vortex strength, and the drag force increase. The base pressure, wake width, vortex-shedding frequency may increase or decrease as one approaches the synchronization region. These are merely some of the simply-observable or measurable flow features which in reality reflect the changes in the fine-grain flow structure due to the complicated interaction between the oscillator and the oscillated. Thus, it may be said that the lock-in phenomenon over a range of velocities owes its occurrence to the precarious nature of the base flow. The more precarious the basic flow features are about the body, the more susceptible is the body to synchronous oscillations in a wider velocity range. In other words, a body's ability to alter the flow features through its oscillations or simply to amplify the lift force is a measure of its ability to hydrodynamic response. It is not reasonable to think that the flow characteristics about an oscillating body would be the same as those about a body at rest. Should this have been the case, there would have been resonance at one particular velocity of flow only, namely, when the Strouhal

frequency is equal to the natural frequency of the body.

The interplay between the different physical quantities involved in the phenomenon can be adequately established and a deeper insight could be gained into the physics of the flow only through an analytical model. To a degree, the difficulties in devising a model stem from an inadequate knowledge of the precise mechanism of flow separation and its consequences in steady flow past a stationary body. To be sure, analytical models in which the equations of motion are conditioned in a manner analogous with experimental techniques, such as conditioned sampling, for instance, could also assist in exposing the details of the physical phenomena. On the other hand, models contrived to suit the available experimental data give only an illusion of understanding of the physics of the flow and become at best an interpolation between various experimental results.

So far, it has not been possible to calculate, by appropriate viscous or inviscid modeling, the development of coiled-up vortex sheets springing from two- or three-dimensional separation lines on a body of general shape. Thus, isolating a small number of flow features either to describe the wake development about a stationary body or the differences between the characteristics of stationary and oscillating body so as to arrive at a theoretical unification of the existing observations and measurements may be an illusive search. However, the end result may be less important than the practical understanding that the effort has brought. In the main, it seems that the computation of the characteristics of the near wake region and the interaction of that region with an oscillating body will continue to remain essentially empirical and the success of numerical schemes will be sensitive to the choice of independent parameters. It appears that heavy reliance on experimental investigations of vortex-induced oscillations and the evolution of essentially empirical models

to bridge between sets of experimental results will dominate the problem of fluid-structure interaction for a long time to come.

C. DISCUSSION OF RELEVANT PHYSICAL PARAMETERS

Flow about an oscillating body necessarily concerns such parameters as the Strouhal number, damping coefficient, natural frequency, added mass, etc. These parameters are variously interpreted, evaluated, or assumed by various workers. Thus, it is necessary that they be discussed here briefly so that the reader can assess the validity of some of the assumptions made in their use in various analytical models.

a. Strouhal Number

The separation process is a time-dependent phenomenon with alternate shedding vortices creating a transverse pressure gradient. Unsteady hydrodynamic loads arising from this pressure gradient acting on the afterbody can excite dynamic structural response as noted earlier. Body natural frequencies near the exciting frequency raise the spector of load and response enhancement. Thus, the spectral content of the forcing functions are important to dynamic structural response analysis. If the shedding process is periodic or quasi-periodic, a simple characteristic Strouhal number $S^0 = f_v^0 D/U$ is defined where f_v^0 is the shedding frequency when the cylinder is at rest. The shedding process may be random (broadband) over a portion of the Reynolds number range for which a statistical response analysis is required based on the spectral content. Also required is a measure of the correlation length along the cylinder. If the correlation lengths are long compared to the cylinder diameter, sectional analyses are valid, and the loads act in concert along the cylinder. If short correlation lengths are present, the structural

analysis must be three-dimensional, and the total load on the body is reduced. Evidently, the characterization of the vortex shedding process by a simple frequency is a practical simplification. Power spectral density analyses of unsteady cylinder loads reveals that in certain Reynolds number regimes the shedding process is periodic and can be characterized by a single frequency. At subcritical Reynolds numbers, the energy containing frequencies are confined to a narrow band, and the Strouhal number is about 0.2 for smooth cylinders. It must, however, be emphasized that only an average Strouhal number may be defined for Reynolds numbers larger than about 20,000. In the critical Reynolds number regime, a broad band power spectral density is usually observed. At higher Reynolds numbers, the Strouhal frequency rises to about 0.3 and the shedding process is quasi-periodic. The spectral content of the exciting forces is particularly important for bodies which may undergo in-line and/or transverse oscillations since the vortex shedding frequency locks onto the frequency of the transverse oscillations of the cylinder.

Various attempts have been made to devise a universal Strouhal number which would remain constant for differently shaped two- or three-dimensional body shapes (e.g., Simmons 1977). Unfortunately, these definitions suffer from the obvious drawback that their definition requires the solution of the wake formation problem first, or the measurement of one or more flow characteristics. Thus, their importance lies not so much in their ability to predict but rather to uncover the intricate relationship between, say, the flow velocity, vortex shedding frequency, wake width, base pressure, the streamwise distance from separation edges to the point of minimum base pressure, or the distance apart of the peaks of the r.m.s. value of the velocity across the wake, etc. It appears that isolating a small

number of simple scales to describe the wake development may not be possible.

As noted earlier, the Strouhal number appears to be a function of the Reynolds number. The fact that inviscid flow models such as the discrete vortex analysis predict the Strouhal number almost exactly in conformity with the experiments in the subcritical Reynolds number range is rather surprising.

The constancy of the Strouhal number over a broad range of Reynolds numbers does not imply that the base pressure remains constant and that a single vortex emanates from a separation line each time a vortex is shed. In reality, there is not only a phase shift between various sections of the vortex, separated by a correlation length, but also variations in both the intensity and the frequency of the vortex segments. The variation of the base pressure with Reynolds number in the range where the Strouhal number remains constant may be related to the variation of the correlation length with the Reynolds number. The net effect of the spanwise variations of the vortex tube is that the lift coefficient obtained from a pressure integration is not necessarily identical with that obtained from the direct total force measurements. Partial spanwise correlation leads to variations in both the frequency and the amplitude of the lift force, the variation of the latter being more pronounced than that of the former. The reasons for these variations and the lack of total spanwise correlation are not quite clear. The end effects, wall-boundary layers, freestream turbulence, non-uniformity of the velocity distribution are mentioned quite often as possible reasons. It is possible that the flow along the cylinder is just as unstable as it is cross to it. The instability of the shear layers to a band of frequencies and the amplification of the disturbances in

response to various frequencies along the cylinder could lead to a three dimensional flow. This, in turn, may give rise to a complicated interaction between the near wake and the mobile separation point on a circular cylinder. It would, however, be wrong to assume that the mobility of the separation points is primarily responsible for the imperfect spanwise coherence. Even bodies such as 90 degree wedges, square cylinders, etc., with fixed separation lines (assuming no reattachment) do not exhibit perfect correlation. To be sure, the variation of the base-pressure coefficient for bodies with mobile separation lines is greater than that for bodies with fixed separation points (Roshko 1970).

Suffice it to note that there is a lack of coherence in the data for the lift coefficient for a cylinder at rest because of the various reasons discussed above. The recognition of the flow instabilities and the three-dimensional nature of the base flow give a greater appreciation of the difficulties encountered in assessing the influence of the dynamic response of the body on the entire flow structure and in devising suitable models.

b. Damping Coefficient

It is a well-known fact that all systems dissipate energy through various mechanisms. The ability of the system to do so is called damping. Its rate depends on the internal friction of the material, the support conditions, and the surrounding medium. The effect of the internal or external fluid medium may be to increase the apparent mass, fluid friction, flow separation, fluid sloshing, or a combination thereof. From a practical point of view, it is simpler and often more desirable to determine the overall damping of a structure in the fluid medium in which it may be subjected to hydroelastic oscillations. This, however, may cause several mathematical and conceptual difficulties. Firstly, the part of

the damping which is attributed to the surrounding fluid is also part of the driving or resisting force, depending on the relative directions of the fluid force and the body velocity. Thus the inclusion in the damping term of a constant damping coefficient would be wrong since the fluid-induced damping is not and cannot be constant. On the other hand, the partition of the effect of the fluid motion partly as fluid damping and partly as driving or resisting force would make the matters worse or hopelessly complex. The inclusion of the entire effect of the fluid motion in the damping term would require the assumption of a highly nonlinear damping coefficient. This, in turn, would give rise to additional assumptions and perhaps to unexplainable conclusions. In spite of these arguments, it has often been assumed that the damping coefficient (and the natural frequency) may be determined by plucking excitation of the cylinder in the fluid medium. Oscillations created in this manner are of small amplitude and often free from vortex shedding, if not from flow separation. For A/D smaller than about unity, the effect of the fluid motion is to increase the linear friction force and the mass of the body by the added mass (not necessarily the displaced mass), (Sarpkaya 1976). On this basis, it is often assumed that frictional effects of the fluid motion may be included in the overall damping coefficient and the added mass effects may be accounted for by properly decreasing the natural frequency. When a body, for example a cylinder, is subjected to transverse oscillations in a steady flow, the fluid forces resulting from vortex shedding (essentially form drag) are taken as the effective driving fluid force. The apparent success of this procedure owes its success to the relatively small amplitude oscillations observed and partly to the difficulty of determining the total force.

The use of a similar procedure for the added mass causes even more difficult problems as will be discussed later. There is no reason in the laws of fluid dynamics that the added mass, or the drifted mass, should be the same for a body oscillating, at its natural frequency, in a fluid otherwise at rest with that oscillating in a fluid in motion. It is of course recognized that it is rather difficult to determine the material damping of a body in vacuum and the added mass as a function of time in a time-dependent flow.

c. Natural Frequency and Added Mass

Natural frequency is perhaps the most important parameter related to the dynamic response of a system since the synchronization takes place at or near to it. The determination of the natural frequency of a body in air (say by plucking excitation) is quite correct since the added mass due to the displaced mass of air is much smaller than the mass of the body. In water, however, the added mass may be quite large and the apparent natural frequency may be significantly lower. The justification for the use of a natural frequency measured by plucking excitation in a fluid otherwise at rest is necessarily based on the assumption that the added mass is approximately equal to its inviscid flow value (not the mass of the fluid displaced by the body!) regardless of mode shape, vibration amplitude, or presence of vortex shedding. Strictly speaking, what is added to the mass of the body is not the "mass of fluid displaced by the body" but rather the added mass obtained by classical potential flow methods for the particular direction of the motion of the body. For example, the displaced mass of a thin rectangular plate is practically zero. Its added mass may be equal to the added mass of the cylinder accepting the plate as its diameter or to zero depending on whether the

plate is oscillating normal or parallel to its surface. It is also important to note that the added-mass and the added-mass moment of inertia coefficient depend, in addition to the direction and type of motion, on the proximity of other bodies and the free surface.

The acceptance of the assumption that the added mass does not depend on the mode of vibration, vibration amplitude, or presence of vortex shedding may lead to unexplainable predictions. The added mass coefficient obtained by plucking excitation of a cylinder in a fluid otherwise at rest does not prove that it remains constant for all types of fluid motion. It rather proves that the added mass calculated from potential flow theory is essentially correct for the conditions approximating the potential flow.

Added mass is one of the least understood and most confused characteristic of time-dependent flows. Several facts need to be made clear. Firstly, added mass exists regardless of whether the fluid and/or the body are accelerating or not. It is a drift of mass resulting from the "elastica shaped" path of the fluid particles during the motion of the fluid about the body (Darwin 1953). This mass, like all masses, reveals its existence only when it is subjected to an acceleration. Thus, the inertial force required to accelerate the fluid about a body at rest is a sum of the force required to accelerate the added mass and the force acting on the displaced mass of the body due to the pressure gradient causing the fluid to accelerate. The inertial force required to accelerate a body in a fluid otherwise at rest is a sum of the force required to accelerate the mass of the body and the force to accelerate the added mass.

Secondly, added mass depends on the type of motion of the body or of the fluid about the body; proximity of other bodies, free-surface, etc.,

and time. It is not always possible, nor advisable, to determine the instantaneous value of the added mass. For example, for a periodic flow characterized by $u = U_{\text{III}} \sin 2\pi t/T$, the added mass coefficient cannot be properly defined at certain times.

Thirdly, the added mass coefficient (or its time averaged value over a suitable time interval) depends on the vortex shedding. For a cylinder undergoing harmonic oscillations with a relative amplitude of A/D nearly equal to unity in a fluid otherwise at rest, there is no vortex shedding and the added mass coefficient is equal to its classical value of unity. For larger values of A/D where there is vortex shedding, the added mass coefficient may even be negative (sarpkaya 1976). Consequently, it is wrong to equate the two flow situations where in one case the cylinder oscillates with amplitudes of A/D smaller than unity in a fluid otherwise at rest and the other case where the cylinder oscillates at similar amplitudes in a transverse direction in steady flow. The former does not involve vortex shedding whereas the latter is accompanied by complex separation and vortex-shedding phenomena even though the amplitude of oscillations is no greater. The empirical models arrived at by ignoring these well established facts require variable empirical constants to simulate the particular set of data and, as noted before, become at best an interpolation between various sets of data.

Suffice it to note that the modeling of the separated flow about an oscillating body requires first of all the elucidation of the correct physics and the separation of the fluid forces acting on the body from such quantities as the actual mass, material damping, and the spring constant of the body. The empirical models (i.e., van der Pol oscillator

model or its improved versions, wake-oscillator models based on a hidden flow variable and the integral-momentum equation, etc.) are highly conditioned by the available experimental data. Thus, their power of prediction is not only uncertain but also limited to the range of the experimental data used in their evolution. It is also unfortunate that the empirical models obscure the physics of the flow and make it impossible to establish a meaningful relationship between certain observed or measured features of the near wake (e.g., narrowing or widening of the wake, the increase or decrease of the wake establishment region, the increase or decrease of the strength of the shed vortices, etc.). As stated earlier, however, the oscillation of a body in a fluid in motion is a further complication added onto an already complex and relatively unstable flow situation. Thus, it does not appear that there will ever be an exact solution or a comprehensive model capable of predicting the observed characteristics of the phenomenon. After all, those who have concentrated on semi-empirical models may have been the wiser in recognizing the need to get to the designer before the understanding of the problem arrives.

II. EXPERIMENTAL EQUIPMENT AND PROCEDURES

The experiments were performed in two separate water tunnels. The first one was a recirculating water tunnel with a capacity of approximately 500 gallons. The galvanized test section, four inches wide, eight inches high and 16 inches long, was closed on top with a removable plexiglass plate to eliminate the free surface effects. A small space adjacent to the side walls was provided to allow the passage of thin leaf arms connecting the cylinder, in the test section, to the driving hardware above the test section. A low RPM, high capacity, 14-inch-diameter discharge centrifugal pump was used to circulate the fluid through the test section. The velocity of the fluid was regulated by a butterfly valve arrangement situated downstream of the test section. Velocities of 0.72 to 1.55 feet-per-second were obtained by adjusting the vanes of the butterfly valve.

The periodic motion was obtained by use of a small, variable speed, electric motor and flywheel and pivot assembly. The amplitude A of the vertical periodic motion was set by adjusting the radial position of the bearing attached to the flywheel. For these experiments the amplitudes ranged from 0.25 to 0.84 inches. The frequency of oscillation was regulated by adjustment of the variable speed motor. The system was designed and constructed to produce essentially sinusoidal oscillation, free of secondary oscillations.

The test specimens used were 0.7 inches and 1.0 inch in diameter and constructed from aluminum tubing. The cylinder was held in the test section by a yoke assembly connected to the pivot arm by a vertically constrained rod. The action of the pivot arm caused the cylinder to

oscillate vertically in the test section, transverse to the flow. The aluminum yoke assembly was instrumented with strain gages and accelerometers to monitor the forces and the acceleration felt by the cylinder.

The mean velocity of the fluid was determined by use of a pitot tube and a hot-film probe installed in the test section upstream of the test cylinder. The velocity was continuously monitored using one channel of a two channel recorder during the experiment.

The frequency and period of oscillation was determined by use of an accelerometer mounted on the yoke assembly. The signal was processed through a filter to remove high frequency, low amplitude, vibrations and was recorded on one channel of a two-channel recorder. The second channel of the recorder was used to record the forces acting on the cylinder. The instantaneous forces were sensed by four piezoelectric strain gages mounted on a cantilever-beam type arrangement, forming the top of the yoke assembly. The yoke was instrumented so as to measure both in-line and transverse forces. Figures 1 through 3 show the test section of the tunnel and the cylinder-yoke assembly.

System checkout and sensor calibration preceded the experimental runs. Several test runs were made to verify the proper operation of the test system, sensors, processing and recording equipment, and to establish the test run procedures to be used. It was verified that the mechanical system produced the required periodicity of oscillation for frequencies below about four cycles per second and amplitudes of about one inch. It was verified that the sensors and processing equipment had adequate sensitivity and phase reproduction to allow measurement of the required physical parameters.

The first set of experiments had as its objective, the measurement

of the mean fluid-induced force on the cylinder, in the direction of the stream flow, (in-line force) for various frequencies and amplitudes of cylinder oscillation transverse to the flow. It was verified by experiment that there was no in-line component of inertial force.

The physical recording of the in-line force was accomplished with a Honeywell recorder. Pitot differential pressure was recorded simultaneously to verify the magnitude and constancy of fluid velocity during the runs. Accelerometer output was recorded on the two channel recorder to provide data on oscillation period and phase angle.

Subsequently, the mean in-line force, the flow velocity, the oscillation period and amplitude, and the cylinder diameter were recorded from the charts. A mean drag coefficient \bar{C}_{di} was calculated from this data for correlation with the frequency parameter $D/\bar{V}T$ and the normalized amplitude A/D for the range of Reynolds numbers under consideration.

The second set of experiments had as an objective the measurement of the time-dependent forces in the direction of cylinder motion, i.e., transverse to the direction of flow. Since, in this case, there was an inertial force in the direction of interest, it was necessary to adjust the experimental procedure in order to identify the instantaneous value of the inertial force. Separation of the inertial force from the total force was required to evaluate the resistive force produced by the fluid alone.

The total force was recorded simultaneously with the acceleration. The water level in the tunnel was alternately raised and lowered for each run in order to allow the recording of the total "wet" force and the inertial "dry" force at a common amplitude and frequency of oscillation. The acceleration trace provided the reference for the time correlation of

the wet and dry force data. Because of the necessity to properly correlate wet and dry phase information, extreme care was taken in verifying the zeros for the acceleration and force recordings.

From force traces similar to Fig. 4, the transverse force was read and recorded from both the wet and dry run curves. Starting from the zero acceleration time (illustrated on Fig. 4) the wet and dry forces were recorded each 0.01 second, for at least three complete cycles. This data was then punched on IBM cards for evaluation.

The second test apparatus consisted of a recirculating water channel. The test section, 12 inches wide, 18 inches high and 36 inches long, was closed on top with a removable plexiglass plate to eliminate the free surface effects. Furthermore, two thin plexiglass plates (10 inches long, 8 inches high, and $1/16$ inches thick) were mounted on the walls of the test section, each at a distance of 0.8 inches away from the wall. The cylinder axis, at its mean position, was at the center of the plate. The test cylinder was placed between these two plates. The gap between the plate and the cylinder end was $1/32$ inches. The purpose of the two plates was to eliminate the effect of the wall boundary layers.

The drive system used in connection with the recirculating tunnel was transferred to the water channel and the test cylinder was connected to it by two thin leaf arms. The velocity of the fluid at the test section was regulated by adjusting the speed of the variable speed pump. Extensive velocity surveys with a hot-film anemometer were made to determine the velocity and turbulence distributions. The velocity was found to be uniform in both the vertical and horizontal directions within 2% of the mean velocity. The turbulence level was about 0.3% for a mean velocity of 1.5 feet per second.

As before, a beam-type accelerometer was mounted on the rigid arm connecting the two driving arms. The acceleration signal was electronically subtracted from the total force signal by means of a differencing unit. The mass of the accelerometer beam and the sensitivity of the signal amplifier were adjusted so as to obtain zero net signal when the cylinder assembly was oscillated in air at desired amplitudes and frequencies. The natural frequency of the accelerometer was about 80 times larger than the largest vortex shedding frequency. The accelerometer had a logarithmic damping coefficient of $\zeta = 0.008$. Thus, it has correctly detected the inertial force acting on the system without any amplification.

Dynamic calibration tests were made by attaching known masses to the cylinder and oscillating them at known fixed amplitudes and frequencies. It was found that the magnification factor of the force transducer-amplifier-recorder system was nearly unity, and the natural frequency of the entire oscillating system was 45 Hz in air and 40 Hz in water.

III. DATA ANALYSIS

The numerical calculations as well as measurements in time-dependent flow yield the resultant force as a function of time for a given set of numerical values of the independent parameters. Thus, it is not possible without a suitable hypothesis, to express the force both as a function of time and remaining independent parameters as one ordinarily would in a closed form solution. Such a working hypothesis is particularly necessary for the cable strumming problem since the results are to be incorporated into the dynamics of the cylinder motion in the form of a forcing function. It should be stated at the outset that there is, at present, no generally accepted hypothesis to decompose the time dependent force into suitable components.

Stokes, in a remarkable paper on the motion of pendulums, showed that the expression for the force on a sphere oscillating in an unlimited viscous fluid consists of two terms, one involving the acceleration of the sphere and the other the velocity. This analysis shows that the inertia coefficient is modified because of viscosity and is augmented over the theoretical value valid for irrotational flow. The drag coefficient associated with the velocity is modified because of acceleration, and its value is greater than it would be if the sphere were moving with constant velocity. In general, the force experienced by a bluff body at a given time depends on the entire history of its acceleration as well as the instantaneous velocity and acceleration. Thus, the drag coefficient in unsteady flow is not equal to that at the same instantaneous velocity in steady flow. Neither is the inertia coefficient equal to that found for unseparated potential flow. As yet, a theoretical solution of the problem for separated flow is difficult and

much of the desired information must be obtained both experimentally and numerically, for example, through the use of the discrete vortex model. In this respect, the experimental studies of Morison and his co-workers (1950) on the forces on piles due to the action of progressive waves have shed considerable light on the problem. The forces are divided into two parts, one due to the drag, as in the case of flow of constant velocity, and the other due to the acceleration of the fluid. The concept necessitates the introduction of a drag coefficient C_d and an inertia coefficient C_m in the expression for force. In particular if F is the force per unit length experienced by the cylinder, then

$$F = 0.5 C_d \rho D |U|U + C_m \pi \rho D^2 / 4 \cdot dU/dt \quad (1)$$

where U and dU/dt represent respectively the undisturbed velocity and the acceleration of the fluid.

On the basis of irrotational flow around the cylinder, C_m should be equal to 2 (cylinder at rest, the fluid accelerating; otherwise $C_m = C_a = 1$), and one may suppose that the value of C_d should be identical with that applicable to a constant velocity. However, numerous experiments show that this is not the case and that C_d and C_m show considerable variations from those just cited above. Even though no one has suggested a better alternative, the use of the Morison's equation gave rise to a great deal of discussion on what values of the two coefficients should be used. Furthermore, the importance of the viscosity effect has remained in doubt since the experimental evidence published over the said period has been quite inconclusive.

The most systematic evaluation of the Fourier-averaged drag and inertia coefficients has been made by Keulegan and Carpenter (1958)

through measurements on submerged horizontal cylinders and plates in the node of a standing wave, applying theoretically derived values of velocities and accelerations. Extensive measurements by Sarpkaya (1976) have shown that the drag, lift, and inertia coefficients depend on both the Reynolds number and the Keulegan-Carpenter number ($U_m T/D$) and that Morison's equation predicts remarkably well the measured force provided that the kinematics of the flow field is known accurately.

It is on the basis of the foregoing that the transverse force acting on a circular cylinder undergoing harmonic oscillations in the transverse direction to a uniform flow is expressed in terms of the Morison's equation as

$$C_L = \frac{F}{\frac{1}{2} \rho_f L D \bar{V}^2} = C_{m1} \pi^2 \left(\frac{U_m T}{D} \right) \left(\frac{D}{\bar{V} T} \right)^2 \sin \frac{2\pi}{T} t - C_{d1} \left(\frac{U_m T}{D} \right)^2 \left(\frac{D}{\bar{V} T} \right)^2 \left| \cos \frac{2\pi}{T} t \right| \cos \frac{2\pi}{T} t \quad (2)$$

where C_{m1} and C_{d1} are the inertia and drag coefficients, respectively. Evidently, the normalized force as well as the drag and inertia coefficients depend on the parameters $U_m T/D = 2\pi\Lambda/D$, and $D/\bar{V}T$. The first parameter is directly proportional to the relative amplitude, and the second parameter may be regarded as the frequency parameter $D/\bar{V}T$ or the reduced velocity $\bar{V}T/D$. Within the range of Reynolds numbers considered herein ($Re = U_m D/\nu$ from about 7,000 to 20,000), in accordance with the specifications of the sponsor, the drag and inertia coefficients are considered to be independent of the Reynolds number (Sarpkaya 1976).

For the purpose under consideration it is more advantageous to expand the $|\cos \omega t| \cos \omega t$ term in series and to retain only the first

term. This procedure yields,

$$C_L = C_{ml} \pi^2 \left(\frac{U_m T}{D}\right) \left(\frac{D}{V_T}\right)^2 \sin \omega t - \frac{8}{3\pi} C_{dl} \left(\frac{U_m T}{D}\right)^2 \left(\frac{D}{V_T}\right)^2 \cos \omega t \quad (3)$$

in which C_{dl} and C_{ml} are given by their Fourier-averages as,

$$C_{dl} = -(3/4) \int_0^{2\pi} (F \cos \theta) d\theta / (U_m^2 D) \quad (4)$$

$$C_{ml} = (2U_m T / \pi^3 D) \int_0^{2\pi} (F \sin \theta) d\theta / (U_m^2 D) \quad (5)$$

In the foregoing, the inertia and drag coefficients have been denoted as C_{ml} and C_{dl} in order to distinguish them from those corresponding to in-line oscillations. The subscript "l" carries the meaning of "lift" or force in the direction transverse to the stream. Furthermore, C_{ml} and C_{dl} were obtained by normalizing F with $0.5\rho D U_m^2$ in Eqs. (4) and (5). If the lift force is normalized by $0.5\rho D \bar{V}^2$ in determining the drag and inertia coefficients, then Eq. (2) reduces to

$$C_L = C_{mh} \sin 2\pi t/T - C_{dh} \cos 2\pi t/T \quad (6)$$

where C_{mh} and C_{dh} are related to C_{ml} and C_{dl} by

$$C_{dh} = C_{dl} [32\pi^2 A^2 / D^2] / [3\bar{V}^2 T^2 / D^2] \quad (7)$$

and

$$C_{mh} = C_{ml} [2\pi^3 A / D] / [\bar{V}^2 T^2 / D^2] \quad (8)$$

It should be noted in passing that C_{dh} and C_{mh} are identical to those used by Hartlen and Currie (1970).

The force acting on the cylinder in the in-line direction due to

the oscillations in the transverse direction is expressed in terms of a mean drag coefficient, denoted by \overline{C}_{di} , given as

$$\overline{C}_{di} = [\text{Force in the in-line direction}] / (0.5\rho D\overline{V}^2) \quad (9)$$

The experimental data are analyzed according to the Eqs. (4)-(9) through the use of appropriate computer programs.

The drag and inertia coefficients obtained as described above were obviously a consequence of the use of Eq. (3) and the method of Fourier averaging. It was, therefore, necessary to compare the predictions of Eq. (3) through the use of the calculated coefficients with those measured directly. Evidently, only such a comparison could show whether the decomposition of the instantaneous force into an in-phase and out-of-phase component is justifiable. The calculations performed along these lines have resulted in computer plots similar to those shown in Figs. 5 through 9. There are three curves on each plot: one marked by COSA is the normalized instantaneous velocity; one marked by CLTM is the normalized instantaneous transverse measured force; and finally, the one marked with CLTC is the normalized instantaneous force calculated through the use of Eq. (3). It is evident that the measured force is fairly well represented by Eq. (3) particularly for $\overline{V}T/D$ values near critical synchronization. Further away from synchronization additional vortex-shedding frequencies appear and require the consideration of higher harmonics in Eq. (3). Such an analysis has been carried out but will not be reported herein.

IV. DRAG AND INERTIA COEFFICIENTS

The results will be discussed in two parts. The first will be the average in-line force acting on the cylinder undergoing forced periodic oscillations in the transverse direction. The second will be the time-dependent lift force and its in-phase and out-of-phase components.

Evidently, the average in-line force is coupled with secondary oscillations due to vortex shedding. However, such oscillations are rather small in both steady and periodic flows and certainly not larger than about 7% of the average force. It is for this reason that only the average of the in-line force acting on the oscillating cylinder is presented herein.

Figures 10-12 show the variation of the normalized in-line force as a function of $D/\bar{V}T$ for representative values of Λ/D . Each figure represents the data obtained with two velocities, namely, $\bar{V} = 0.84$ and $\bar{V} = 1.3$ ft/sec. In normalized form, these velocities correspond to the Reynolds numbers $Re = \bar{V}D/\nu = 7,000$ and $Re = 10,833$. Figure 13 shows a carpet plot of the mean drag coefficient for four representative values of Λ/D .

Evidently, the in-line force increases with Λ/D since the cylinder, undergoing transverse oscillations, presents a larger apparent-projected area to the mean flow. This, however, is only part of the explanation. In addition, the vortex growth and motion are affected by the oscillation of the cylinder which in turn affect the in-line and transverse forces acting on the cylinder. This is evidenced by the fact that the in-line force for a given Λ/D increases at first, reaches a maximum, and then decreases as $D/\bar{V}T$ increases. A simple minded calculation based on the

steady flow drag coefficient for a stationary cylinder and the apparent projected area for the in-line force, which may be written as

$$\overline{C}_{di} = C_{ds} (1 + 2\Lambda/D) \quad (10)$$

yields values which are almost equal to the maximum values given in Fig. 13. It should be noted, however, that the phenomenon is far more complex and that such a simple minded procedure should not generally be used, even though the results are surprisingly good.

Figure 13 shows that the in-line force coefficient reaches its maximum at $D/\sqrt{V}T$ between 0.18 and 0.20. Ordinarily, the Strouhal number for a stationary cylinder would be 0.21 for the Reynolds numbers cited previously, and one would expect that the forces acting on the cylinder will undergo dramatic changes as the vortex shedding frequency given by the Strouhal number coincides with the frequency of the cylinder oscillations. The present results show that such a synchronization takes place at a frequency slightly lower than the Strouhal frequency. The occurrence of synchronization as well as the increase of the amplitude of oscillations in the force trace are shown most dramatically in Fig. 14. This figure was obtained by setting the free stream velocity at 0.84 ft/sec and the Λ/D ratio equal to 0.5. Then, beginning with the case of non-oscillating cylinder, the frequency of the oscillations was gradually increased up to about 4 Hz and the resulting in-line force was continuously recorded. The figure shows that the in-line force increases rapidly but with very little oscillations superimposed on it. As soon as the frequency of oscillations nears the Strouhal frequency, the amplitude as well as the frequency of the force oscillations increases. This fact is worth remembering in connection with the difficulty of obtaining the drag and

inertia coefficients at oscillation frequencies in the vicinity of the Strouhal frequency.

From an engineering viewpoint, the significance of the magnitude of the in-line force is that a cylinder or cable excited by the flow to oscillate in the transverse direction may be subjected to in-line forces several times larger than those assumed in its design. Furthermore, the deflections caused by the in-line force of sufficiently flexible cylinders tend to couple with transverse oscillations and not only affect the magnitude of the transverse oscillations but also the path of the cylinder motion.

The time-dependent transverse force is described, as noted earlier, in terms of a drag coefficient C_{dl} or C_{dh} and an inertia coefficient C_{ml} or C_{mh} [see Eqs. (3) and (6)] as a function of $V_r = \bar{V}T/D$. Figures 15 through 24 show C_{dl} and C_{ml} for representative values of Λ/D , ($\Lambda/D = 0.13, 0.25, 0.50, 0.75$, and 1.03).

It is seen from these figures that important variations occur in C_{dl} and C_{ml} particularly in the vicinity of the Strouhal frequency where the natural eddy-shedding is both enhanced and correlated by the oscillations. The inertia coefficient or the normalized in-phase component of the transverse force undergoes a rapid drop as the frequency of oscillations approaches the Strouhal frequency. In other words, synchronization or lock-in is manifested by a rapid decrease in inertial force and a rapid increase in the absolute value of the drag force. Thus, the lock-in is a phase transformer. Equally important is the fact that C_{ml} reaches a value of about 2 at a V_r value slightly under that corresponding to the perfect synchronization. It has been noted earlier that C_{ml} is equal to

unity for a cylinder oscillating in a quiescent fluid and is equal to 2.0 for a flow oscillating about a cylinder at rest. Thus, the data presented herein show that the net effect of the cylinder-flow interaction near synchronization is not unlike that of a periodic flow about a cylinder at rest. In other words, the fluid becomes the oscillator. The data also show that the use of an inertia or added-mass coefficient equal to unity, as determined by oscillating the cylinder in a fluid otherwise at rest, is not correct in modeling the vortex-induced oscillations. None of the existing flow-induced vibration models predict the inertia coefficient accurately as far as the present data are concerned.

The data for all values of Λ/D show that the peak value of C_{m1} decreases from about 2 to unity as Λ/D increases from 0.75 to 1.03. In other words, the wake gradually ceases to behave like an oscillator as Λ/D approaches unity. For very small values of V_r , well below the synchronization range, C_{m1} drops to unity, as would be expected on physical grounds. For values of V_r above that corresponding to the perfect synchronization, C_{m1} first drops sharply and then becomes negative. A similar phenomenon is observed in a harmonic flow about a cylinder at rest (Sarpkaya, 1976), (or when a cylinder is oscillated in a quiescent fluid) for $U_m T/D$ values from about 8 to 40, depending on the particular value of $D^2/\nu T$. This is a consequence of fractional vortex shedding as discussed by Sarpkaya (1976) and simply means that the total drift mass during the period of flow deceleration is larger than that during the period of acceleration.

The dramatic variation of C_{m1} in the vicinity of the synchronization

region shows that the fluid motion just before the perfect synchronization is significantly different from that just after the synchronization. For example, Griffin and Volaw (1972) have observed that "vibration frequencies above and below the natural frequency f_n respectively decrease and increase the longitudinal spacing from its value at the natural frequency" and that "both the vortex formation region and the longitudinal spacing are influenced in the same way by the frequency, resulting in an expansion and contraction of the wake at the lower and higher frequencies."

The drag coefficient C_{dl} or the normalized out-of-phase component of the total instantaneous transverse force given in Figs. 15 through 19 becomes negative for V_r values in the neighborhood of 5. Outside this range the drag is mostly positive, thus in the opposite direction to the motion of the cylinder. Within the range of V_r values cited above, the drag force is in phase with the direction of motion of the cylinder and helps to magnify the oscillations rather than damp them out. For this reason, the region in which C_{dl} is negative is sometimes referred to as the negative damping region. The fact of the matter is that this is not damping in the proper use of the word but rather an energy transfer from the fluid to the cylinder via the mechanism of synchronization. The values of V_r at which C_{dl} or C_{dh} changes its sign depend on Λ/D . The maximum absolute value of C_{dl} in the synchronization range decreases rapidly as Λ/D increases. Field studies have shown that synchronization does not occur for relative amplitudes larger than about unity. The trend of the present data is in conformity with such observations.

Finally, an unexpected and previously unknown observation in connection with the variation of C_{dl} will be described. For normalized velocities V_r in the neighborhood of 4, the data yield once again negative drag

coefficients for Λ/D smaller than about 0.5. The occurrence of this second region of synchronization at higher frequencies shows that there is not a single region of lock-in and that there are at least two and possibly more regions of frequency in which synchronization can occur. The narrowness of the regions in the second region of synchronization makes it rather difficult to observe the phenomenon. In fact, one may easily miss such a region by simply not taking smaller increments in frequency. It suffices to note that a cylinder may be excited first at frequencies near the Strouhal frequency and then at the multiples of the Strouhal frequency. However, the largest energy transfer from the fluid to the cylinder occurs in the first synchronization region near the Strouhal frequency.

The variations of C_{dh} and C_{mh} with V_r for representative values of Λ/D are shown in Figs. 25 through 34. Evidently, this particular set of data, obtained from C_{dl} and C_{ml} , carry the same information as C_{dl} and C_{ml} . A careful examination of the data shows that in the synchronization region C_{dh} increases at first gradually and then more rapidly with Λ/D , reaching a value of about -1.0. Subsequently, C_{dh} decreases rapidly with increasing Λ/D and becomes positive near $\Lambda/D = 1.0$. Similarly, C_{mh} increases with increasing Λ/D and reaches a maximum value of about 1.65 at $\Lambda/D = 0.8$. For larger values of Λ/D , C_{mh} decreases rapidly as Λ/D approaches unity.

The values of C_{dh} and C_{mh} corresponding to the V_r value at the point of perfect synchronization were entered into the computer and the equation of motion was solved, as described later, through the use of a fourth-order Runge-Kutta numerical procedure. This method has enabled the prediction of the dynamic response of cylinders at perfect synchronization.

V. ANALYSIS

The equation of motion for an elastically mounted, linearly damped, and periodically forced cylinder may be written as (see Fig. 35)

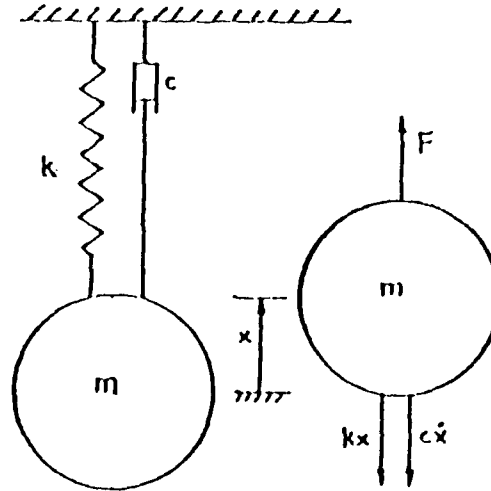


Fig. 35 Elastically mounted, linearly-damped cylinder

$$m\ddot{x} + c\dot{x} + kx = F = 0.5\rho_f D L \bar{V}^2 C_L \quad (11)$$

where m represents the mass of the cylinder, c the linear material damping, and k the spring constant. The derivatives of x are taken with respect to real time t , i.e., $d^2x/dt^2 = \ddot{x}$, etc.

Defining,

$$\begin{aligned} \omega_m &= \sqrt{k/m}, \quad \omega_n = 2\pi f_n, \quad \tau = \omega_n t, \quad x/D = x_r, \\ \zeta &= \frac{c}{2m\omega_n}, \quad \omega_o = f_s/f_n = S\bar{V}/f_n D, \quad x_r = \Lambda/D \\ \Omega &= f_c/f_n, \quad a = \frac{\rho_f L D^2 f_s^2}{2m\omega_n^2 S^2 \omega_o^2}, \quad \ddot{x}_r = \frac{\partial^2 x_r}{\partial \tau^2} \end{aligned} \quad (11a)$$

equation (11) may be reduced to

$$\ddot{x}_r + 2\zeta\dot{x}_r + x_r = \rho_r \Omega^2 [C_{ml} \sin \Omega \tau - (16/3\pi^2) x_r C_{dl} \cos \Omega \tau] \quad (12)$$

in which $\rho_r = \rho_f/\rho_s = 2\pi^3 a S^2$

Equation (12) may be solved exactly only for constant values of C_{ml} and C_{dl} . There is of course no difficulty in solving this equation either for assumed values of the force coefficients or for theoretically or experimentally obtained coefficients. The purpose of this report is to solve Eq. (12) through the use of the experimentally obtained force-transfer coefficients, particularly for perfect synchronization, and compare the results with those obtained experimentally by others under comparable conditions.

Equation (12) may also be written in terms of C_{mh} and C_{dh} as

$$\ddot{x}_r + 2\zeta\dot{x}_r + x_r = a\omega_0^2 (C_{mh} \sin \Omega \tau - C_{dh} \cos \Omega \tau) \quad (13)$$

from which one easily obtains the normalized relationship between the amplitude and phase as

$$a^2 \omega_0^4 (C_{mh}^2 + C_{dh}^2) = [(1 - \Omega^2)^2 + (2\zeta\Omega)^2] (\Lambda/D)^2 \quad (14)$$

Solving for Ω , one has

$$\Omega^2 = (1 - 2\zeta^2) - [(1 - 2\zeta^2)^2 + W - 1]^{1/2} \quad (15)$$

where W is given by

$$W = a^2 \omega_0^4 (C_{dh}^2 + C_{mh}^2) / (\Lambda/D)^2 \quad (16)$$

Equations (13) and (14) constitute a set of coupled differential equations. For a given value of ω_0 , C_{dh} and C_{mh} may be expressed in

terms of Λ/D through the use of the experimental data. Then the Eqs. (13) and (14) may be solved together for given values of 'a' and ζ . For this purpose Ω is solved from Eq. (15) for the previously calculated value of Λ/D and the corresponding values of C_{dh} and C_{mh} . Then, Eq. (13) is integrated through the use of a fourth order Runge-Kutta method for a half cycle and a new value of Λ/D is calculated. This value is then inserted into the Eq. (15) together with the corresponding new values of C_{dh} and C_{mh} and the entire procedure is repeated until a steady state is reached. The computer program which carries out the stated calculations is given in Appendix-A.

The purpose of the application of the above procedure to self-excited oscillations of cylinders was three fold: (a) to establish the validity of the force-transfer coefficients within the range of Reynolds numbers under consideration; (b) to investigate as to whether the steady-state response of the cylinder is determined primarily by the ratio $S_G = \zeta/a$ (see e.g., Skop, Griffin, & Ramberg, 1976) or by both ζ and 'a'; and finally, (c) to examine the stability of the differential equation when the cylinder reaches a steady-state. Evidently, if it can be demonstrated that the calculations predict accurately the steady-state amplitudes of self-excited oscillations obtained under entirely different circumstances, then one can conclude that the force-transfer coefficients presented herein should form the basis for comparison with those obtained from other numerical or heuristic models.

The foregoing may be accomplished only through the use of carefully conducted experiments for which the material damping ratio (obtained in vacuo), the mass ratio 'a', the critical frequency ω_0 , and the steady-

state amplitude are recorded. To the author's knowledge only Griffin and Koopmann (1977) were able to obtain such data which are tabulated below:

	Damping ratio ζ	Mass ratio a	Response parameter $S_G = \zeta/a$	Amplitude Λ/D
I	6.78×10^{-4}	8.62×10^{-3}	0.079	0.47
II	3.31×10^{-4}	2.43×10^{-3}	0.14	0.275
III	1.62×10^{-4}	5.17×10^{-4}	0.31	0.14

This data set formed the basis of comparative calculations reported herein. Before proceeding with the calculations, however, it was necessary to investigate the behaviour of the differential equation and the accuracy of the numerical procedure used. For this purpose, C_{d1} and C_{m1} were assumed to remain constant and the differential equation, [Eqs. (12) or (13)], was solved in closed form to yield

$$y_r = [\sin(-\alpha-\phi)/\sin\beta]e^{-\zeta\tau} \sin(\sqrt{1-\zeta^2}\tau + \beta) - \sin(\Omega\tau - \alpha - \phi) \quad (17)$$

in which $y_r = x/\Lambda$ and

$$\alpha = \arctan(16AC_{d1}/3\pi^2 DC_{m1}) \quad , \quad \phi = \arctan(2\zeta\Omega)/(1-\Omega^2)$$

and

$$\beta = \arctan[(\sqrt{1-\zeta^2})/[\zeta + \Omega \cot(-\alpha-\phi)]] \quad (18)$$

Then the accuracy of the numerical integration through the use of the fourth order Runge-Kutta method has been checked by comparing results with those obtained from the exact solution for various sets of identical input parameters. In all cases the solutions were perfectly identical in

both the transient and steady states. Sample plots of the evolution of the oscillations are shown in Figs. 36 through 38. Such calculations have also shown that a lowly damped system may result in an initial overshoot of the amplitude before it reaches a steady state provided that the force-transfer coefficients remain constant. A highly damped system, on the other hand, reaches its steady-state gradually from initial rest position. It should be kept in mind, however, that the purpose of these parametric calculations was not to investigate the role played by damping but rather to compare the predictions of the exact solution with those obtained with the numerical procedure. In a system in which the force-transfer coefficients vary with amplitude, such an overshoot may not take place.

Subsequent to the foregoing parametric studies, computations were carried out using the data obtained by Griffin and Koopmann (1977) and the experimentally determined values of C_{dh} and C_{mh} through the use of the numerical procedure described earlier. The envelopes of the transient and steady-state oscillations for the three cases under consideration are shown in Figs. 39 through 41. The predicted and measured relative amplitudes are tabulated below:

	<u>Predicted Λ/D</u>	<u>Measured Λ/D, [Griffin & Koopmann]</u>	<u>S_G</u>
S-I	0.43	0.47	0.079
S-II	0.235	0.275	0.14
S-III	0.11	0.14	0.31

Evidently, the measured and calculated relative amplitudes compare quite well. The relatively small differences may be attributed to the experimental errors in the determination of both Λ/D and the force-transfer coefficients,

to the difficulties encountered in the determination of the critical damping factor in vacuo, and to the variation in the mass ratio 'a'. Furthermore, it should be noted that the relative amplitudes reported by Griffin and Koopmann (1977) are the maximums and that the mean values of Λ/D at synchronization are somewhat lower and certainly closer to those predicted by the numerical analysis.

It appears, at least on the basis of the foregoing, that the force-transfer coefficients presented herein could be used with confidence in the range of Reynolds numbers from about 5,000 to 25,000 to predict the dynamic response of elastically mounted cylinders provided that the material damping and the mass ratio are given. Evidently, additional data are needed to test the power of prediction of the computer code developed in this investigation for all practically important values of S_G from about 0.01 to 5.0.

Next to consider was the investigation of the role played by S_G , known as the stability or response parameter. Among others, Griffin, Skop, and Ramberg (1975) have attempted to show that the value of Λ/D is uniquely determined by the value of a response or stability parameter S_G which is itself related to certain physical properties of the strumming structure, i.e., $S_G = \tau/a$. Vickery and Watkins (1962) were the first to arrive at such a conclusion on the basis of dimensional analysis and energy-balance considerations. Griffin, Skop, and Ramberg (1975) obtained a least squares fit to the existing data (see Fig. 42) and arrived at the following empirical formula:

$$2\Lambda/D = 1.29/(1 + 0.43 S_G)^{3.35} \quad (19)$$

It should be noted that the $2A/D$ values in Fig. 42 show large variations (as much as 100%) for a given value of S_G particularly for S_G values from about 0.2 to 1.0. It should also be noted that the response parameter used in Eq. (19) and in Fig. 42 was obtained by using the damping ratios which include both structural and fluid effects.

The equation of motion [Eq. (13)] shows that the response of the system is independently governed by ζ and 'a' and that the said equation cannot be expressed in terms of a single response parameter. One can, however, explore the reasons for the apparent correlation of the experimental data with S_G (determined as noted above) through the use of Eq. (14). For this purpose, let $\Omega = 1 - \epsilon$, (since Ω is often very close to unity). Inserting this value in Eq. (14), ignoring terms such as ϵ^3 , $\zeta\epsilon^2$, i.e., all third and higher order terms, and simplifying, one has

$$2A/D = \omega_0^2 C_L / [\epsilon^2/a^2 + S_G^2]^{1/2} \quad (20)$$

in which $C_L = [C_{mh}^2 + C_{dh}^2]^{1/2}$

Evidently, if it is assumed that C_L and ϵ/a remain nearly constant then and only then one can conclude that there is a unique relationship between $2A/D$ and S_G . In fact, the insertion of fairly reasonable values of C_L , ω_0 , and ϵ/a into the Eq. (20) suggest that $2A/D$ may be represented by

$$2A/D = 0.35/[0.12 + S_G^2]^{1/2} \quad (21)$$

However, there is no physical reason that the two constants in Eq. (21) should remain constant for all values of the parameters cited above.

In fact the large variations in $2A/D$ for a given value of S_G in Fig. 42 (particularly for S_G from about 0.2 to 2.0) suggest that the lack of

correlation rather than the experimental errors is responsible for the scatter. Thus, it was deemed necessary to investigate the effect of S_G on Λ/D by carrying out a parametric study. For this purpose, in one set of calculations ζ was kept constant and 'a' was varied. In another set of calculations, 'a' was kept constant and ζ was varied so as to arrive at the same S_G values. The following table gives the ζ and 'a' values used:

ζ	a	ζ/a	Λ/D (calculated)
6.8×10^{-4}	1.36×10^{-3}	0.5	0.23
"	6.8×10^{-4}	1	0.12
"	3.4×10^{-4}	2	0.054
4.3×10^{-3}	8.6×10^{-3}	0.5	0.26
8.6×10^{-3}	"	1	0.18
1.7×10^{-2}	"	2	0.11 (unstable)

As conjectured above, identical S_G values did not result in identical Λ/D ratios. However, surprisingly enough, the Λ/D values for the two sets of parameters did not significantly differ. Even though, additional calculations are definitely necessary to reach firmer conclusions, one can tentatively state that the governing equation is not very sensitive to the individual variations of the damping and mass ratios provided that S_G remains constant. This particular behavior of the differential equation plus the use of combined fluid and material damping may be primarily responsible for the observed correlation.

It is noted from the above table that one set of calculations became unstable even though the damping ratio was fairly large and an

error limit of 10^{-8} was used in the Runge-Kutta integration scheme, (see Fig. 43). It is not clear whether the observed instability is a consequence of the numerical integration, or of the inherent instability of the differential equation for certain sets of the governing parameters, or of the actual behavior of the corresponding dynamic system. It will be most desirable to perform calculations with a set of damping and mass ratios for a system which has exhibited such unstable oscillations near synchronization.

VI. CONCLUSIONS

The results presented herein warrant the following conclusions:

- a. The in-line force acting on a cylinder undergoing harmonic oscillations in the transverse direction increases with Λ/D . The force coefficient reaches its maximum at $D/\bar{V}T$ between 0.18 and 0.20;
- b. The Fourier-averaged transverse force coefficients exhibit significant variations in the vicinity of the Strouhal frequency. The inertia coefficient is larger than unity for oscillation frequencies larger than the Strouhal frequency and may be negative for oscillation frequencies lower than the Strouhal frequency;
- c. The variation of the inertia coefficient with $\bar{V}T/D$ and Λ/D is not in conformity with the predictions of the oscillator models;
- d. The use of the experimentally obtained drag and inertia coefficients for the transverse force together with a numerical integration procedure accurately predicts the dynamic response of a self-excited cylinder in the synchronization region;
- e. A parametric study of the separate and combined effects of material damping ratio, mass ratio, and response parameter show that the maximum response of the cylinder is primarily governed by the response parameter. Additional data and calculations are needed to explore the effect of these parameters further;
- f. It appears, on the basis of somewhat limited observations, that the governing equation may become unstable for certain combination of the damping and mass ratios.

VII. REFERENCES

- Blevins, R. D., (1977), Flow-Induced Vibration, Van Nostrand Reinhold Co., New York.
- Darwin, C. G., (1953), "Virtual Mass and Drift", Proc. Camb. Phil. Soc., Vol. 49, pp. 342-354.
- Griffin, O. M. and Koopmann, G. H., (1977), "The Vortex-Excited Lift and Resistance Forces on Resonantly Vibrating Cylinders", (to be published).
- Griffin, O. M., Skop, R. A., and Ramberg, S. E., (1975), "The Resonant, Vortex-Excited Vibrations of Structures and Cable Systems", Offshore Technology Conference Paper OTC 2319, Houston, TX.
- Griffin, O. M. and Votaw, C. W., (1972), "The Vortex Street in the Wake of a Vibrating Cylinder", J. Fluid Mech., Vol. 55, pp. 31-48.
- Hartlen, R. T. and Currie, I. G., (1970), "Lift-Oscillator Model of Vortex-Induced Vibration", Proc. ASCE, EMS, pp. 577-591.
- Keulegan, G. H. and Carpenter, L. H., (1958), "Forces on Cylinders and Plates in an Oscillating Fluid", Journal of Research, NBS, Vol. 60, pp. 423-440.
- Morison, J. R., et al., (1950), "The Force Exerted by Surface Waves on Piles", Petroleum Trans., Vol. 189, pp. 149-157.
- Roshko, A., (1954), "On the Drag and Shedding Frequency of Two-Dimensional Bluff Bodies", NACA TN 3169.
- Sarpkaya, T., (1976), "Vortex Shedding and Resistance in Harmonic Flow About Smooth and Rough Cylinders at High Reynolds Numbers", Naval Postgraduate School, Technical Report No.-NPS-59SL76021, Monterey, Calif.
- Simmons, J. E. L., (1977), "Similarities Between Two-Dimensional and Axisymmetric Vortex Wakes", The Aeronautical Quarterly, Vol. XXVIII, pp. 15-20.
- Skop, R. A., Griffin, O. M., and Ramberg, S. E., (1976), "Seacon-II Strumming Predictions", NRL Memorandum Report 3383.
- Vickery, B. J. and Watkins, R. D., (1962), "Flow-Induced Vibration of Cylindrical Structures", Proc. of the First Australian Conference, Held at the University of Western Australia.

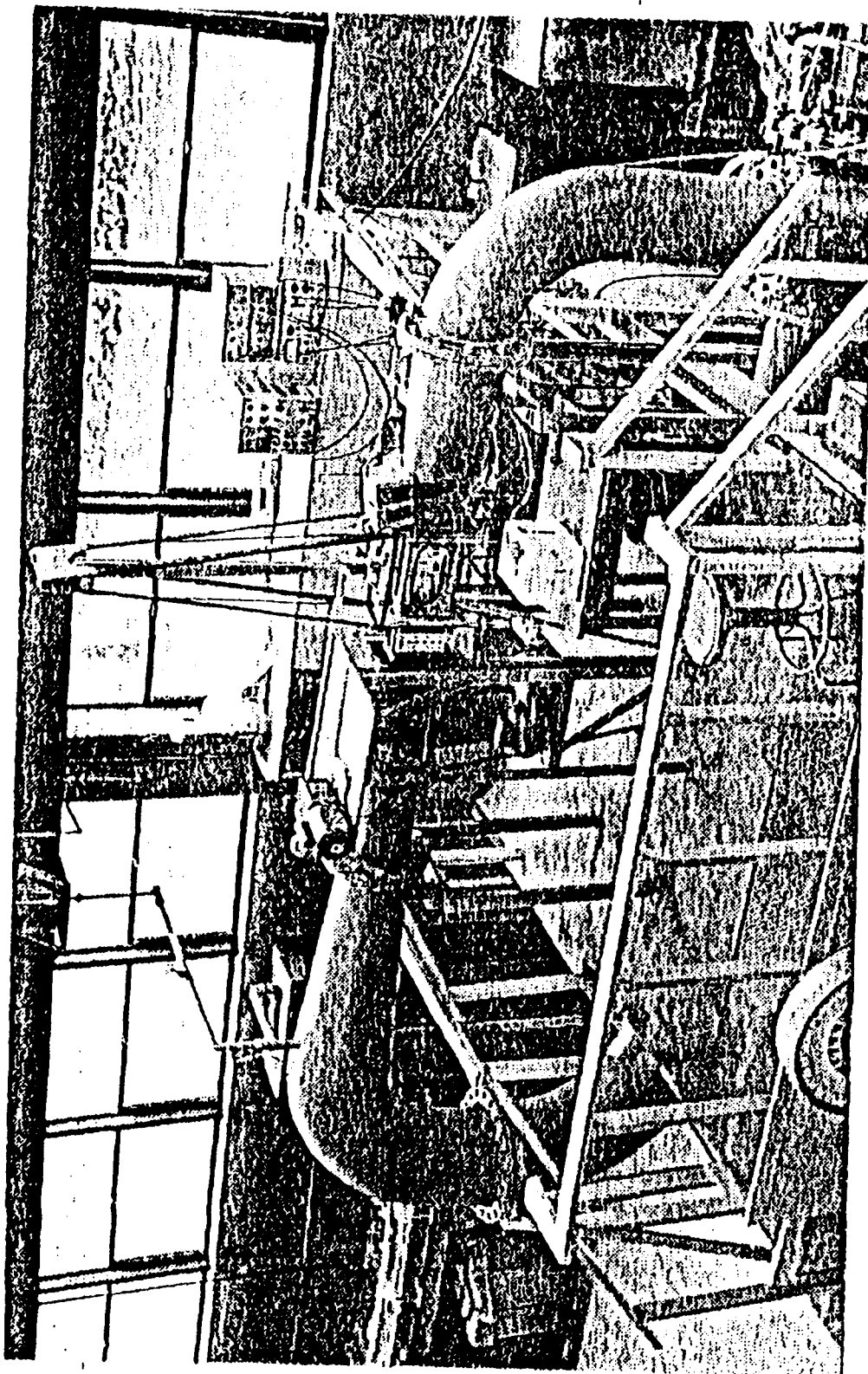


Figure 1. NPS water tunnel.

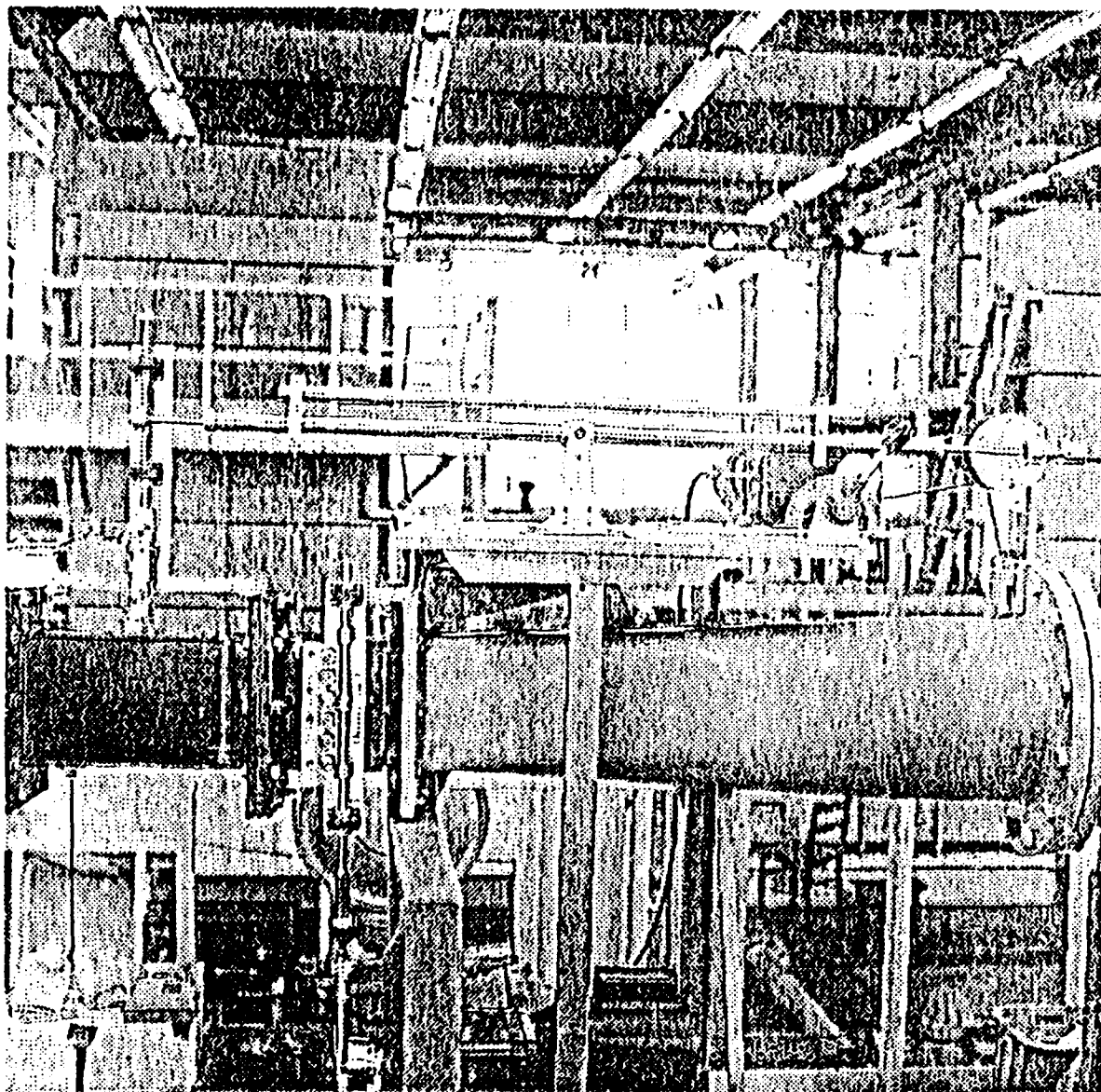


Fig. 2 Motor, Flywheel and Pivot Assembly

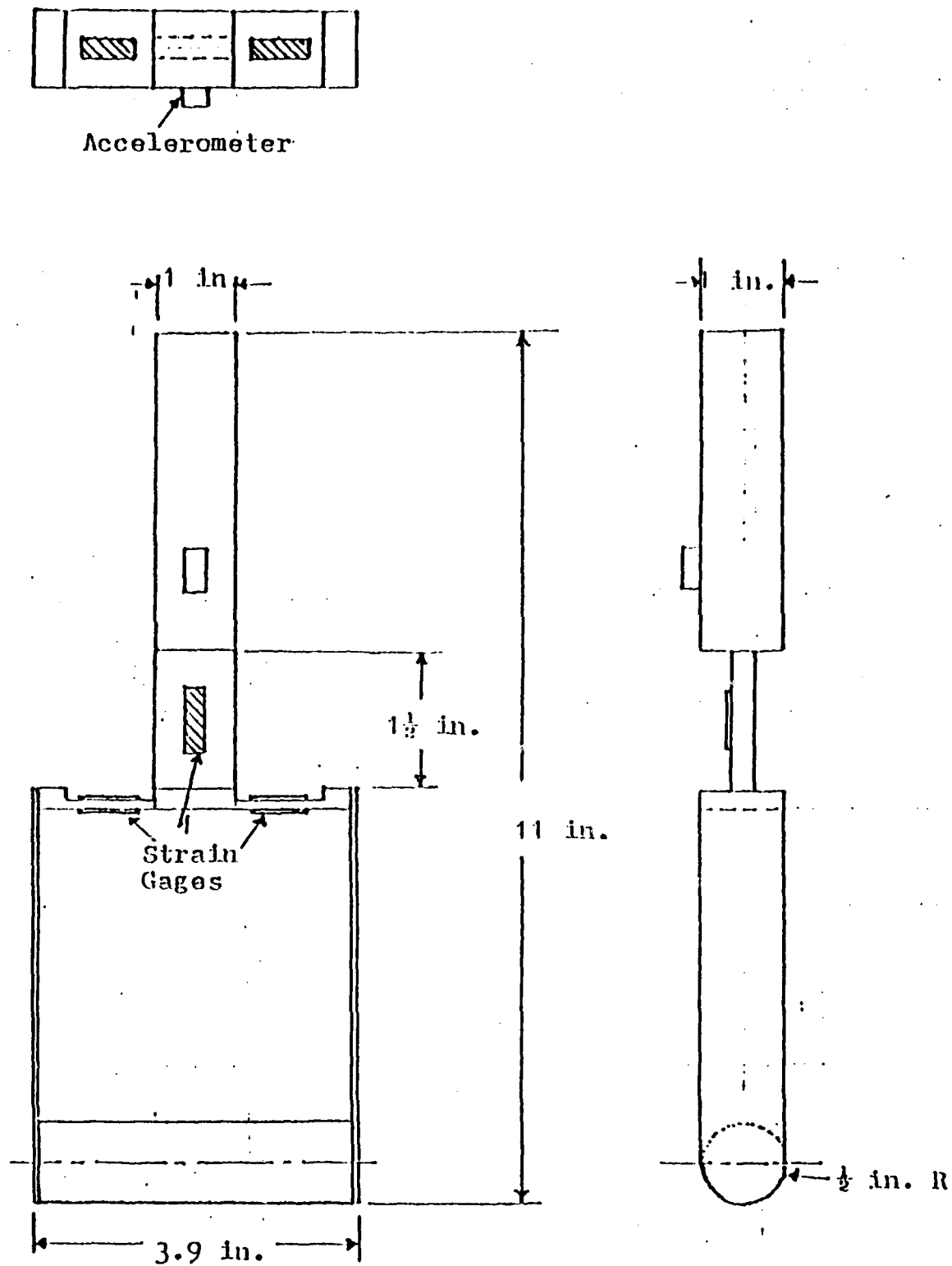


Fig. 3 Aluminum Yoke—Force Transducer

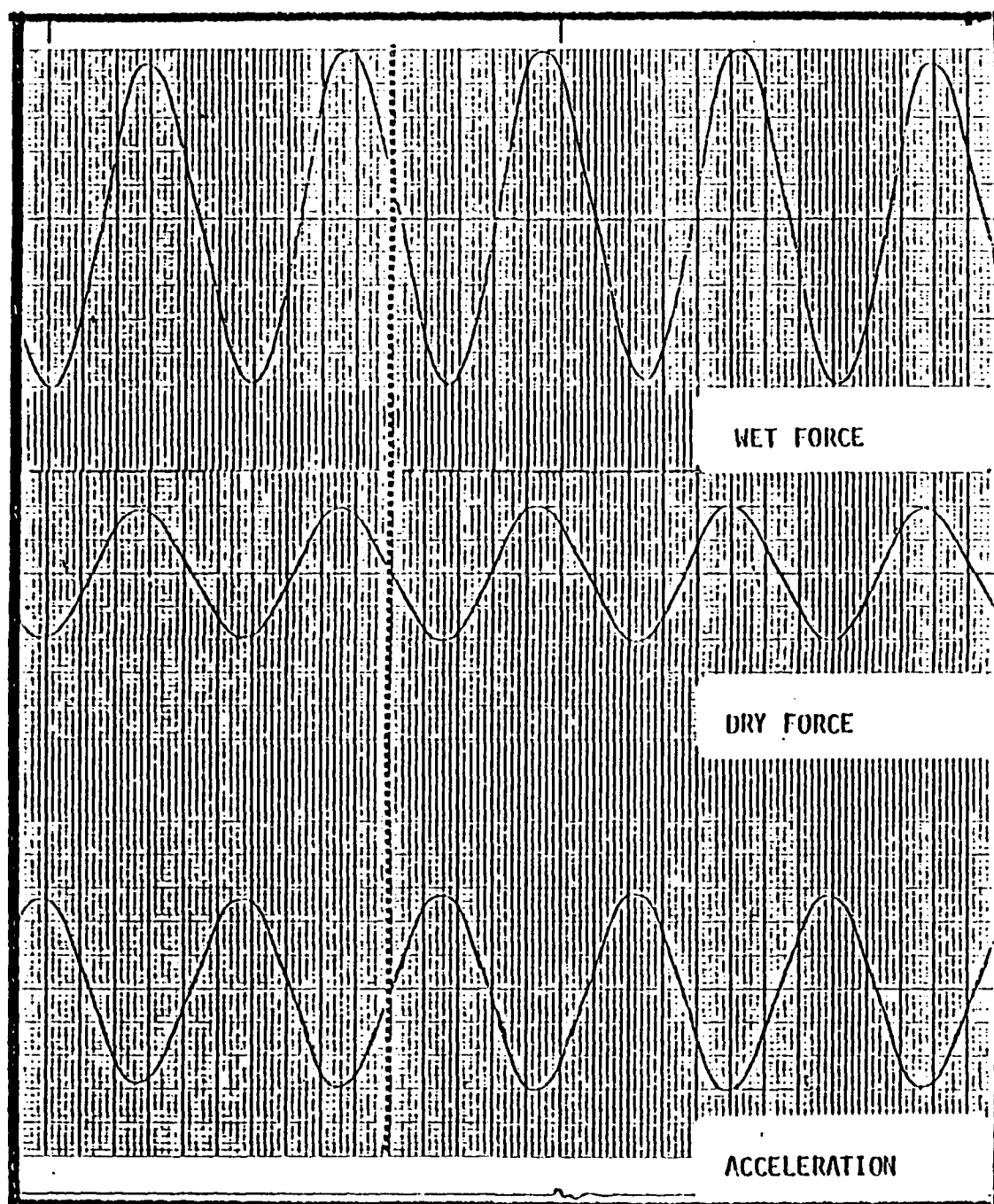


Fig. 4 Force and Acceleration Traces

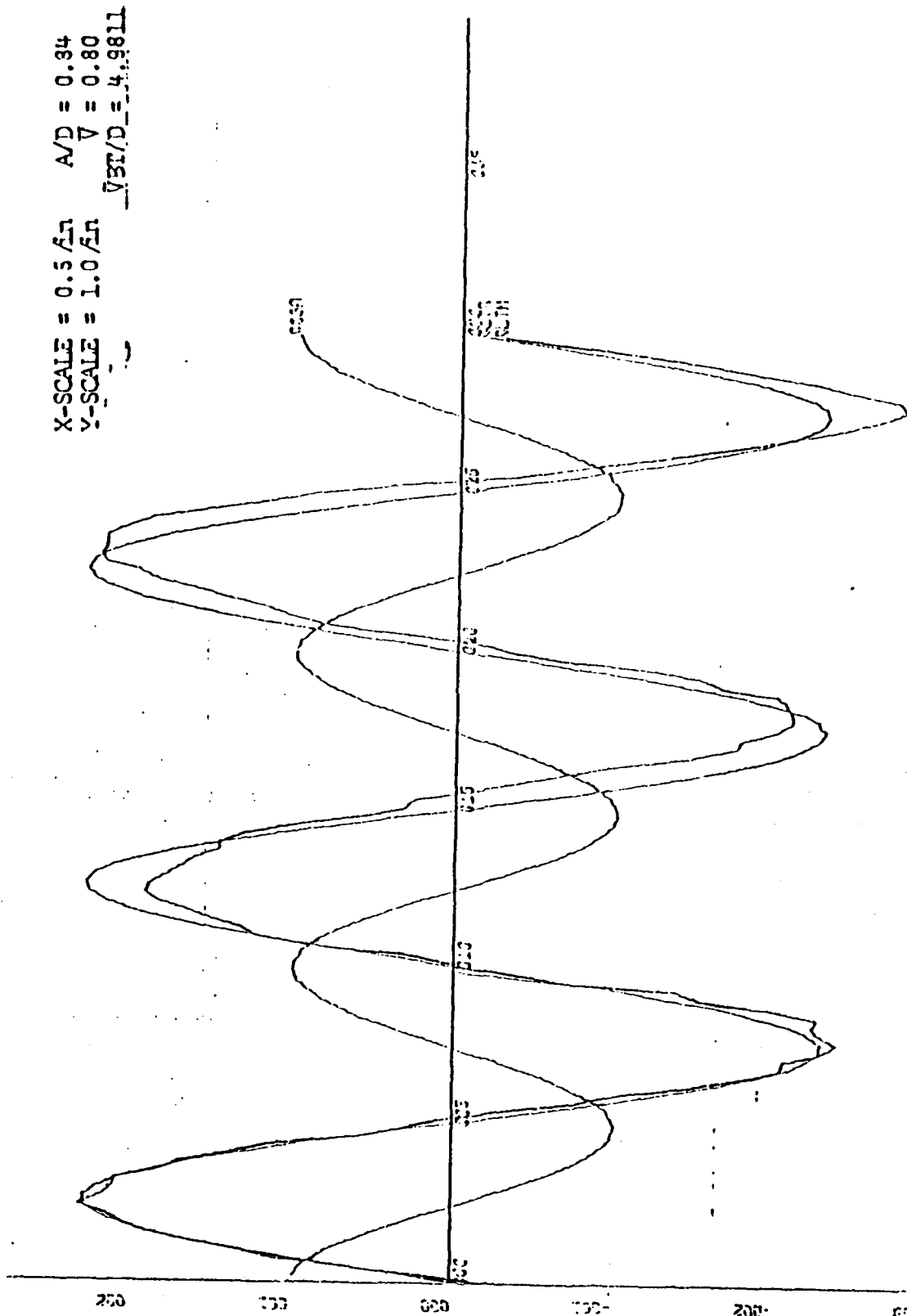


Figure 5. Comparison of calculated and measured lift forces, $A/D = 0.34$, $\bar{V}T/D = 4.9811$.

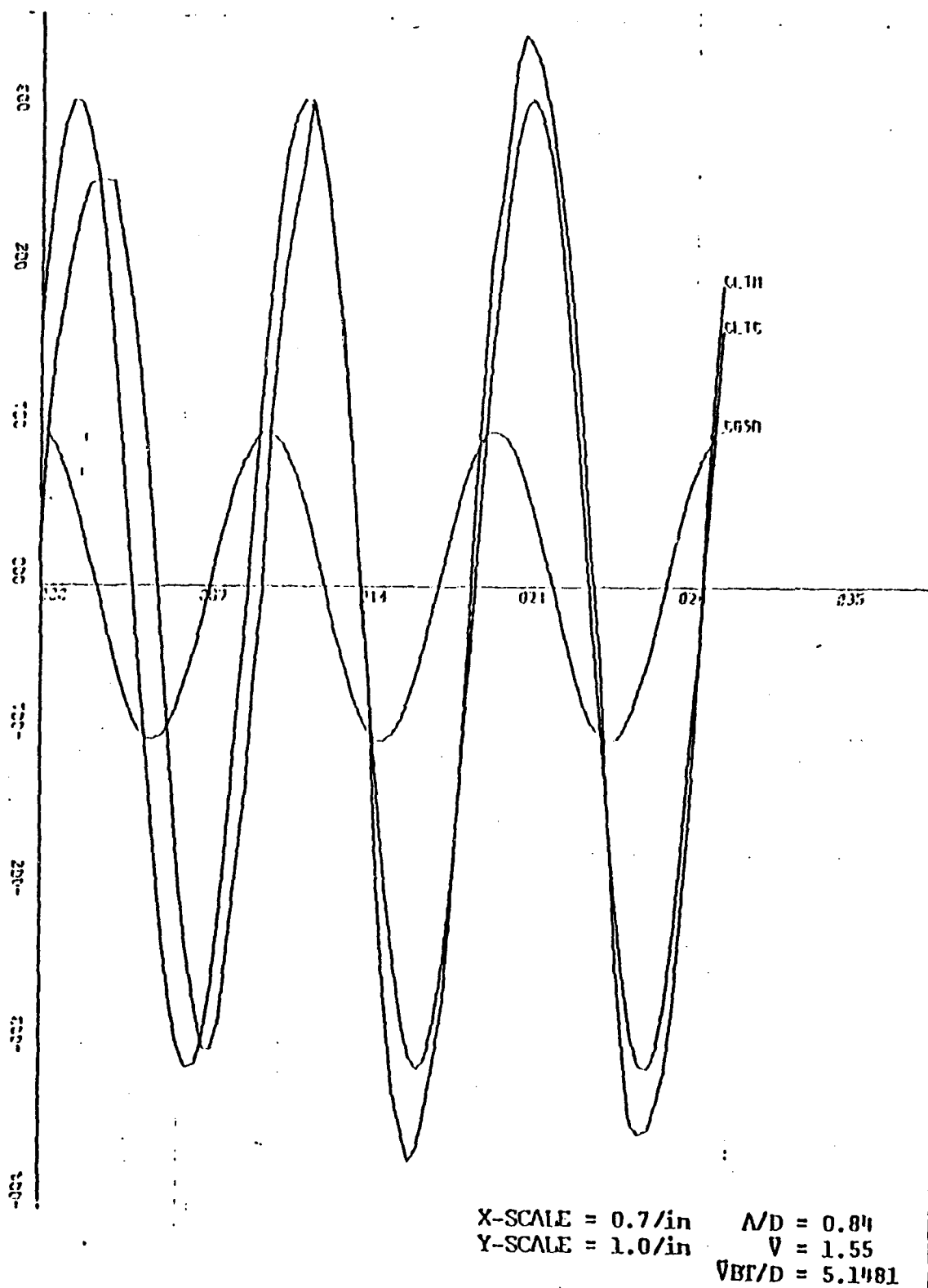


Figure 6. Comparison of calculated and measured lift forces,
 $\Lambda/D = 0.84$, $\sqrt{VT}/D = 5.1481$.

$X\text{-SCALE} = 0.5/\text{in}$ $A/D = 0.84$
 $Y\text{-SCALE} = 1.0/\text{in}$ $V = 0.80$
 $\bar{V}T/D = 5.4888$

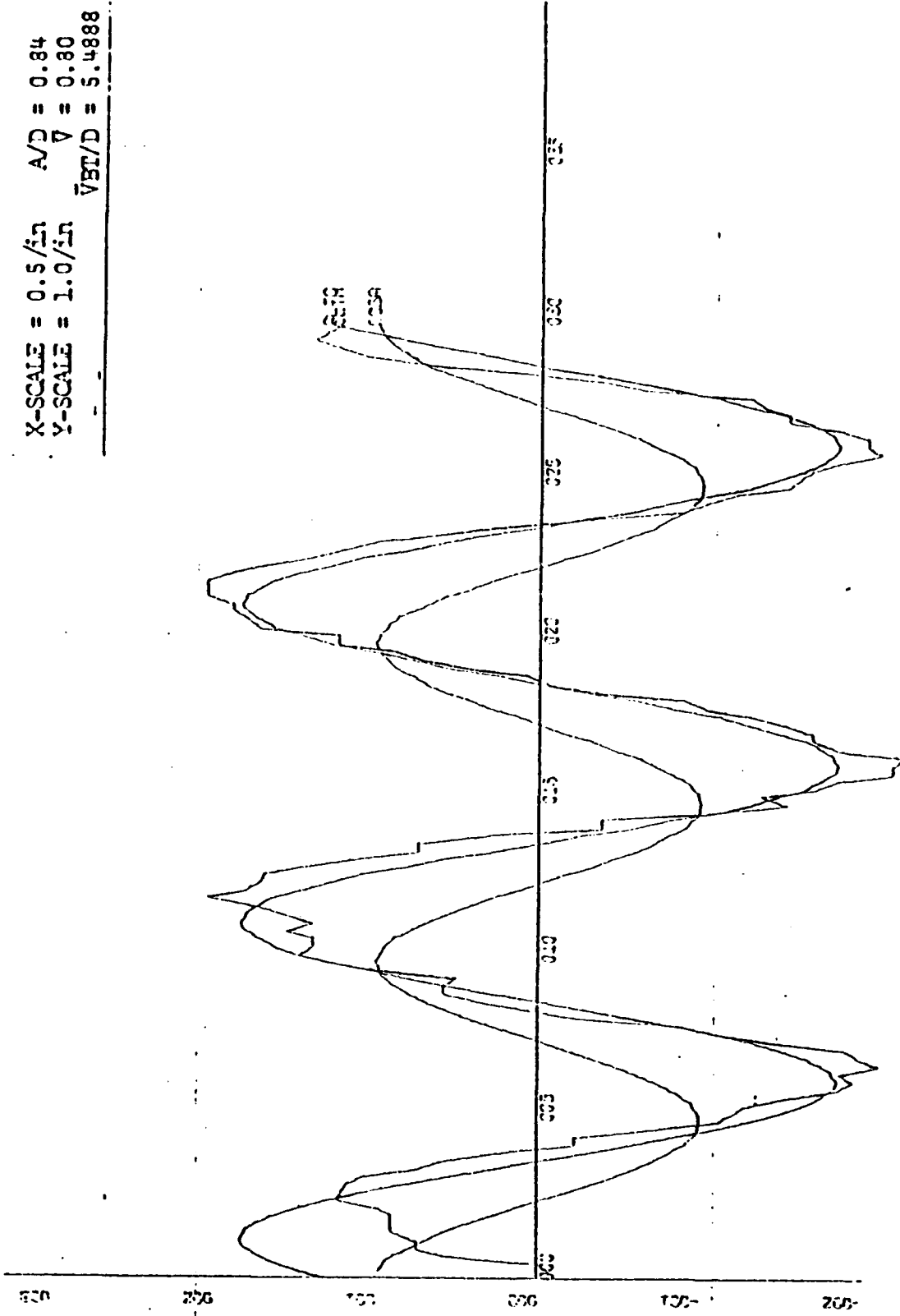


Figure 7. Comparison of calculated and measured lift forces, $A/D = 0.84$, $\bar{V}T/D = 5.4888$.

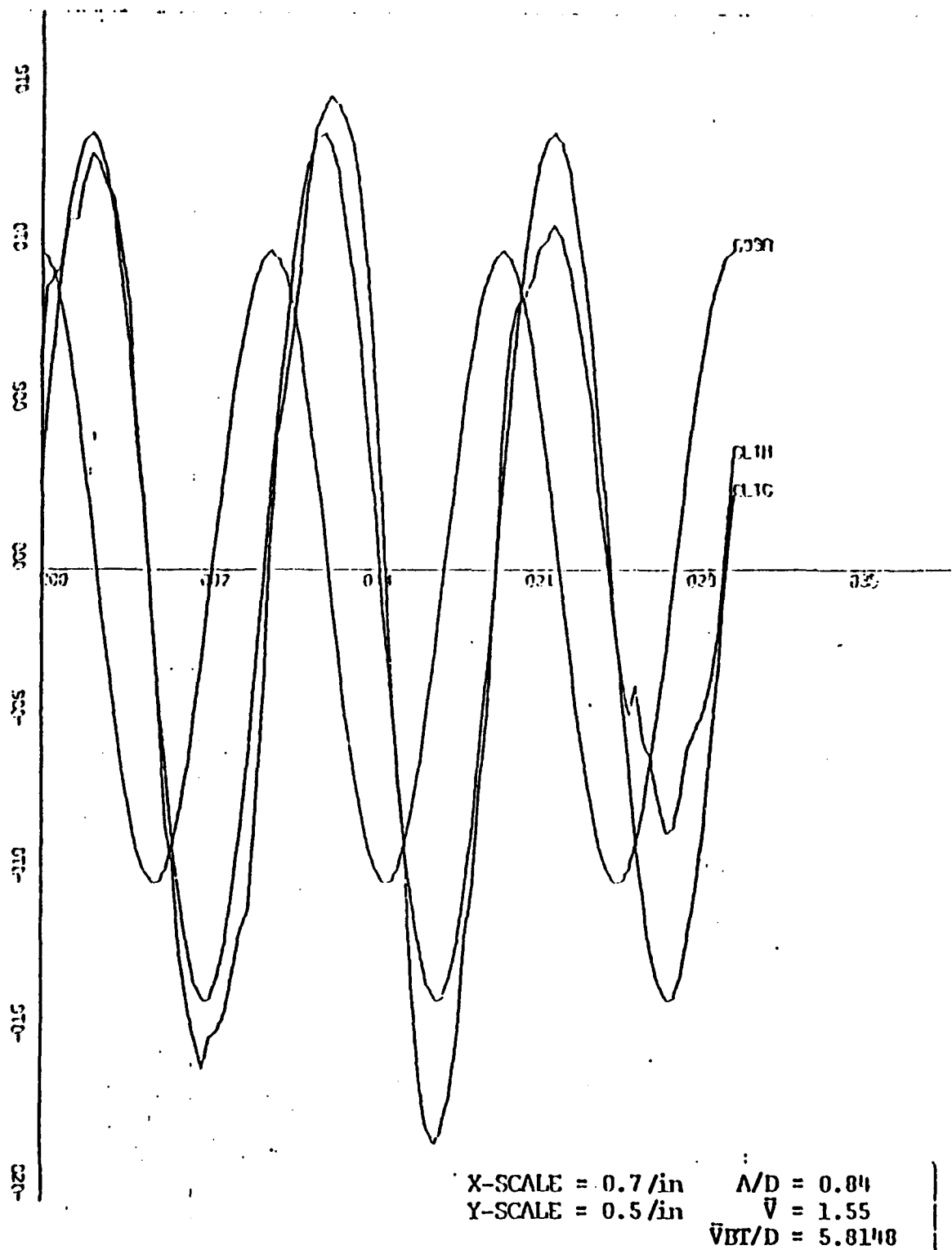


Figure 8. Comparison of calculated and measured lift forces,
 $\Lambda/D = 0.84$, $\bar{V}T/D = 5.8148$.

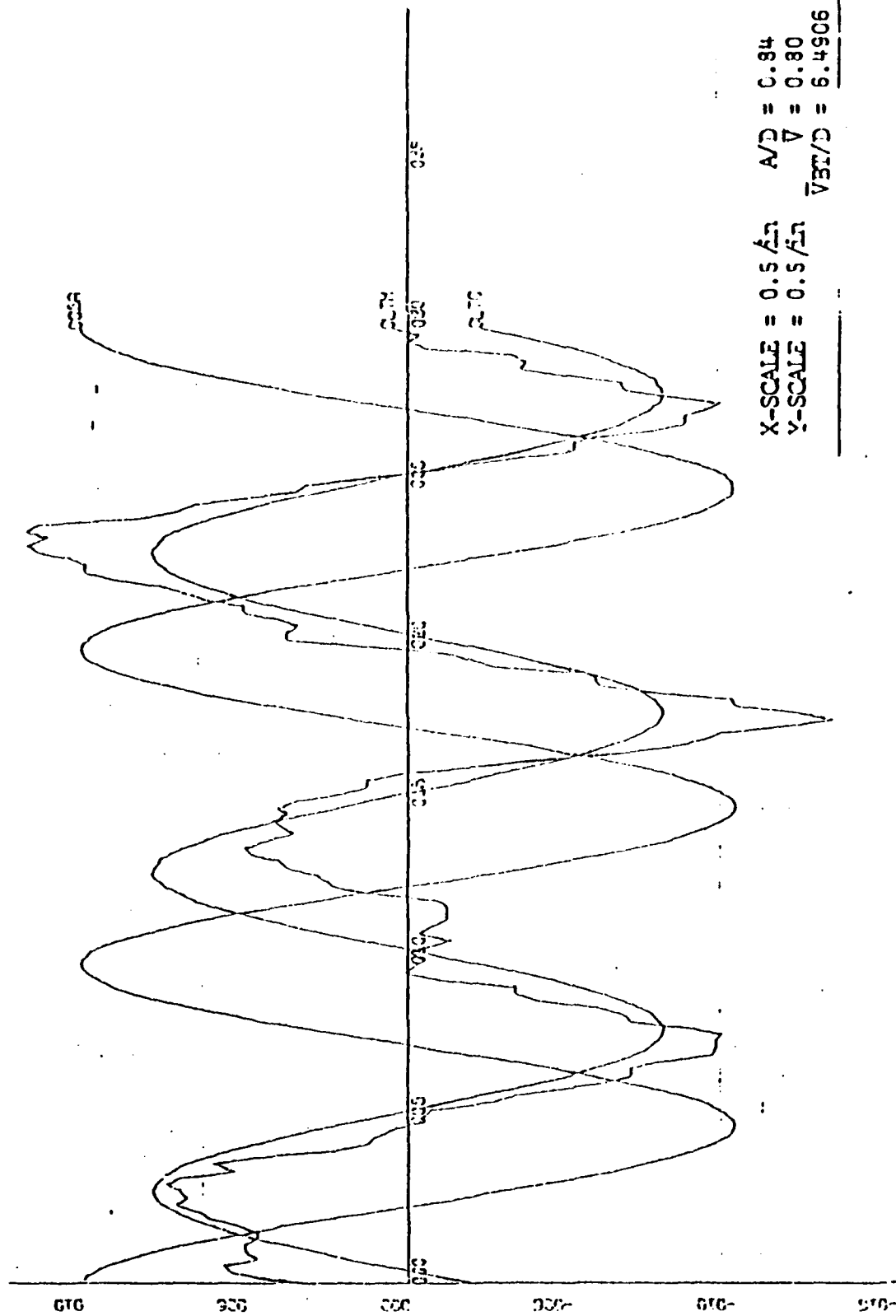


Figure 9. Comparison of calculated and measured lift forces, $A/D = 0.84$, $\bar{V}T/D = 6.4906$.

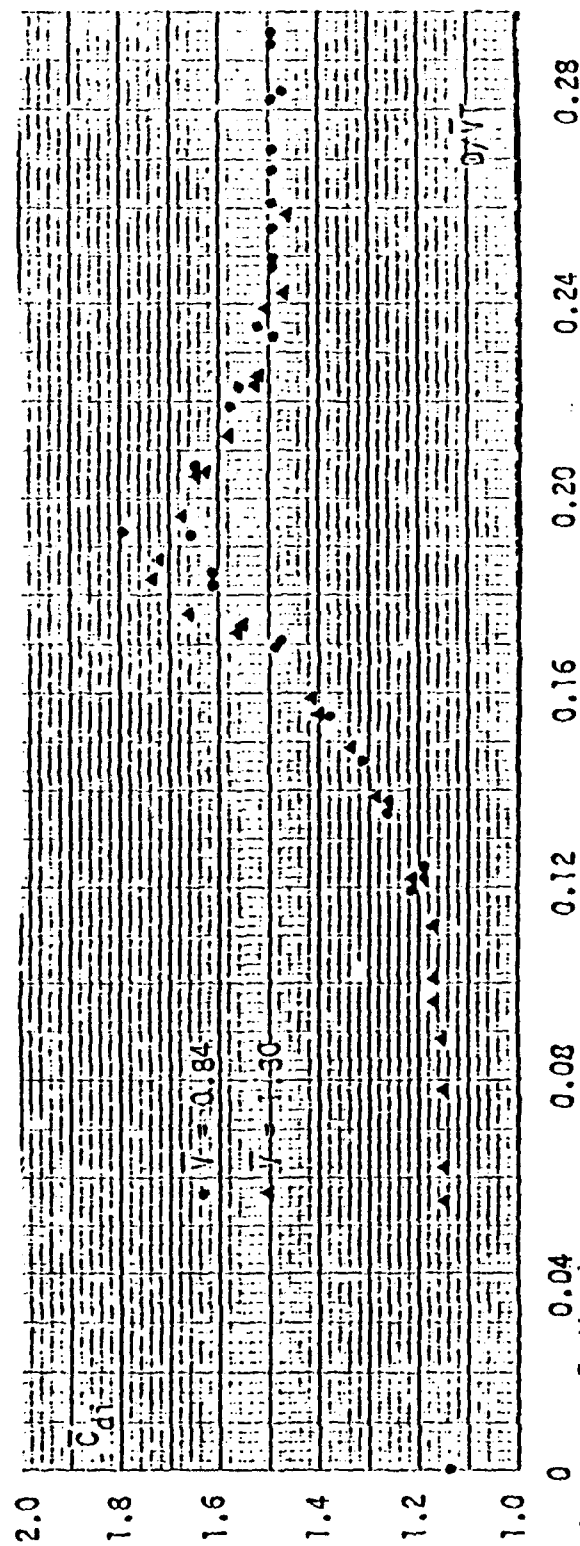


Fig. 10.- Mean in-line drag coefficient versus D/\sqrt{V} for $A/D = 0.25$

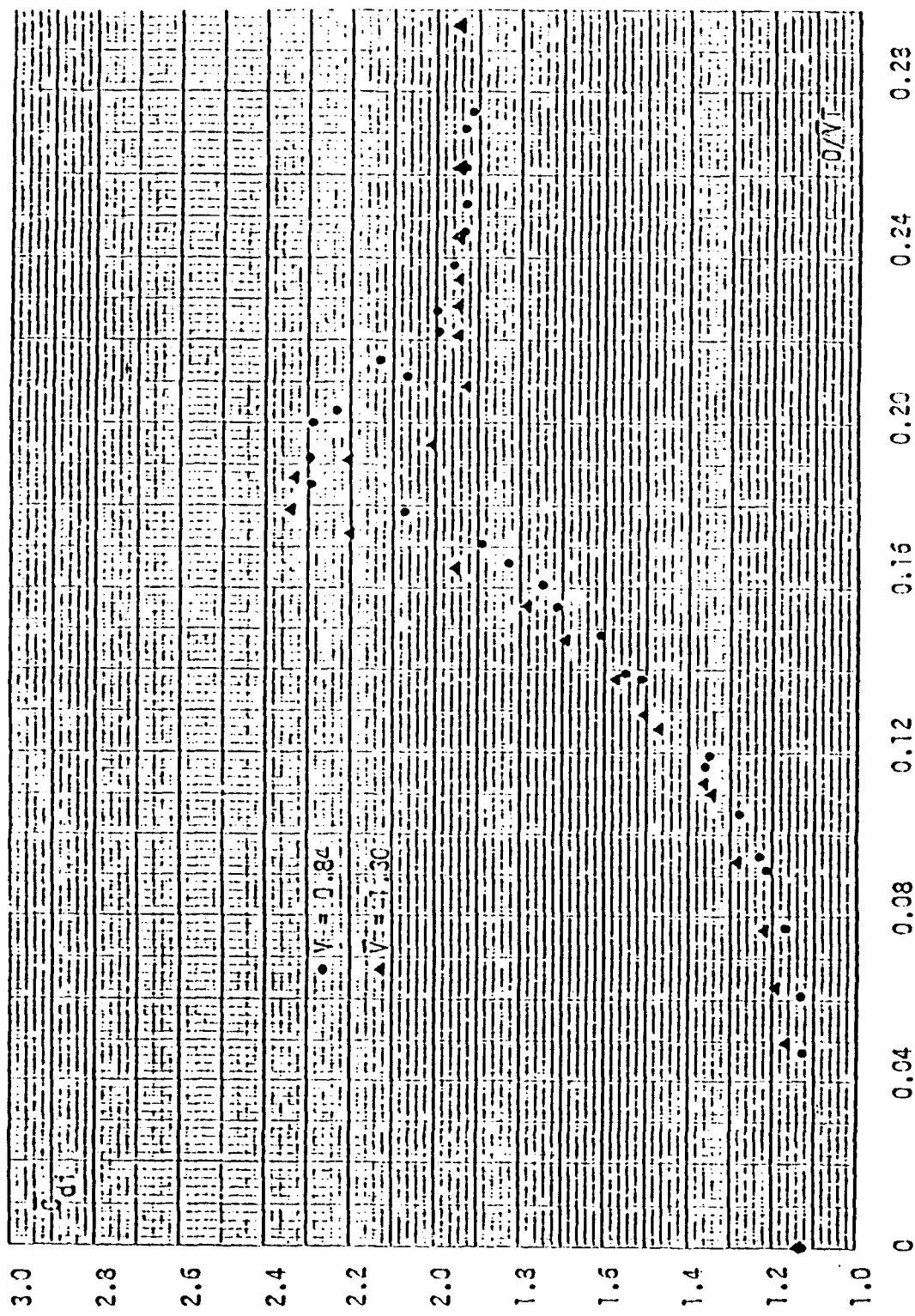


Fig. 11. Mean in-line drag coefficient versus U/UT for $A/D = 0.50$

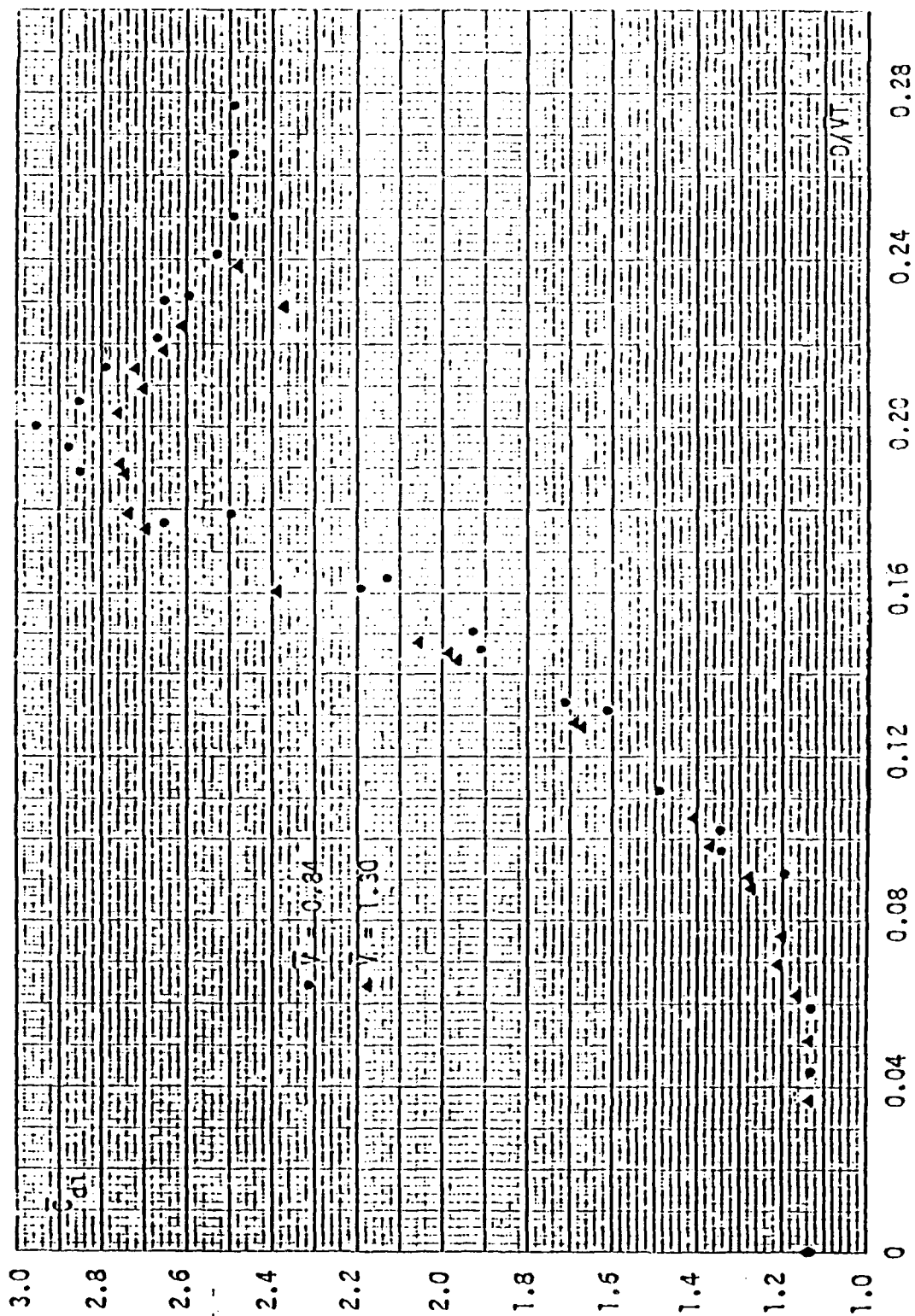


Fig. 12 Mean in-line drag coefficient versus U/\sqrt{T} for $A/D = 0.75$

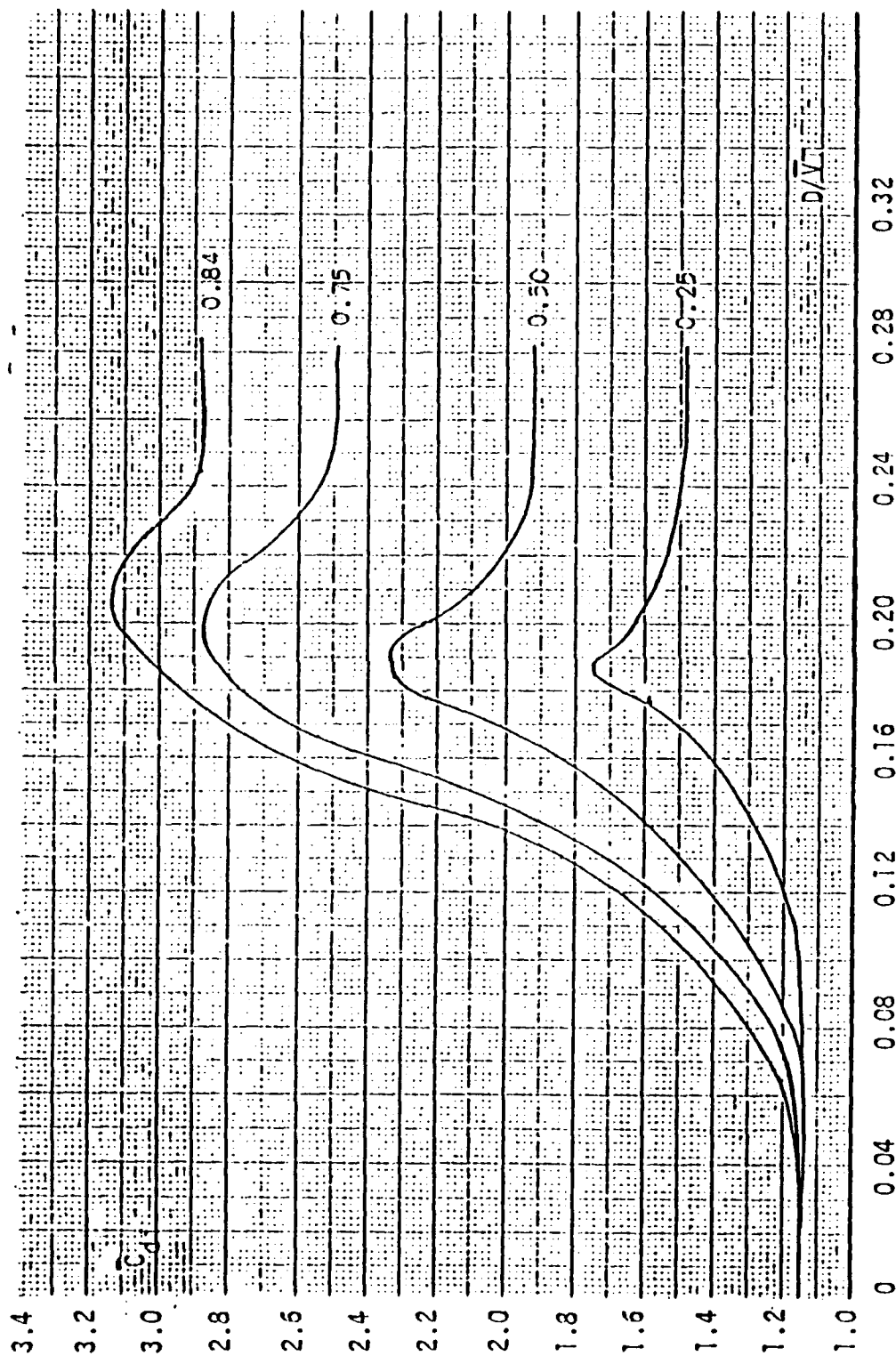


Fig. 13 Comparison curves: Mean in-line drag coefficient versus D/\sqrt{T} for $A/D = 0.25, 0.50, 0.75$, and 0.84 .

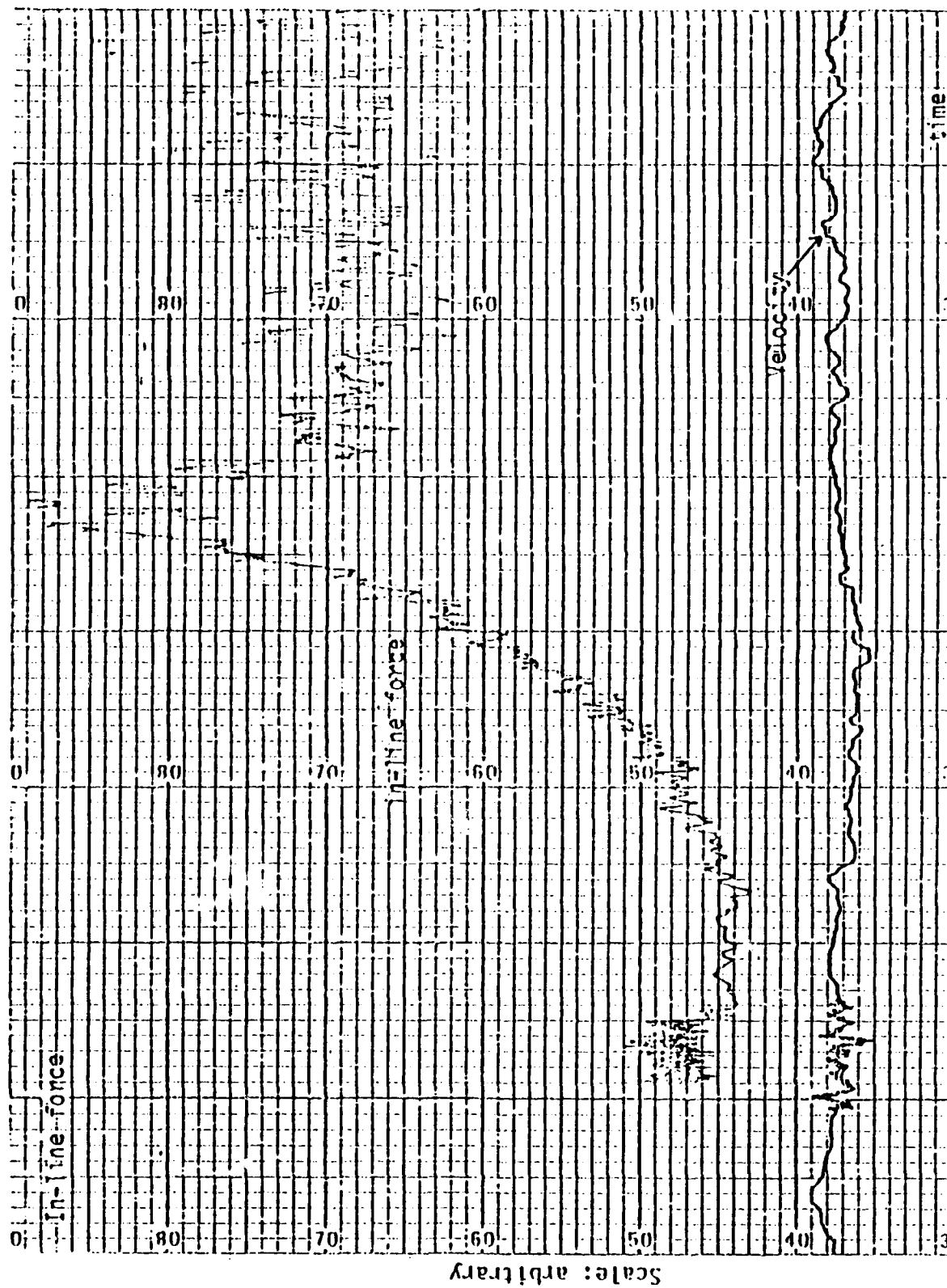


Fig. 14. Phenomenological Demonstration: in-line force versus time while increasing oscillation frequency, ($\Lambda/D = 0.50$, $V = 0.84$, $D/\sqrt{\tau} = 0$ to 0.31).

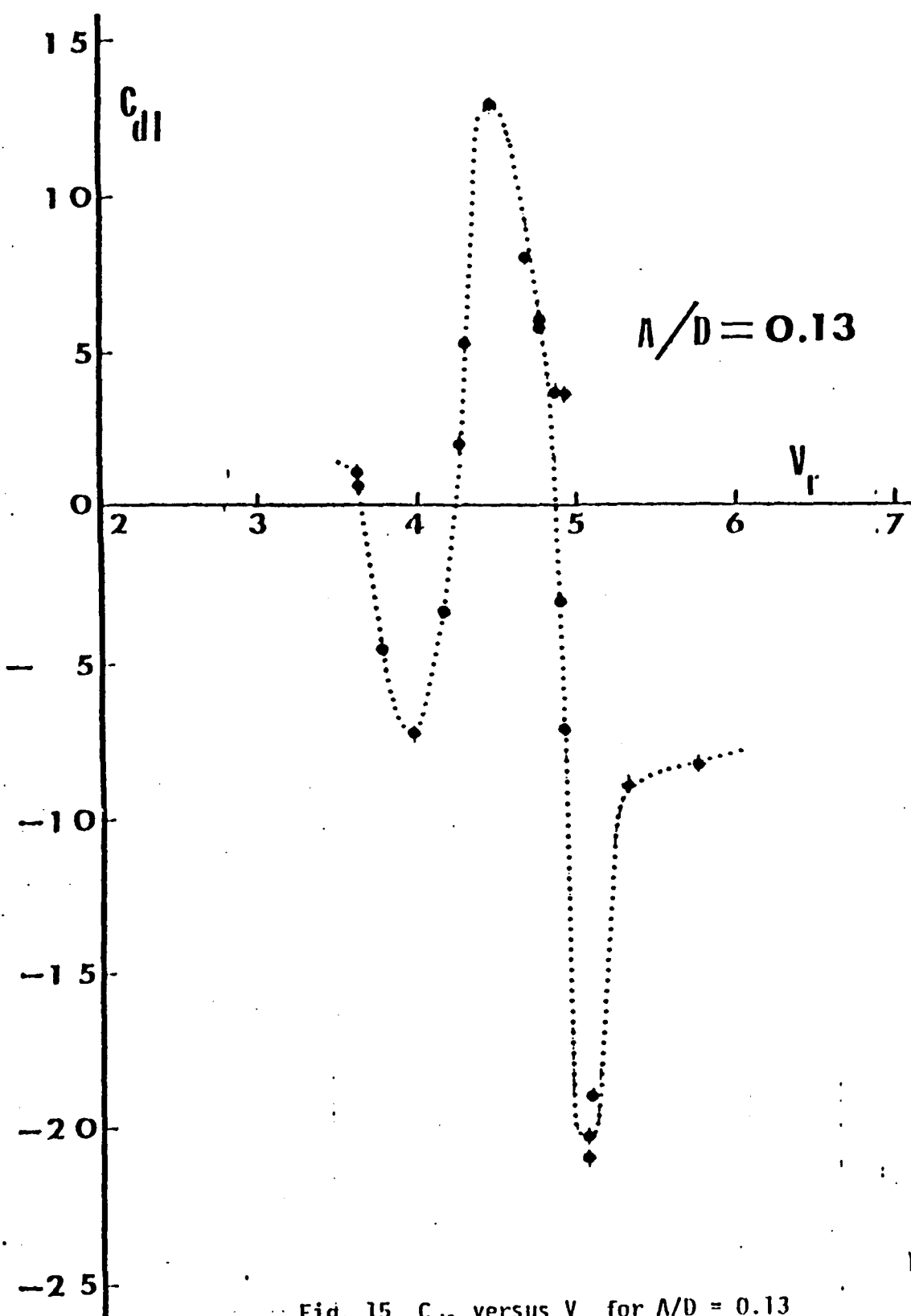


Fig. 15 C_{d1} versus V_r for $\Lambda/D = 0.13$

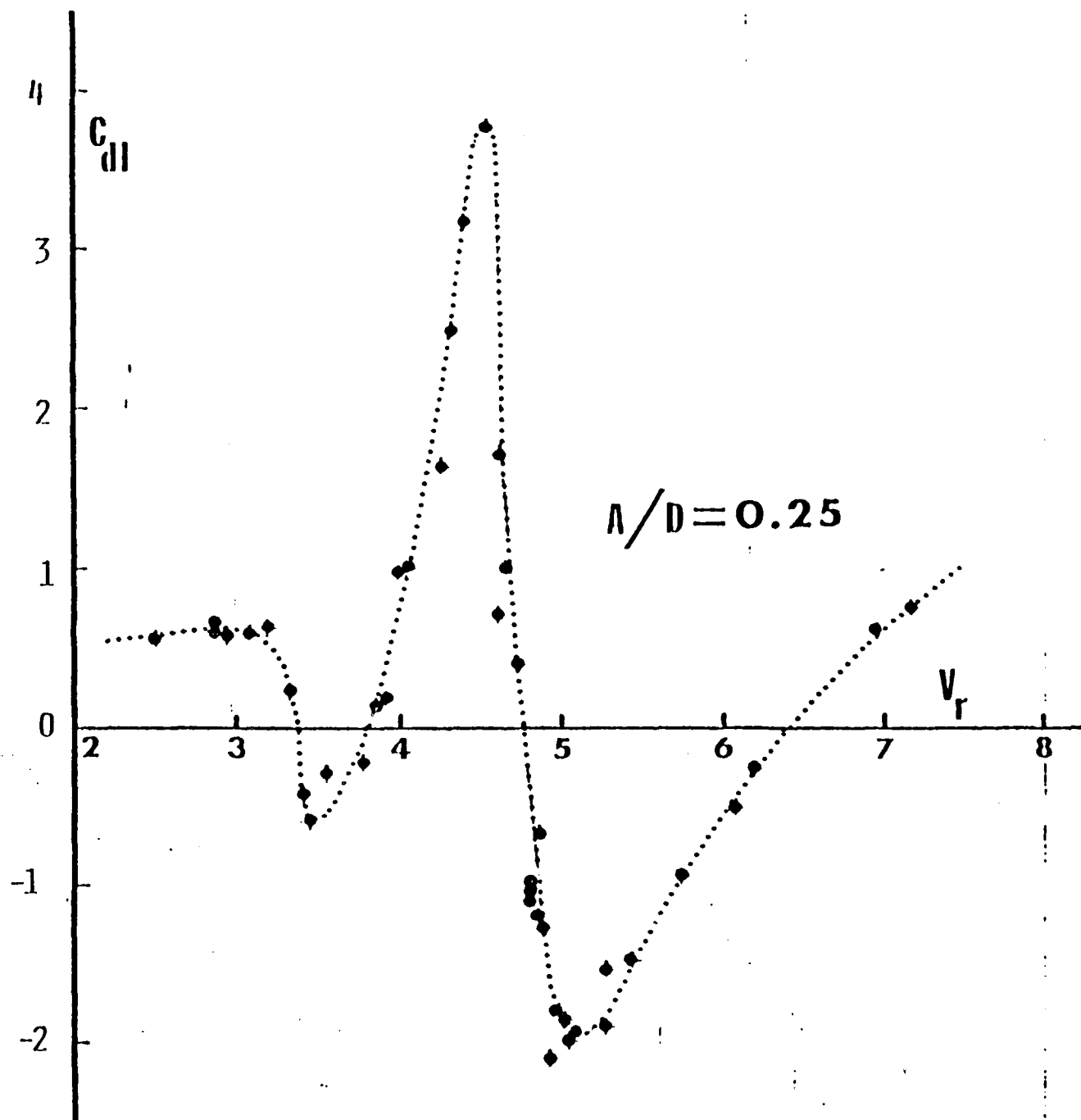


Fig. 16 C_{dl} versus V_r for $\Lambda/D = 0.25$

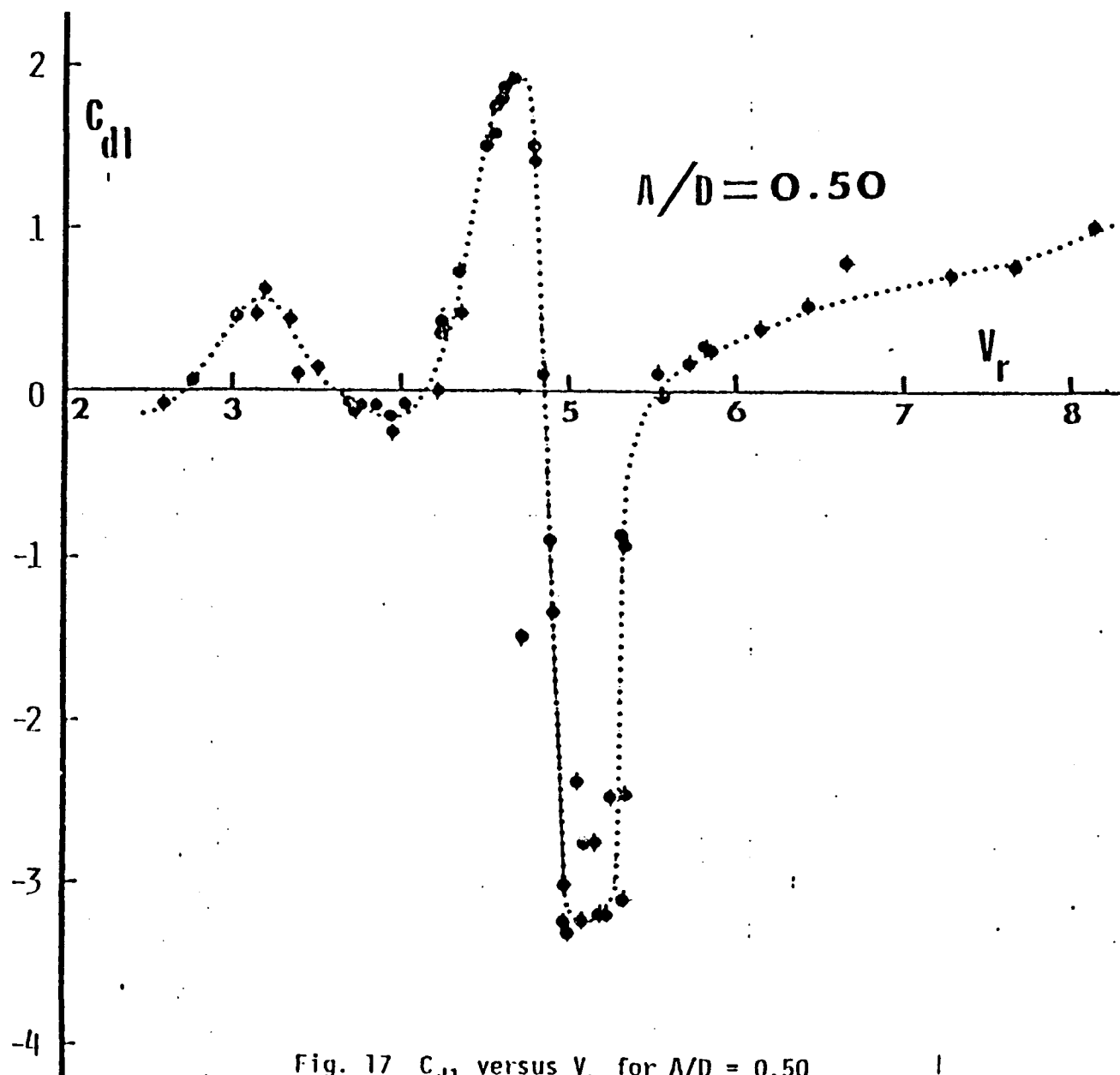


Fig. 17 C_{d1} versus V_r for $\Lambda/D = 0.50$

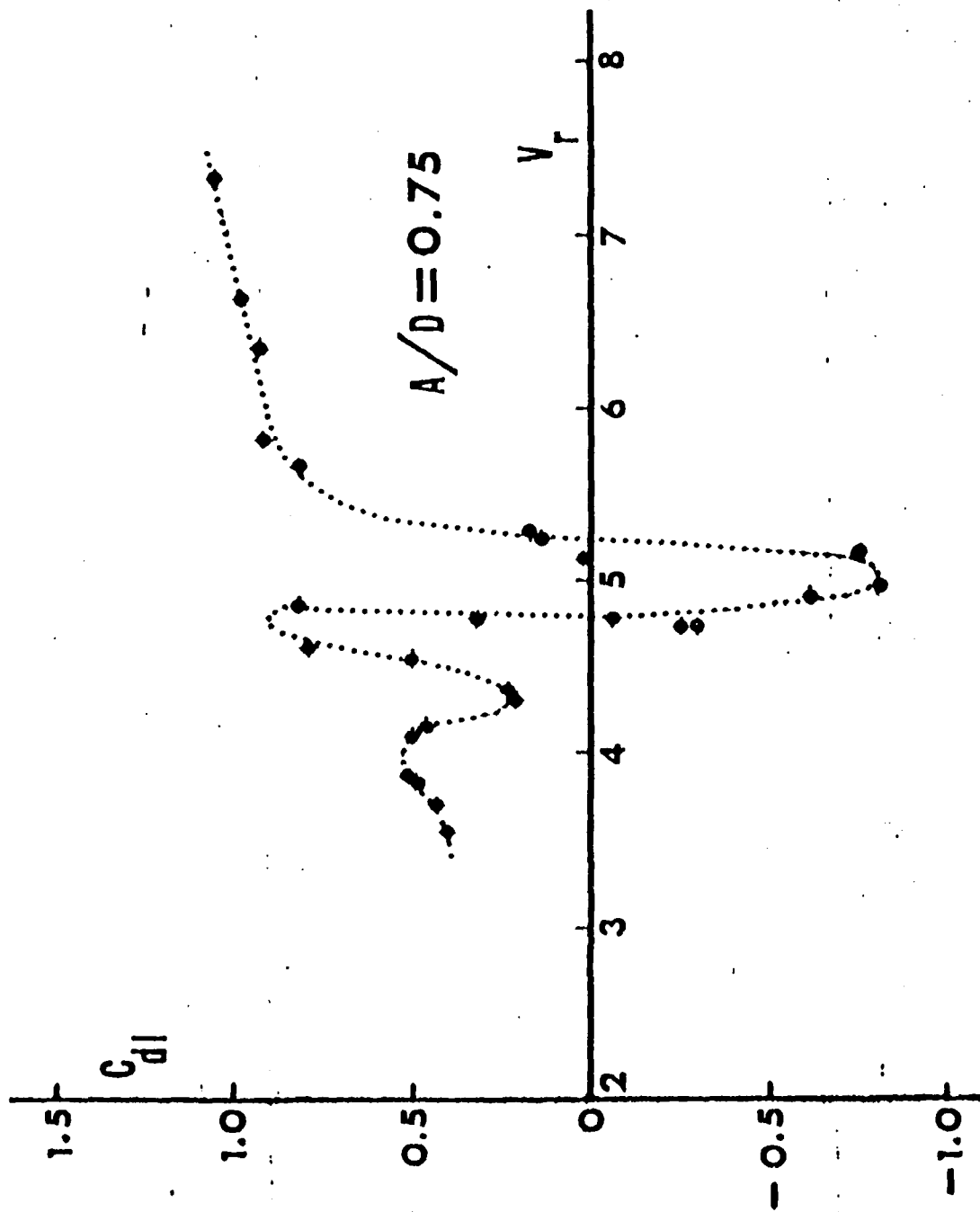


Fig. 18 C_{dI} versus V_r for $A/D = 0.75$

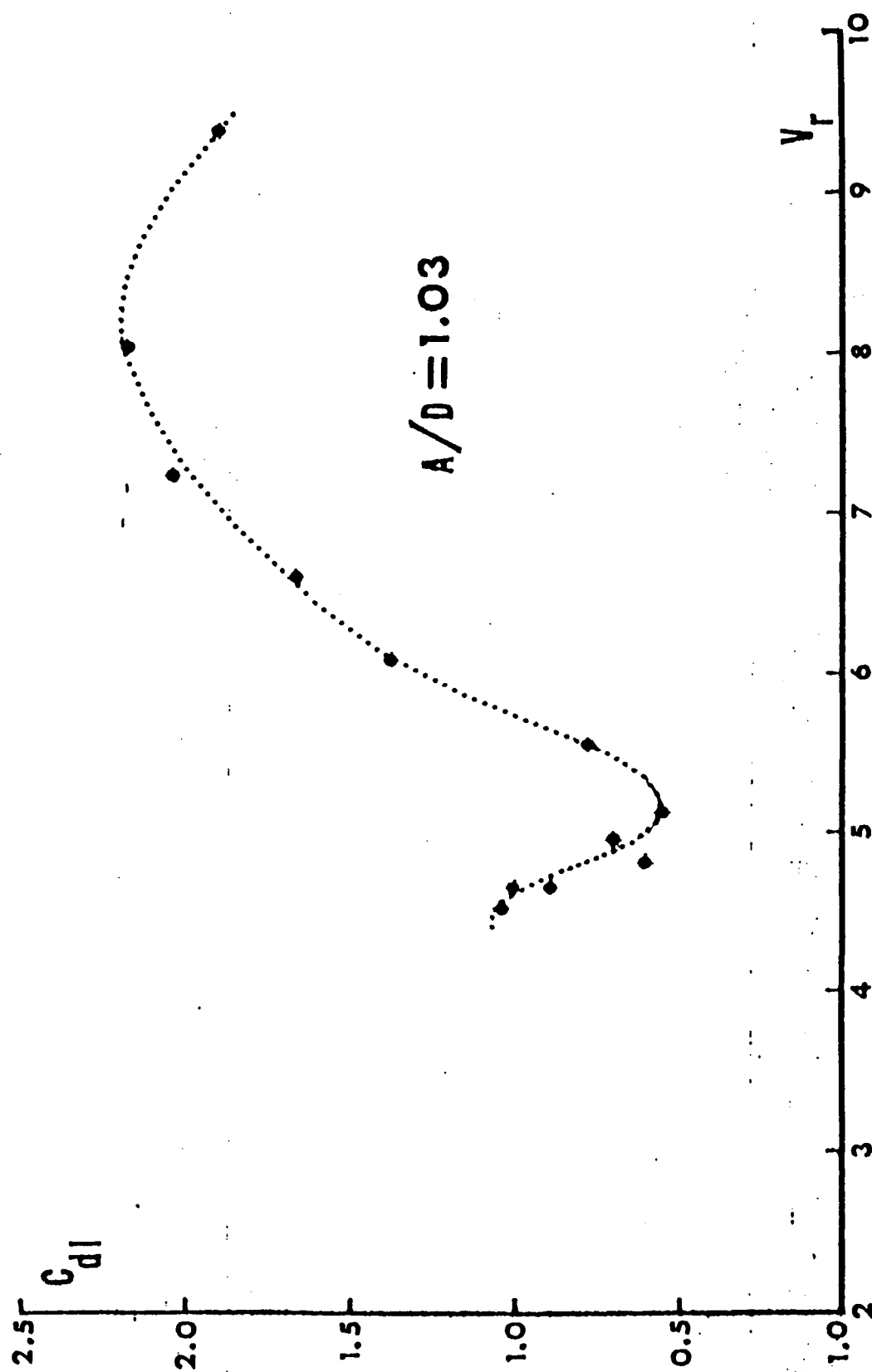


Fig. 19 C_{d1} versus V_r for $A/D = 1.03$

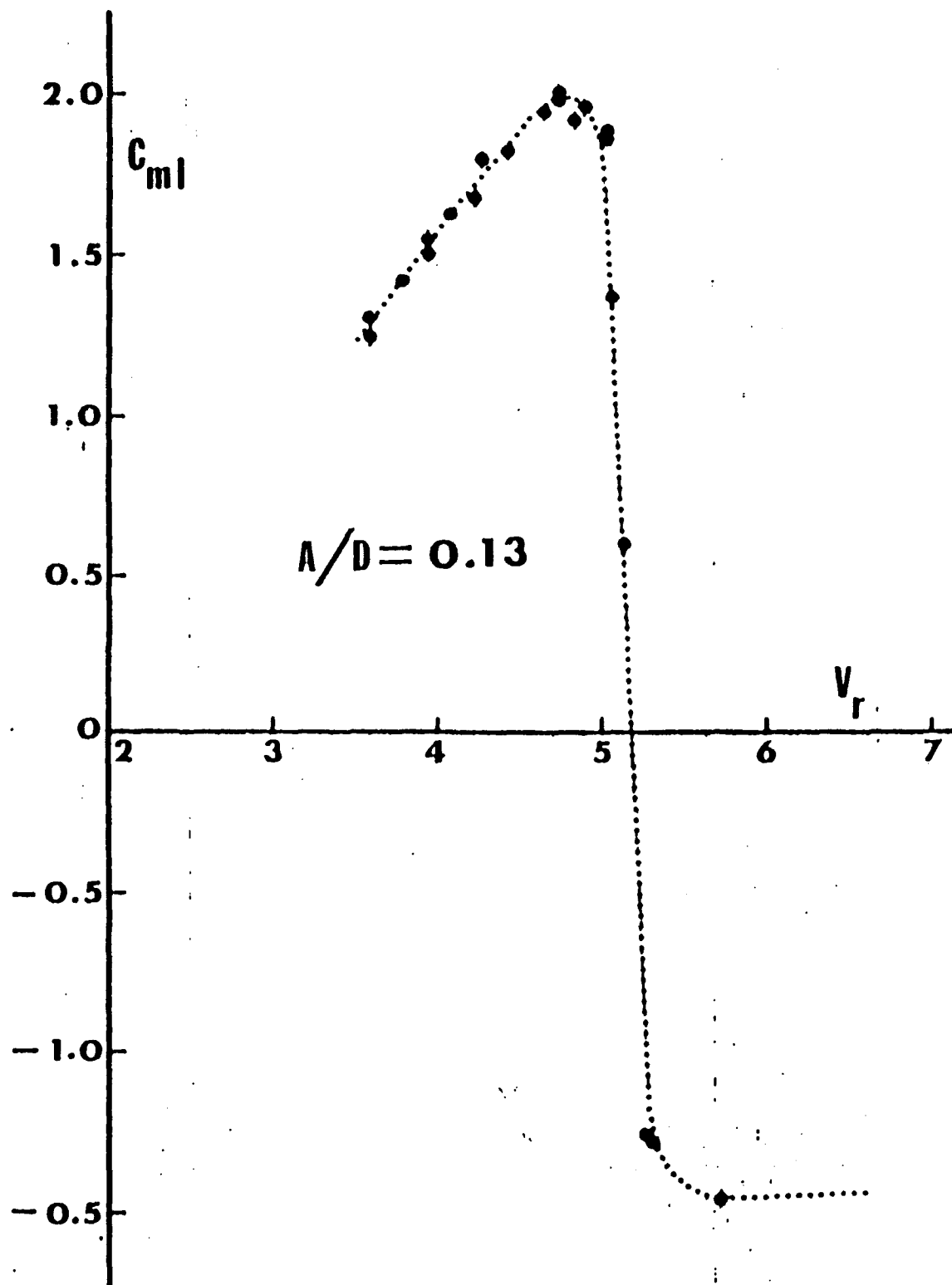


Fig. 20 C_{m1} versus V_r for $\Lambda/D = 0.13$

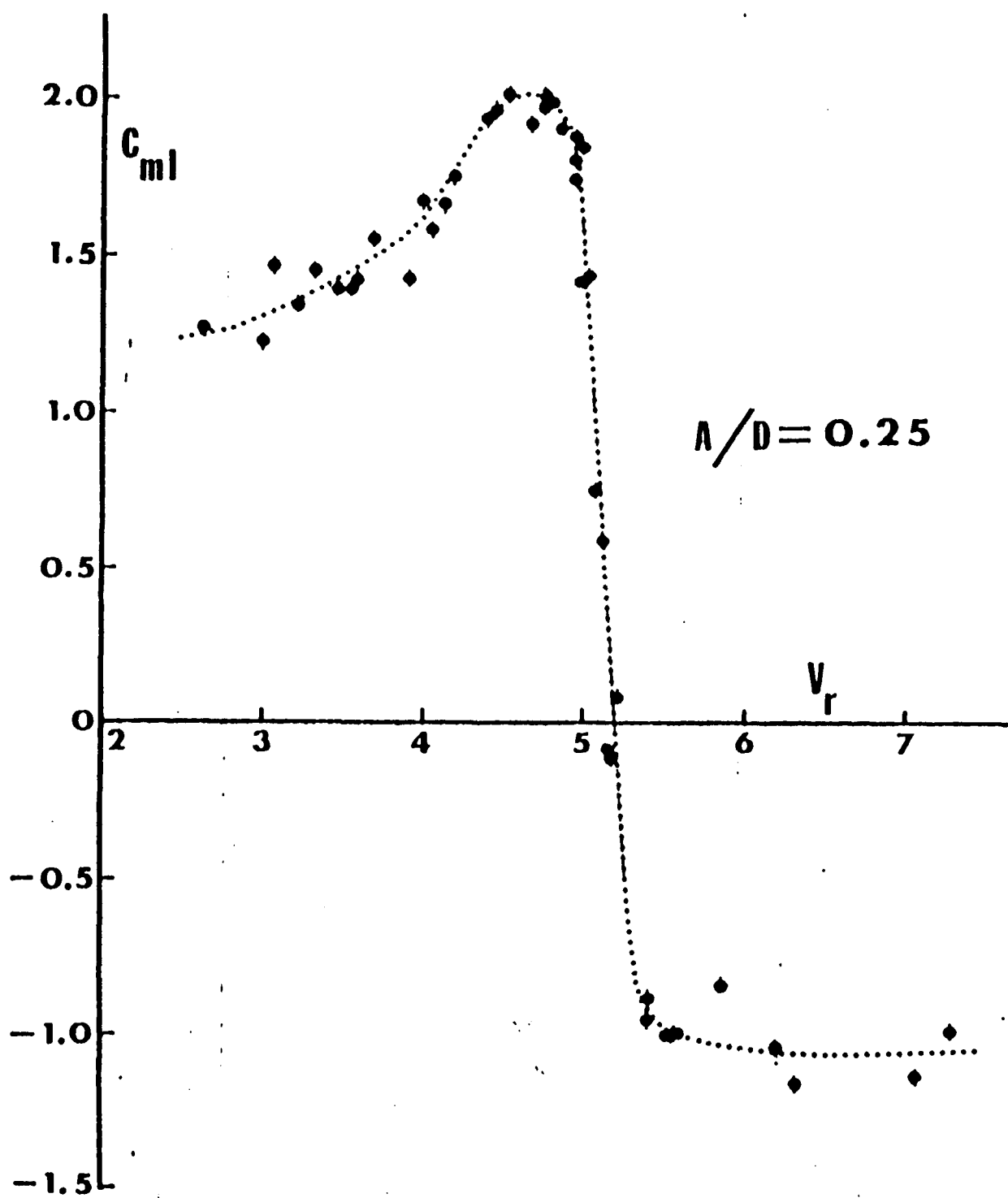


Fig. 21 C_{mI} versus V_r for $\Lambda/D = 0.25$

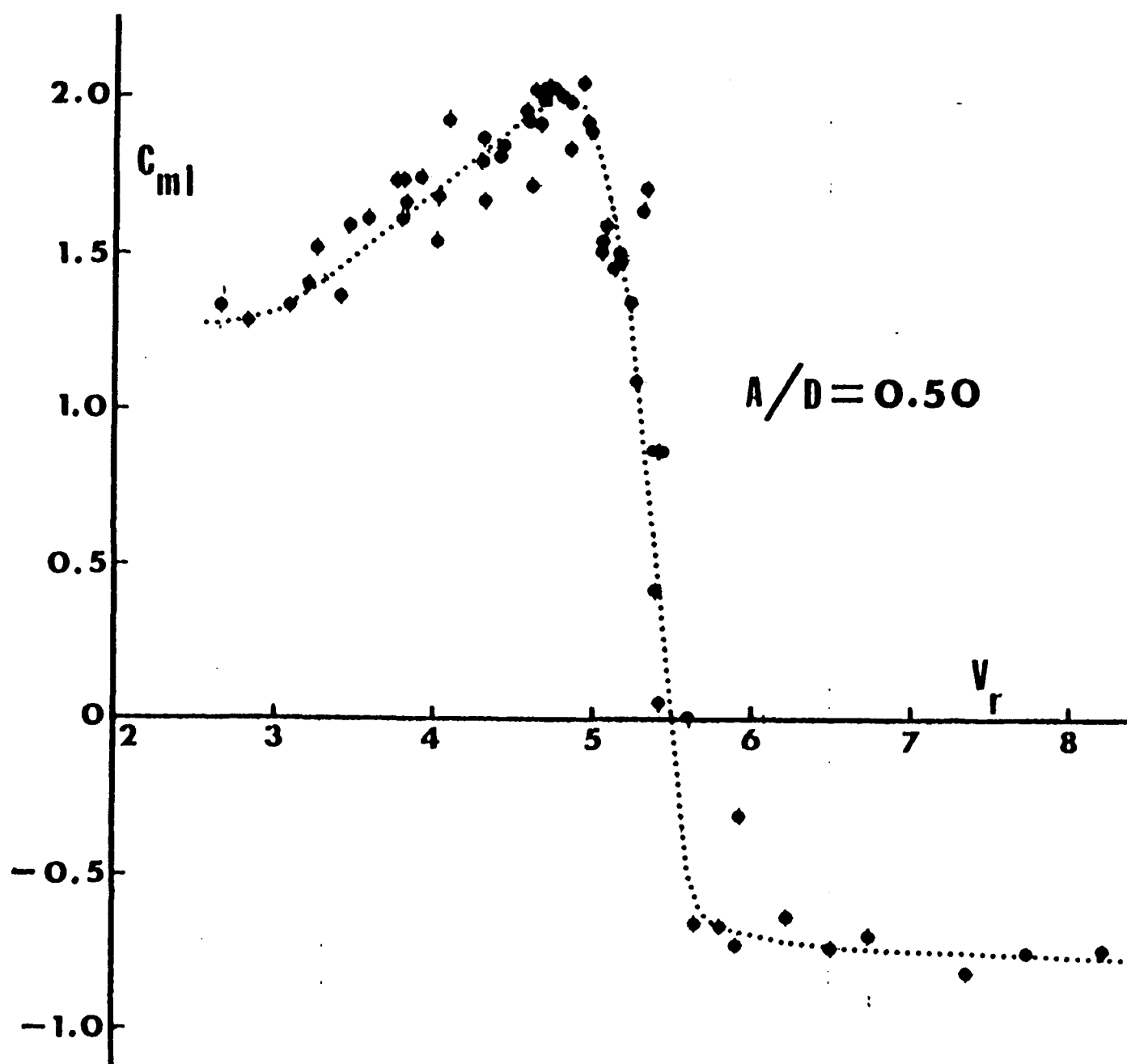


Fig. 22 C_{m1} versus V_r for $A/D = 0.50$

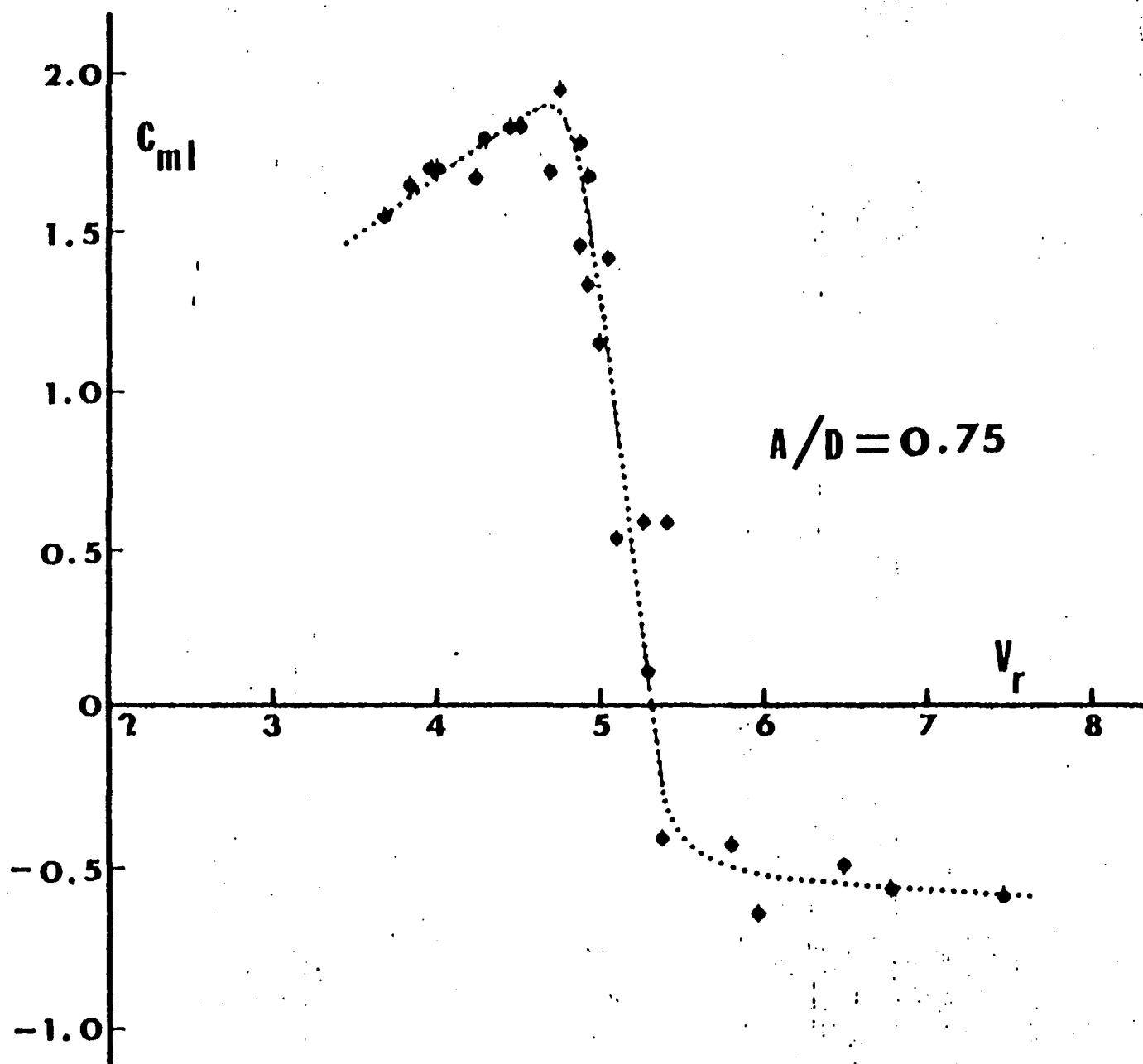


Fig. 23 C_{mI} versus V_r for $\Lambda/D = 0.75$

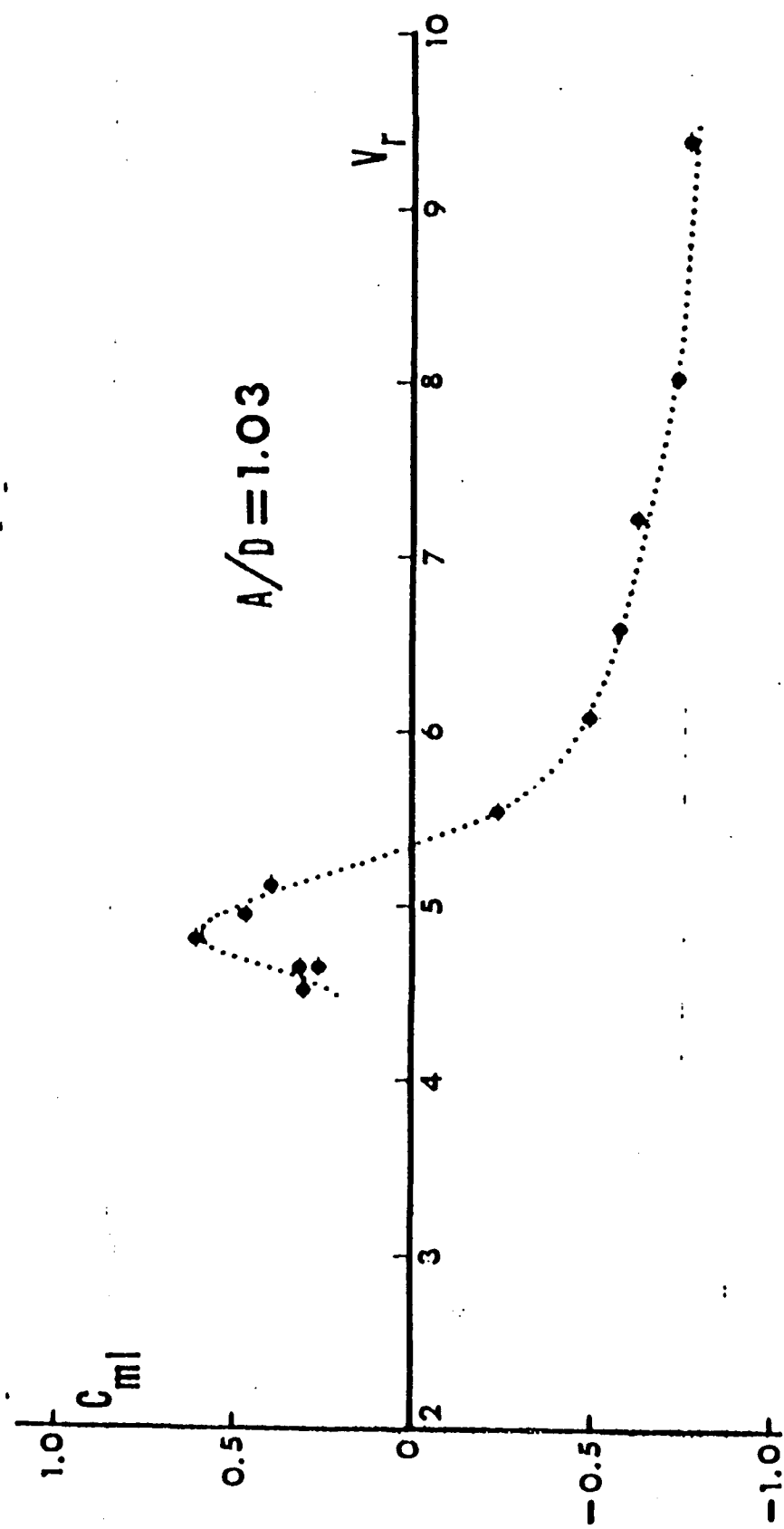


Fig. 24 C_m versus V_r for $A/D = 1.03$

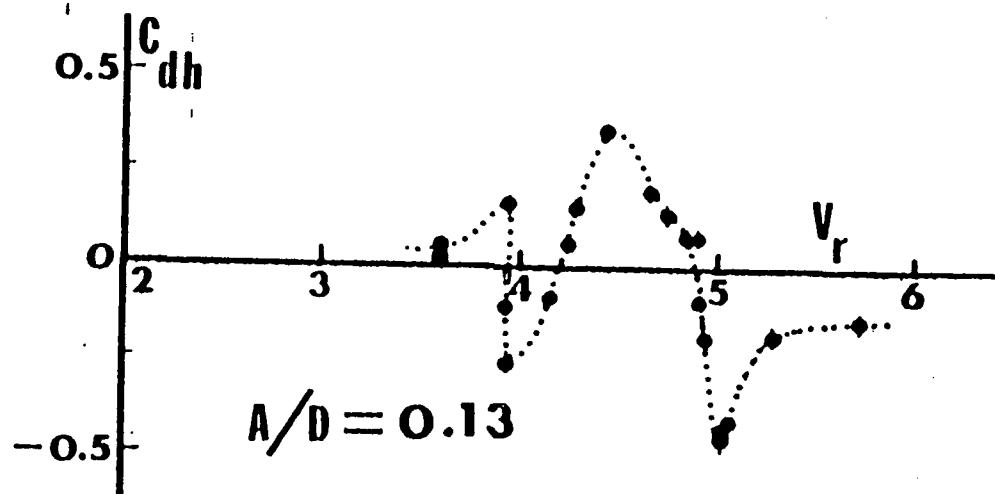


Fig. 25 C_{dh} versus V_r for $\Lambda/D = 0.13$

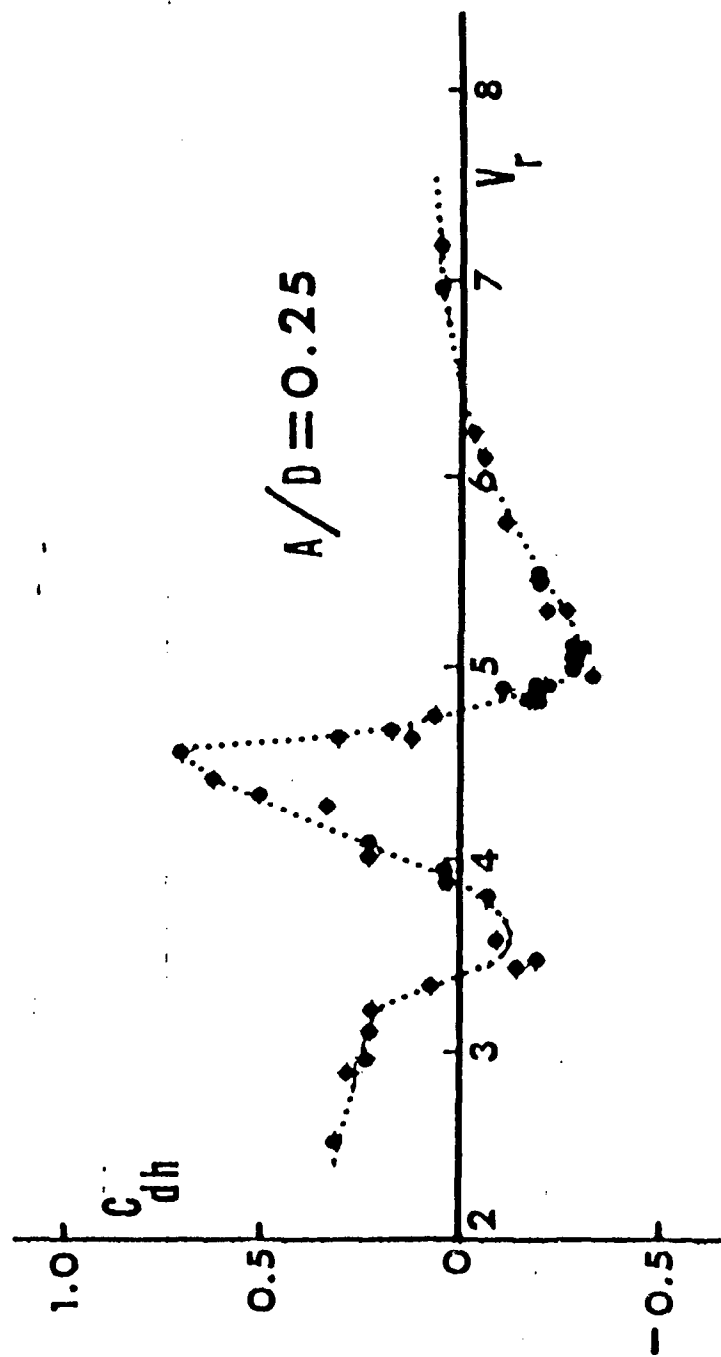


Fig. 26 C_{dh} versus V_r for $A/D = 0.25$

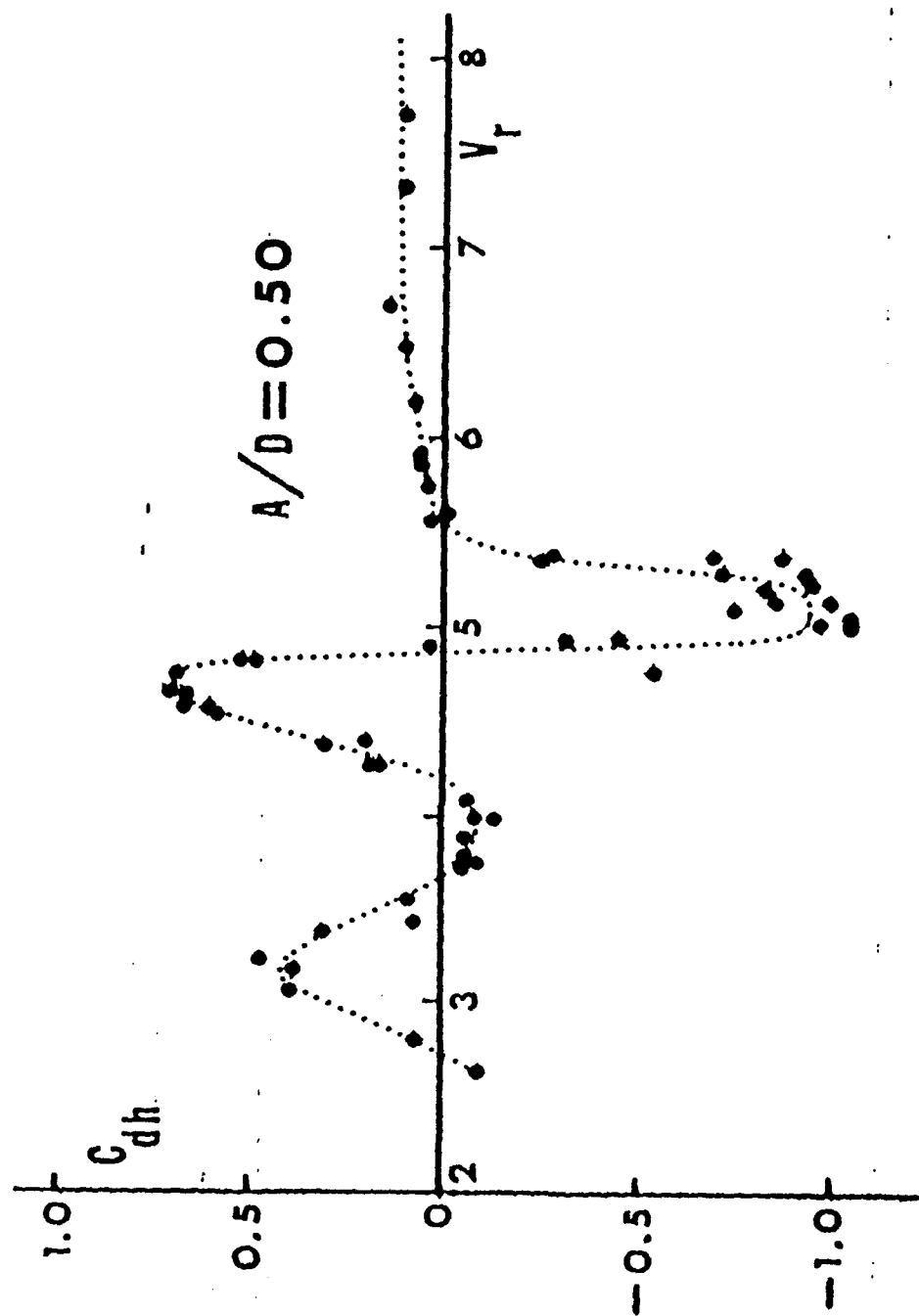


Fig. 27 C_{dh} versus V_r for $A/D = 0.50$

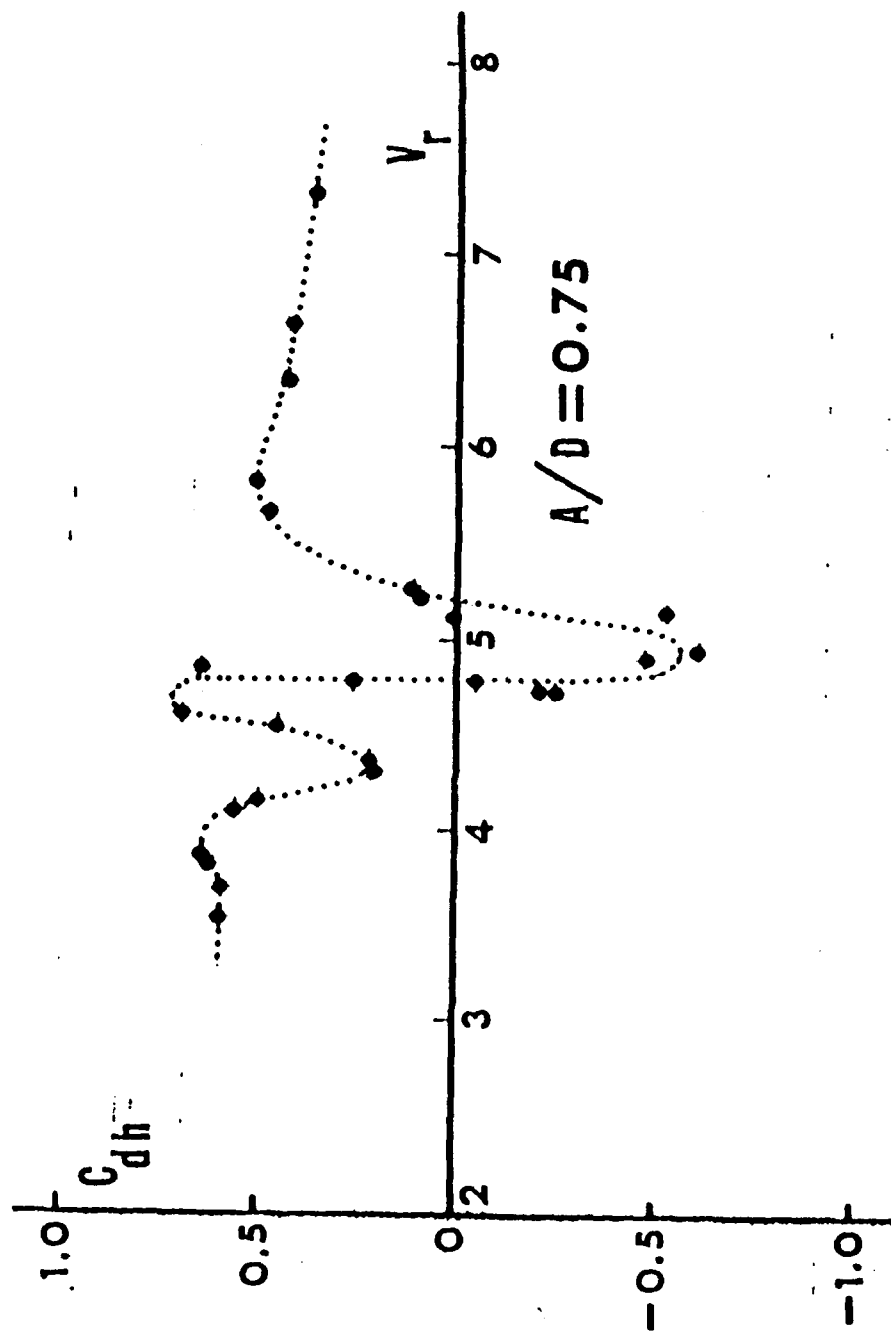


Fig. 28 C_{dh} versus V_r for $A/D = 0.75$

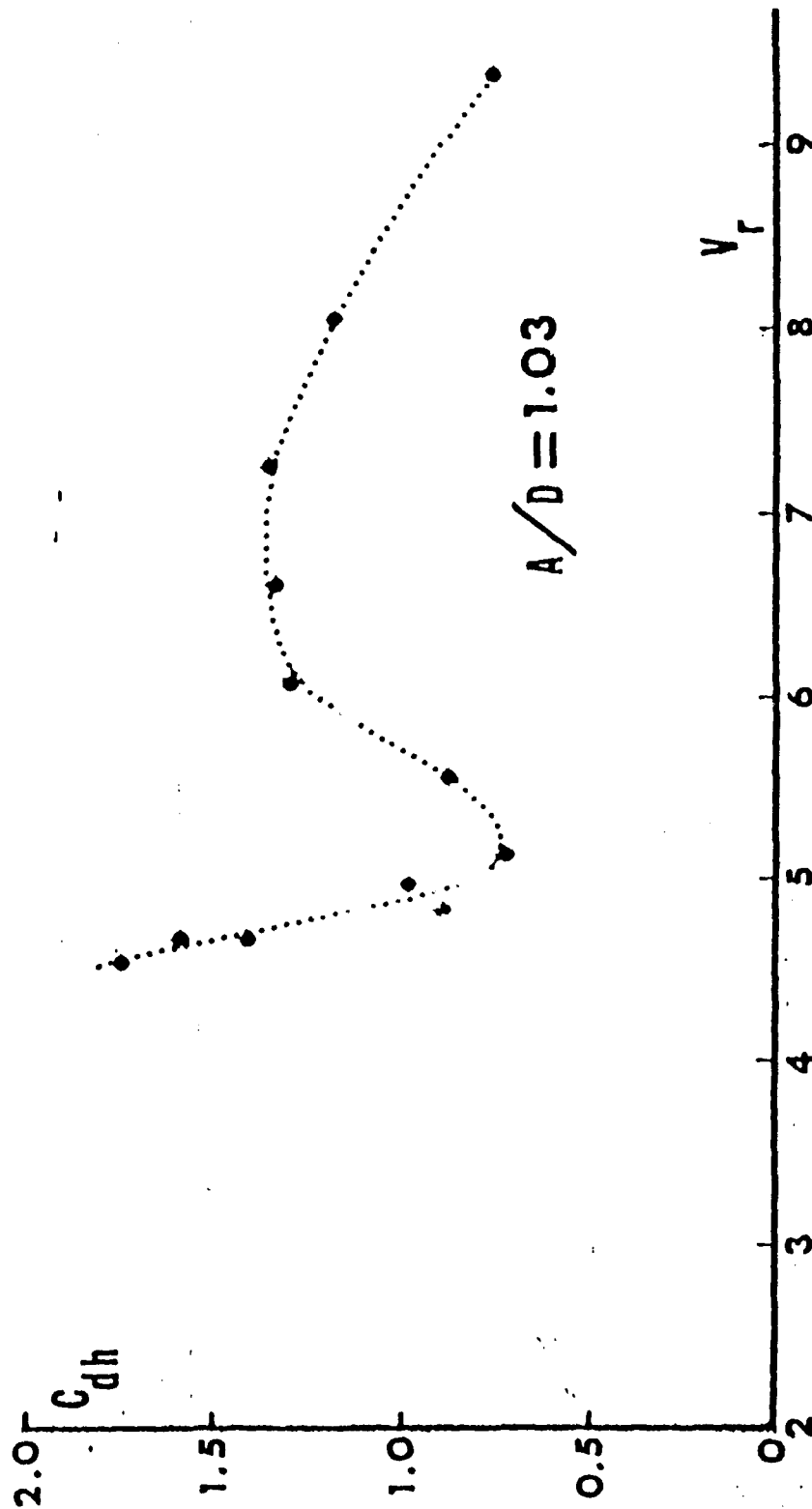


Fig. 29 C_{dh} versus V_r for $A/D = 1.03$

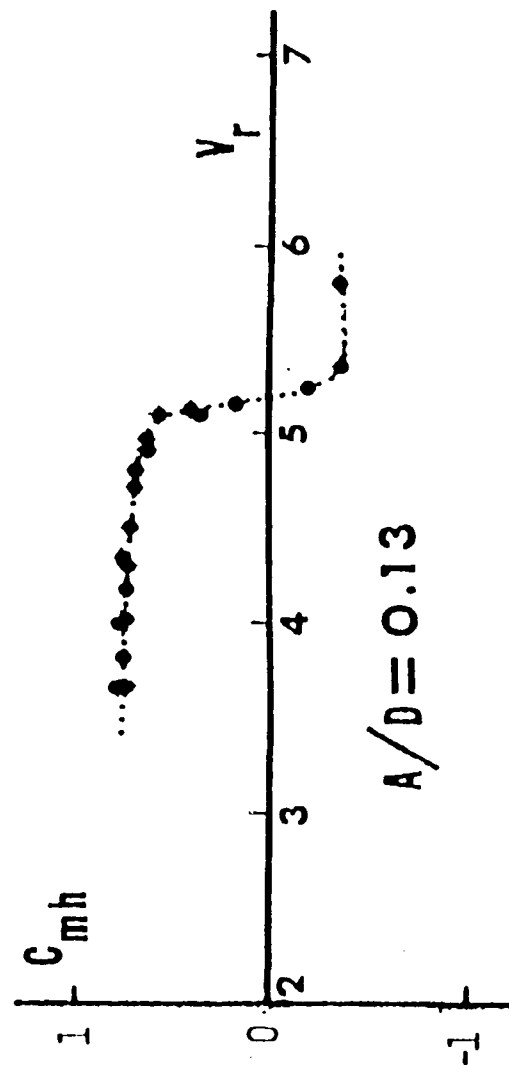


Fig. 30 C_{mh} versus V_r for $A/D = 0.13$

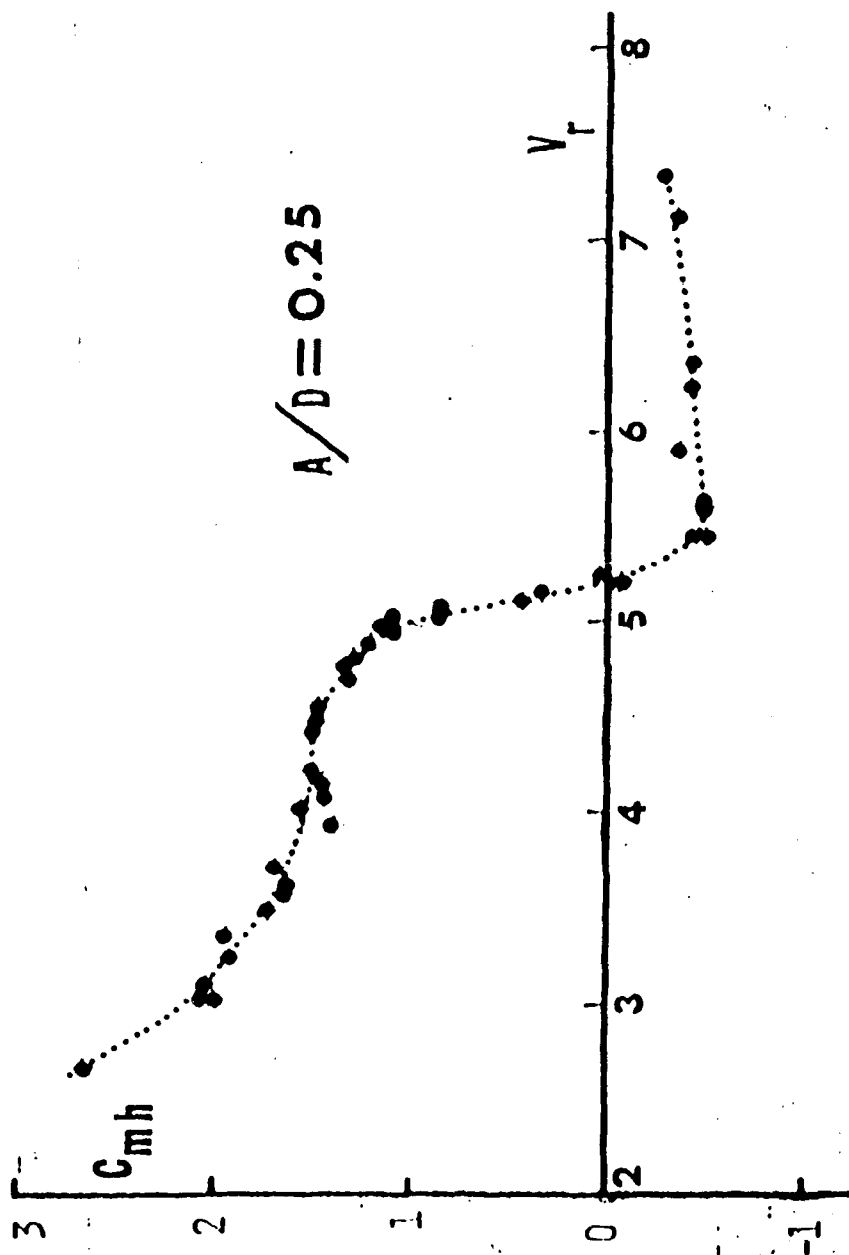


Fig. 31 C_{min} versus V_r for $A/D = 0.25$

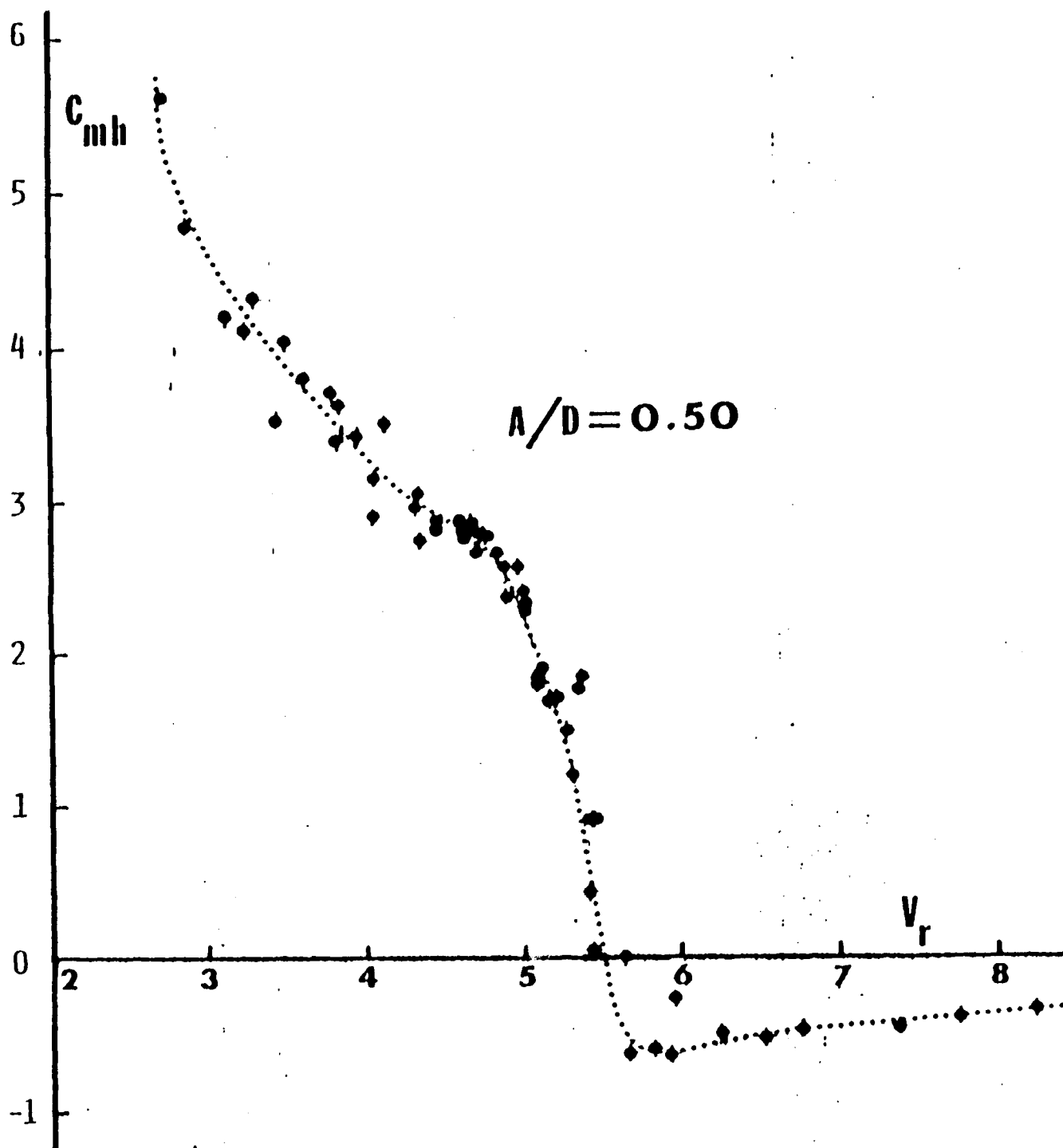


Fig. 32 C_{mh} versus V_r for $\Lambda/D = 0.50$

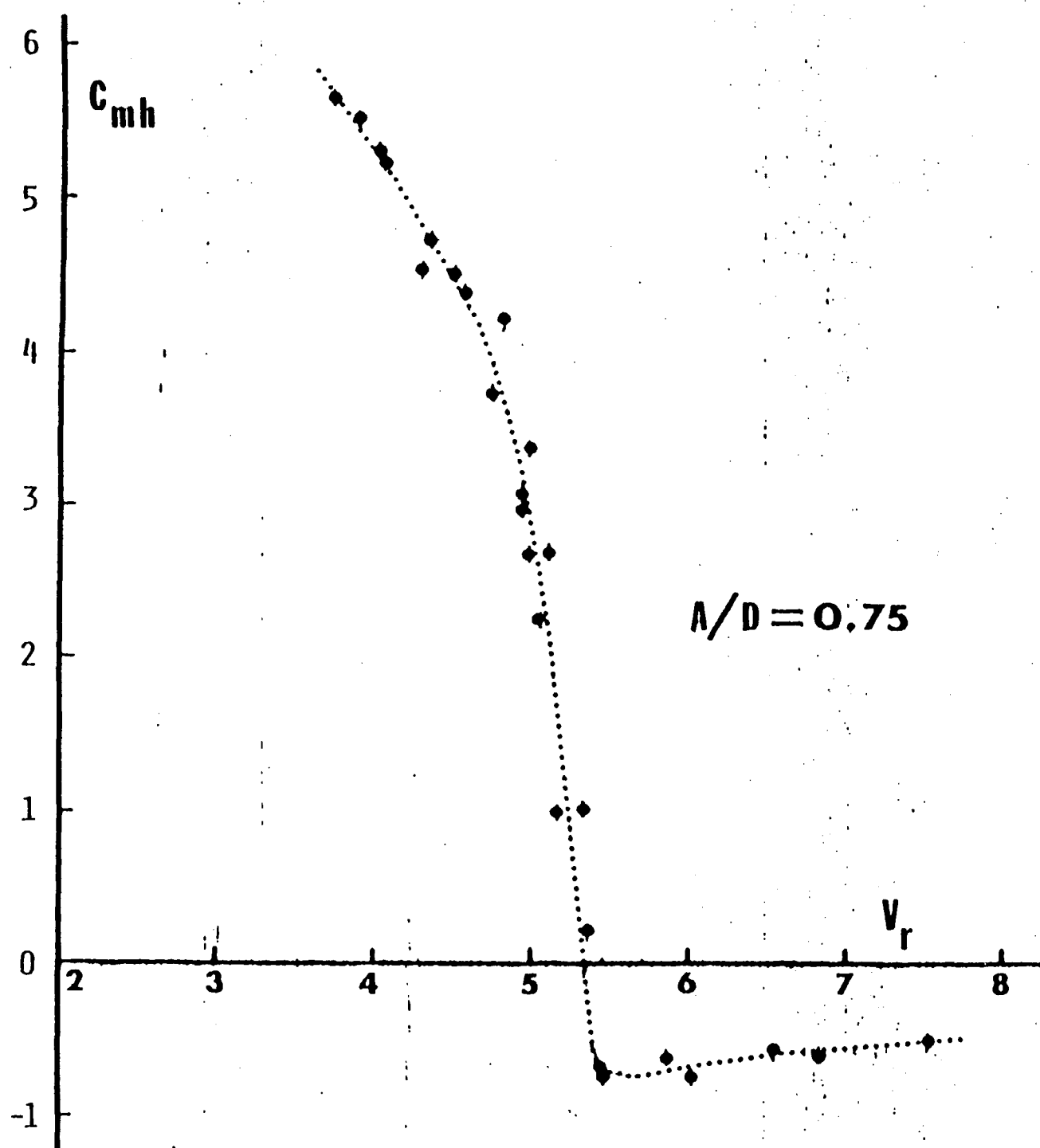


Fig. 33 C_{mh} versus V_r for $\Lambda/D = 0.75$

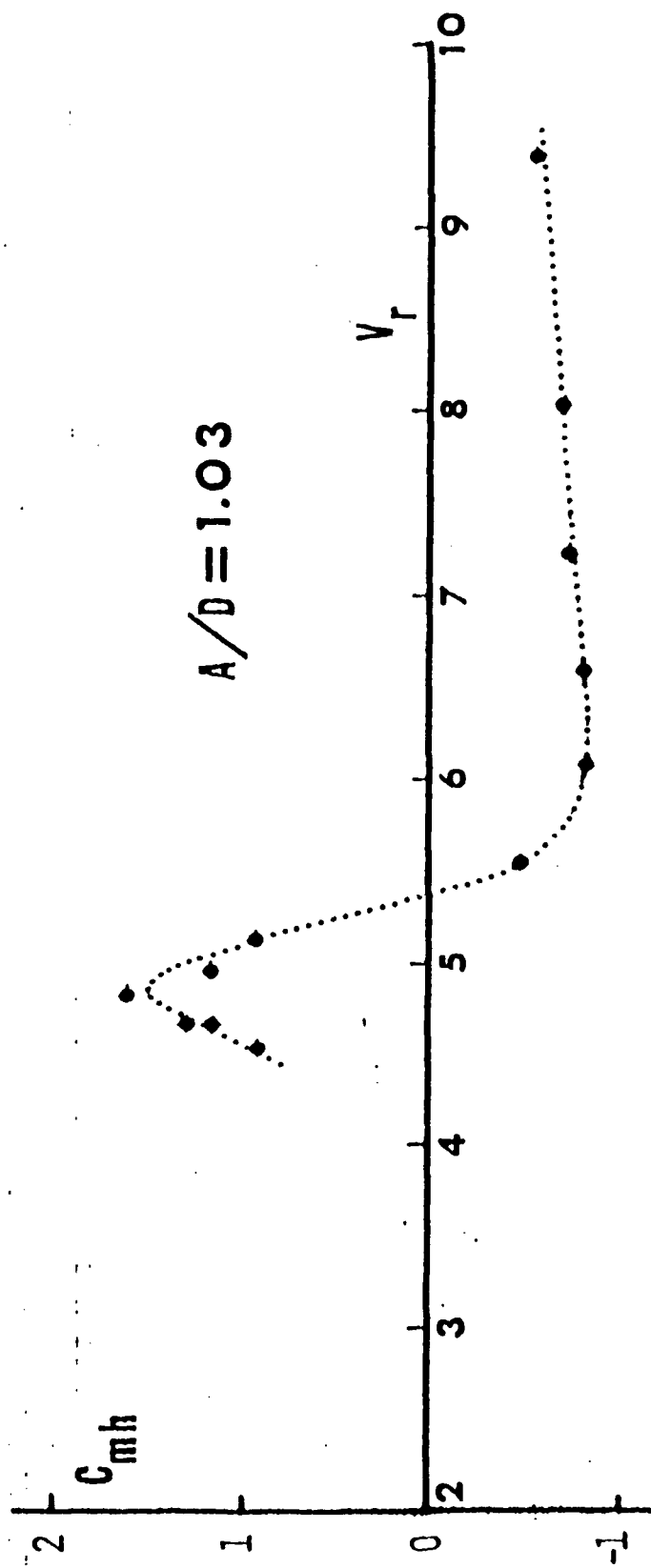


Fig. 34 C_{mh} versus V_r for $A/D = 1.03$

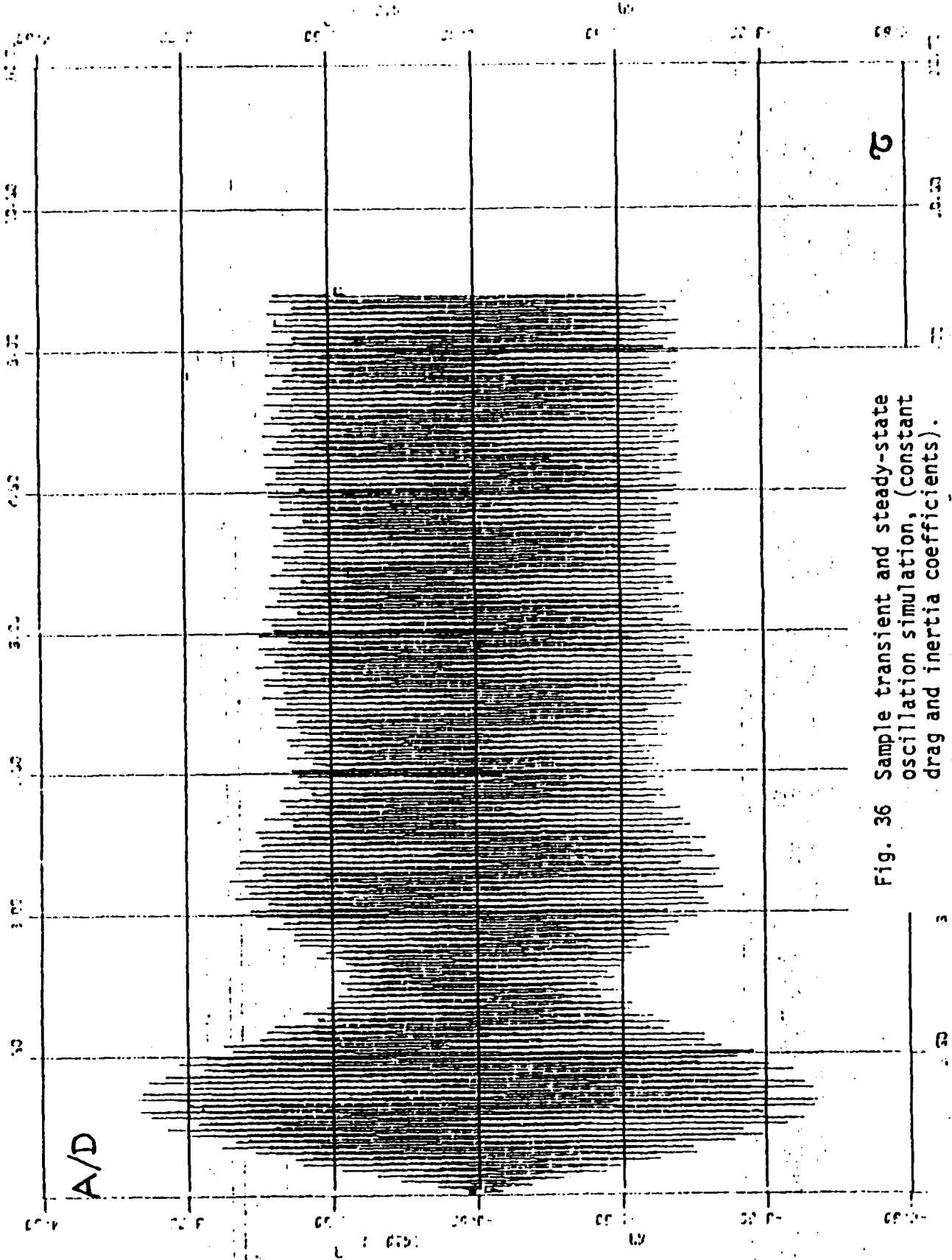


Fig. 36 Sample transient and steady-state oscillation simulation, (constant drag and inertia coefficients).

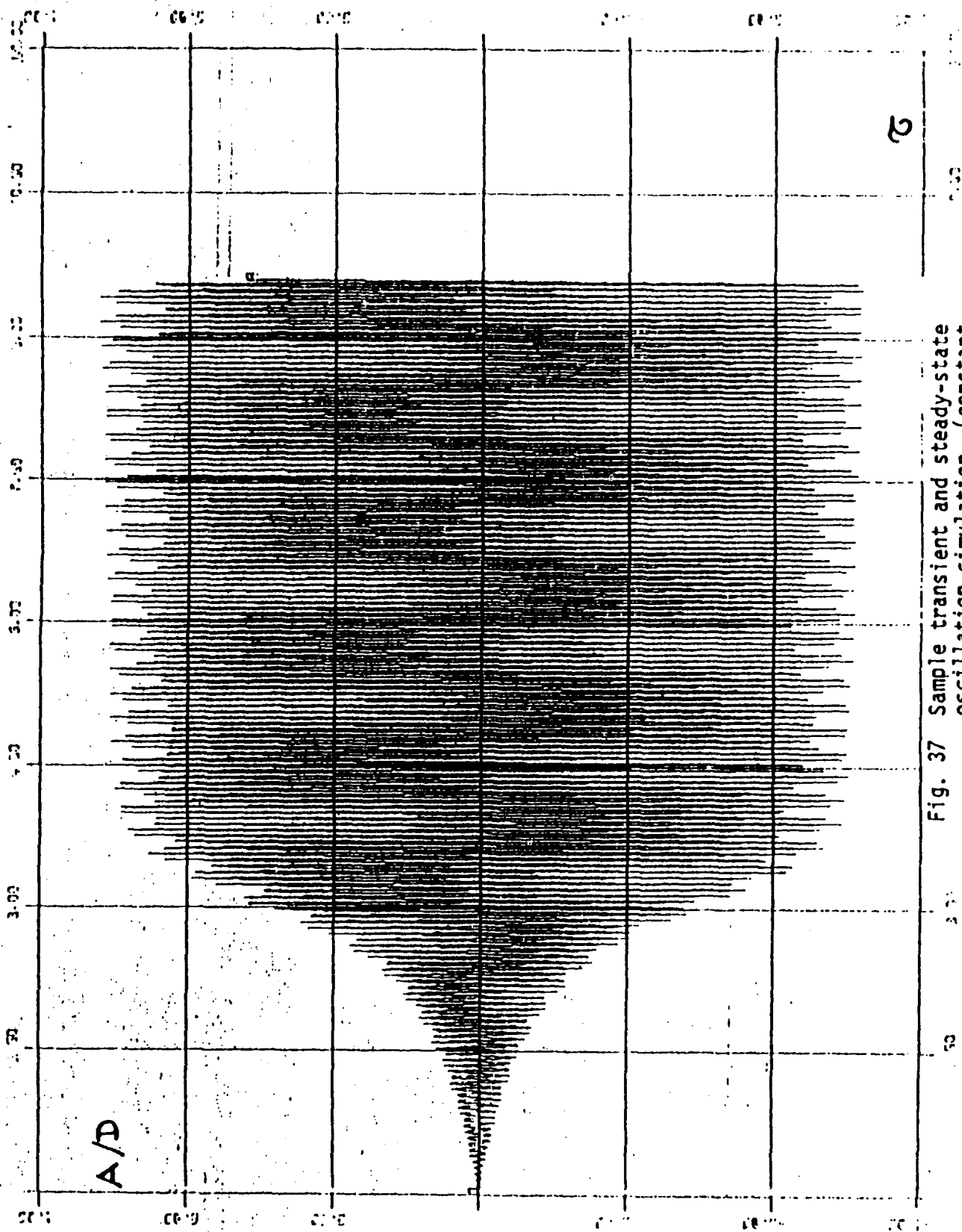


Fig. 37 Sample transient and steady-state oscillation simulation, (constant drag and inertia coefficients).

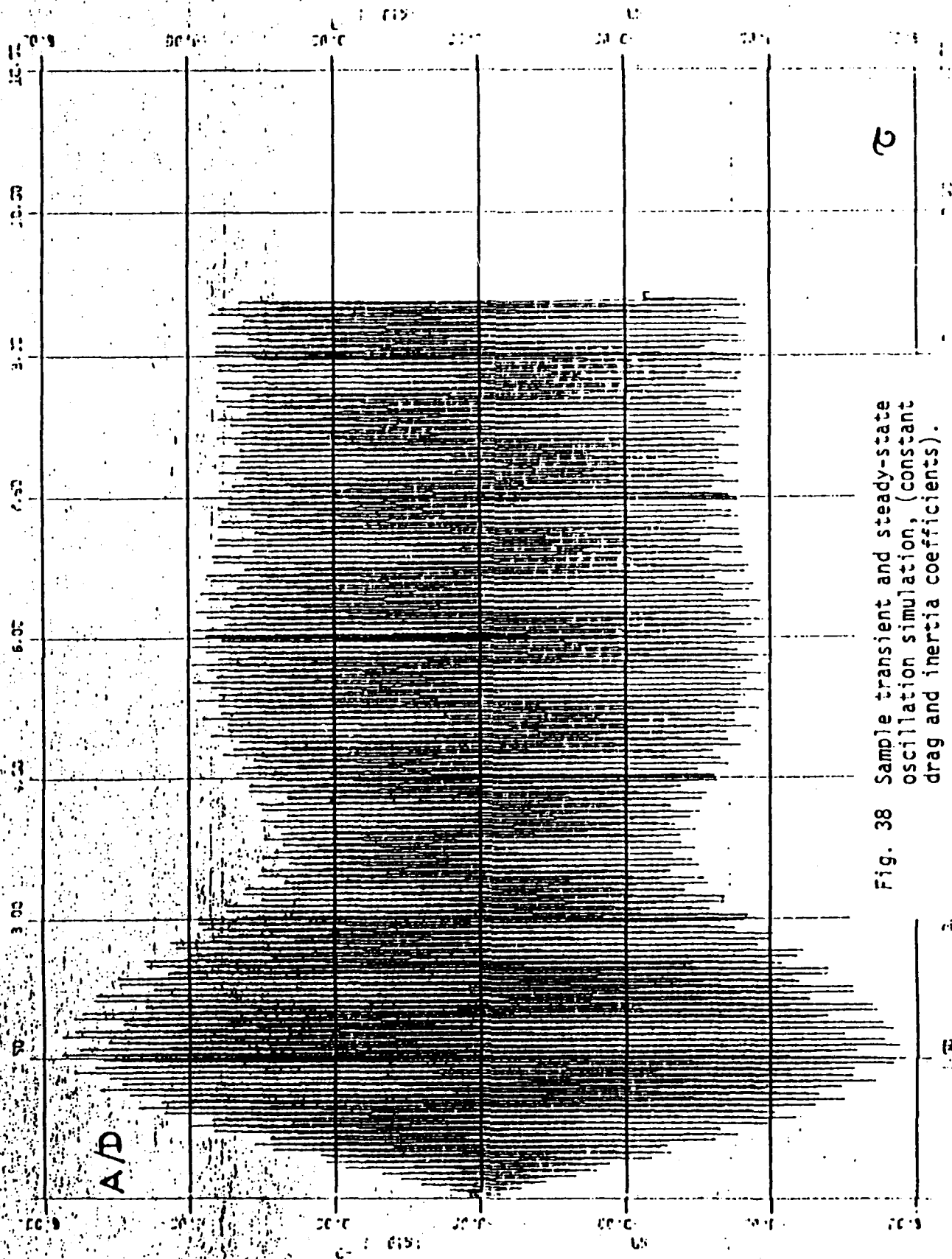


Fig. 38 Sample transient and steady-state oscillation simulation, (constant drag and inertia coefficients).

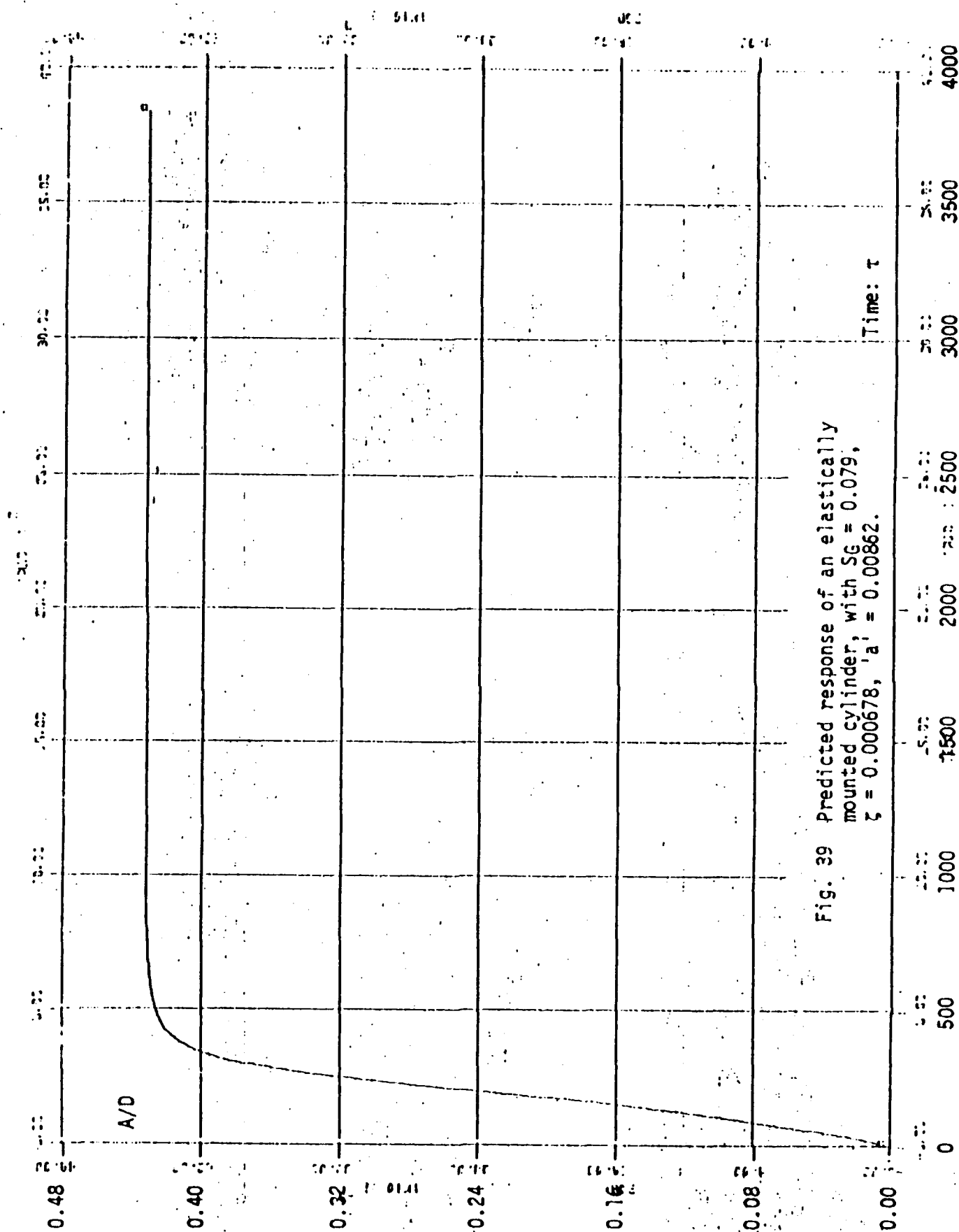


Fig. 39 Predicted response of an elastically mounted cylinder, with $SG = 0.079$, $\zeta = 0.000678$, $'a' = 0.00862$.

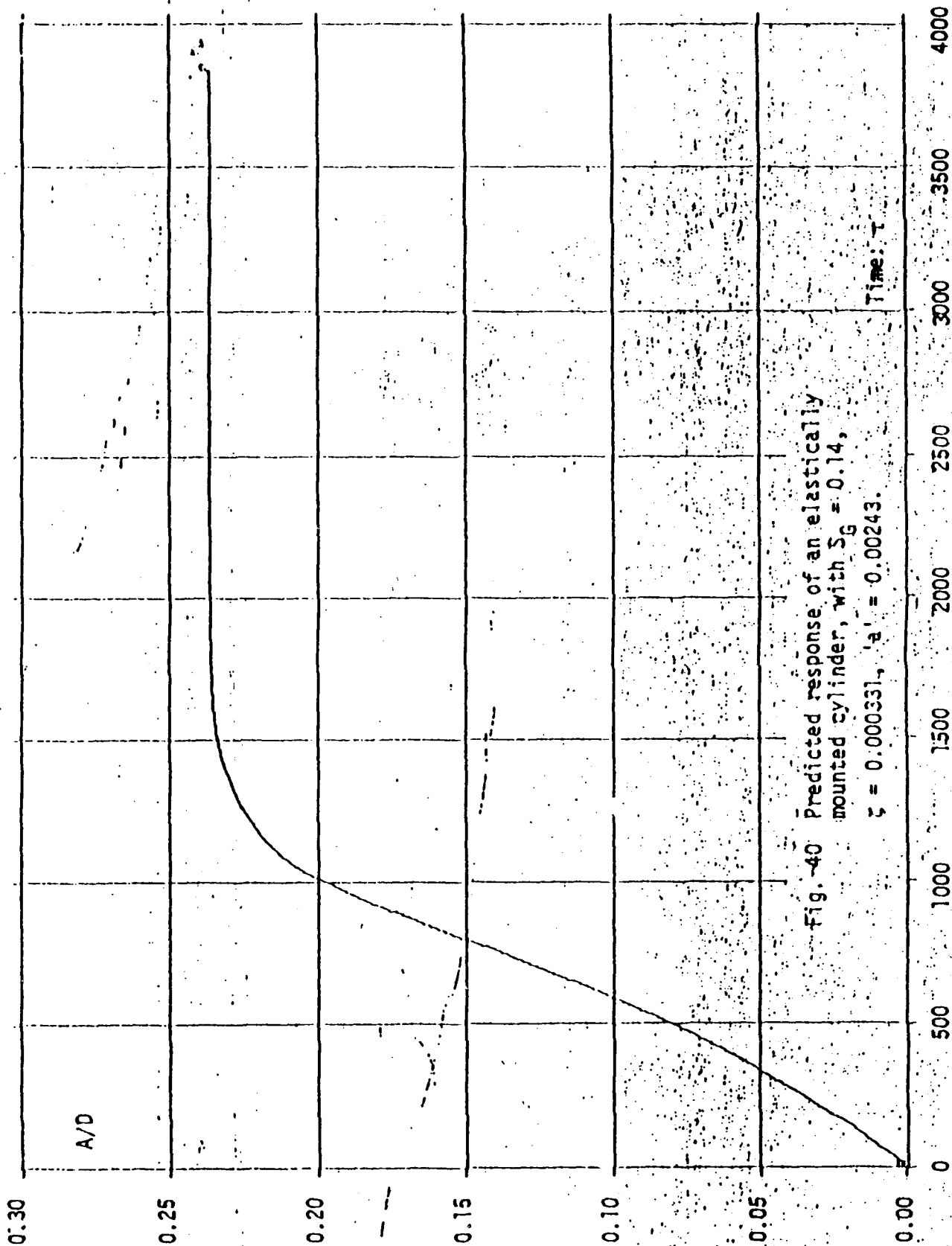


Fig. 40 Predicted response of an elastically mounted cylinder, with $S_g = 0.14$, $\zeta = 0.000331$, $a' = 0.00243$.

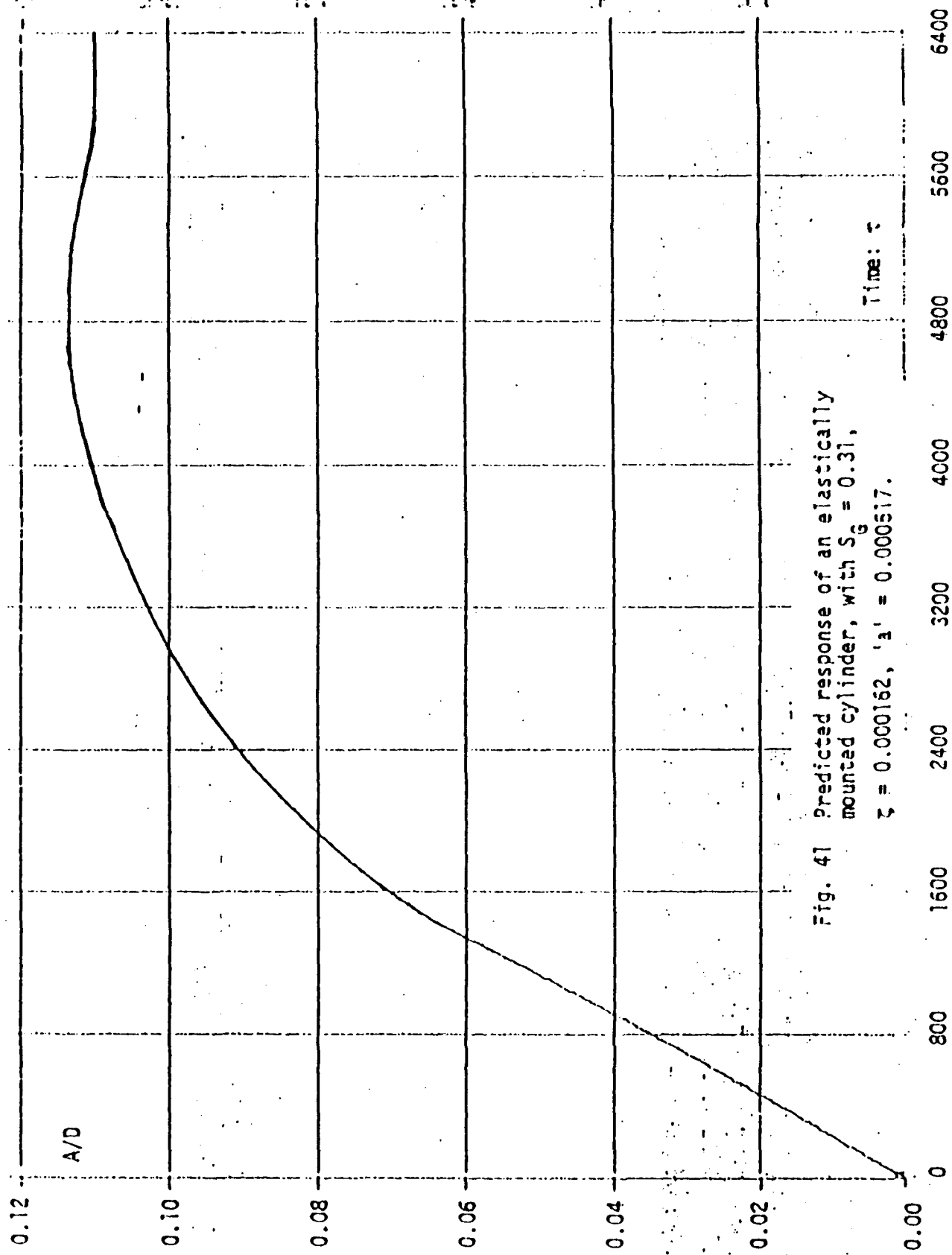


Fig. 41 Predicted response of an elastically mounted cylinder, with $S_g = 0.31$, $\zeta = 0.000162$, ' λ ' = 0.000517.

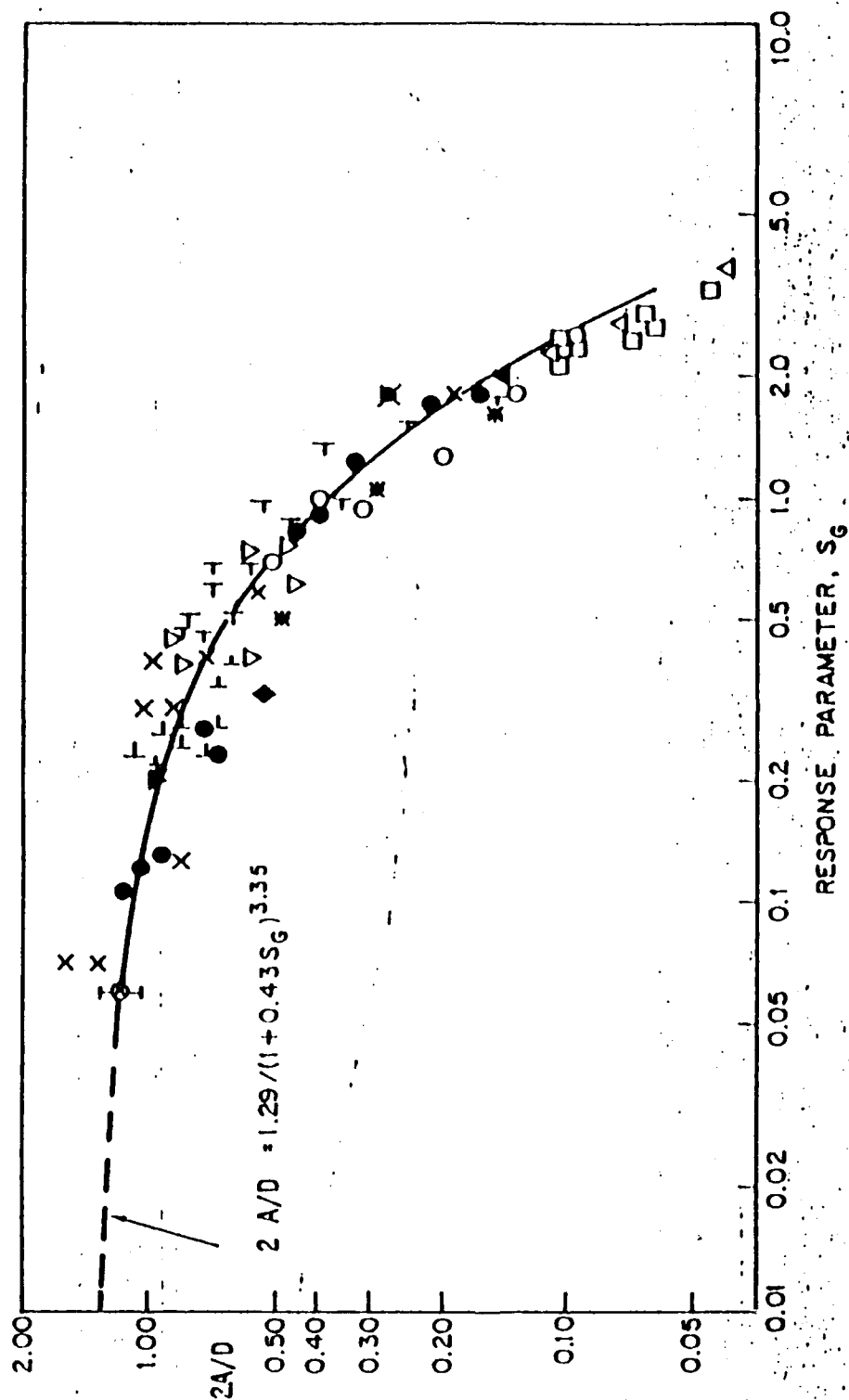


Fig. 42 $2A/D$ versus response parameter, [from Skop, Griffin, & Ramberg (1976)]

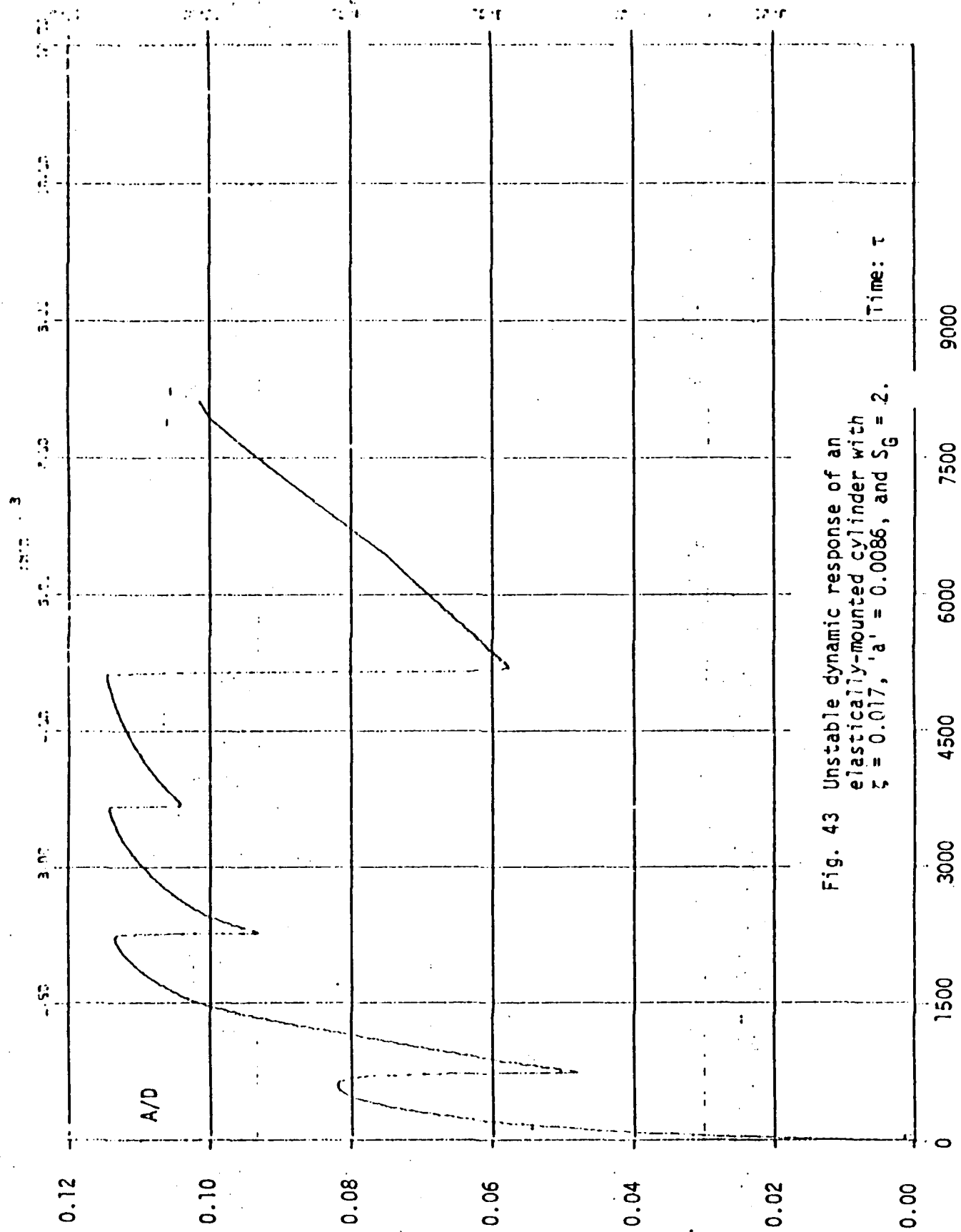


Fig. 43 Unstable dynamic response of an elastically-mounted cylinder with $\zeta = 0.017$, $a' = 0.0086$, and $S_G = 2$.

APPENDIX-A COMPUTER PROGRAM

```

INITIAL
CONSTANT P1=3.14159, ZETA=0.2
CONSTANT XZETA=0.0, XADZ=0.0
CONSTANT OMEGA=1.15
CONSTANT OMEGA1=1.0
CONSTANT SMALLA=8.0E-03
CONSTANT ADD1A=1.4E-04
CONSTANT CAPINT=0.1475000
CONSTANT ZETA=4.3E-03
C1=SMALLA
A1=C1*C1
C2=OMEGA*OMEGA
A2=C2*C2
C3=C1*C2
B1=A1+A2
Z=2.0*ZETA
DYNAMIC
PROCEDURE ADD, CHPL, CDPL, CAPME, ALPHA, FEFUNCT(XR)
IF (TIME.NE.0.0) GO TO 2
XRM2=XR
XRM1=XR
ADD=ADD1A
CMPL=0.01
CDPL=-0.12
S1=B1*(CMPL*CHPL+CDPL*CDPL)
FF=SQRT(S1)
RATIO=CDPL/CMPL
ALPHA=ATAN(RATIO)
CAPME=CAPINT
GO TO 3
2 IF (EOR(XRM1-XRM2,XR-XRM1).EQ.1.0) CALL PRINT
IF (EOR(XRM1-XRM2,XR-XRM1).EQ.1.0) KEY=1
IF (KEY.NE.1) GO TO 3
XRM2=XRM1
XRM1=XR
IF (KEY.NE.1) GO TO 3
IF (KEY.EQ.1) ADD=ABS(XR)
KEY=0
CHPL=AFGEN(ONE,ADD)
CDPL=AFGEN(TWO,ADD)
RATIO=CDPL/CMPL
ALPHA=ATAN(RATIO)
S1=0.1*(CMPL*CMPL+CDPL*CDPL)
FF=SQRT(S1)
T1=S1/(ADD*ADD)
PART1=1.0-Z*Z*Z
PART2=T1-1.0
SUM=PART1+PART1*PART2
RATIO=SQRT(SUM)
RATIO=PART1-RATIO
CAP1=SQRT(ABS(RATIO))
BOUND=ADD-ADD*ADD
CAPME=FEFUNCT(BOUND,CAPINT,CAPINT,CAP1)
3 CONTINUE
ENDPROCEDURE
ANGLE=CAPME*TIME-ALPHA
F=FF*STH(ANGLE)
XROD=(F-Z*XR-X)
XRO=INTGRL(XROZ,XRO)
X=INTGRL(XAZ,XRO)
METHOD RK4
PAINT,XRO,XR,ALPHA,TIME,ADD,CMPL,CDPL,CAPME
OUTPUT,TIME,ADD(0.0,0.5)
PAGE XPLOI,HEIGHT=2.0,WIDTH=3.0
LABEL ZETA
LABEL CSMP SIMULATION OF THE SYSTEM BY TUNG-KUTTA FOURTH ORDER
TUNG-KUTTA METHOD=1.0,0.0,0.0,0.2,0.1,0.1,0.1,0.1
END

```


INITIAL DISTRIBUTION LIST

	No. Copies
1. Defense Documentation Center Cameron Station Alexandria, Virginia 22314	2
2. Chairman, Department of Mechanical Engineering, Code 69 Naval Postgraduate School Monterey, Calif. 93940	2
3. Civil Engineering Laboratory Naval Construction Battalion Center Port Hueneme, CA. 93043	2
4. Library, Code 0212 Naval Postgraduate School Monterey, CA. 93940	2
5. Prof. T. Sarpkaya, Code 69SL Mechanical Engineering Naval Postgraduate School Monterey, Calif. 93940	5
6. Dr. O. M. Griffin Ocean Technology Division Naval Research Laboratory Washington, D. C. 20375	1